UNIVERSITA' VITA-SALUTE SAN RAFFAELE

CORSO DI DOTTORATO DI RICERCA INTERNAZIONALE IN MEDICINA MOLECOLARE

Curriculum in GENE AND CELL THERAPY

MOBILIZATION-BASED CHEMOTHERAPY-FREE ENGRAFTMENT OF GENE EDITED HEMATOPOIETIC STEM CELLS

DoS: Prof. Luigi Naldini

Second Supervisor: Prof. Vincenzo Calvanese

Tesi di DOTTORATO di RICERCA di GABRIELE PEDRAZZANI

matr. 017577

Ciclo di dottorato: XXXVI

SSD: BIO/11, BIO/18, MED/03

Anno Accademico 2022/2023

CONSULTAZIONE TESI DI DOTTORATO DI RICERCA

Il/la sottoscritto/*I*	Gabriele Pedrazzani
Matricola / *registration number*	017577
nato a/ *born at*	Cremona
il/*on*	20/10/1996

Autore della tesi di Dottorato di ricerca dal titolo / *author of the PhD Thesis titled*

"MOBILIZATION-BASED CHEMOTHERAPY-FREE ENGRAFTMENT OF GENE EDITED HEMATOPOIETIC STEM CELLS"

AUTORIZZA la Consultazione della tesi / AUTHORIZES *the public release of the thesis*

X NON AUTORIZZA la Consultazione della tesi per 12 mesi /DOES NOT AUTHORIZE *the public release of the thesis for* 12 *months*

a partire dalla data di conseguimento del titolo e precisamente / *from the PhD thesis date, specifically*

Dal / *from* 20/12/2023 Al / *to* 20/12/2024

Poiché /*because*:

□ l'intera ricerca o parti di essa sono potenzialmente soggette a brevettabilità/ *The whole project or part of it might be subject to patentability;*

X ci sono parti di tesi che sono già state sottoposte a un editore o sono in attesa di pubblicazione/ *Parts of the thesis have been or are being submitted to a publisher or are in press;*

□ la tesi è finanziata da enti esterni che vantano dei diritti su di esse e sulla loro pubblicazione/ *the thesis project is financed by external bodies that have rights over it and on its publication.*

E' fatto divieto di riprodurre, in tutto o in parte, quanto in essa contenuto / *Copyright the contents of the thesis in whole or in part is forbidden*

Data /Date 27/11/2023 Firma /Signature 

DECLARATION

This thesis has been:

- composed by myself and has not been used in any previous application for a degree. Throughout the text I use both 'I' and 'We' interchangeably.
- has been written according to the editing guidelines approved by the University. Permission to use images and other material covered by copyright has been sought and obtained (Italian legislative Decree no. 68/2003).

All the results presented here were obtained by myself, except for the following results that were obtained in a joint effort:

1) Mobilization experiments were performed with the help of Dr. Attya Omer-Javed, Luisa Albano, and Sherash Ghaus in Naldini lab (SR-Tiget)
2) Experiments on non-human primate cells have been performed by myself in the lab of Prof. Hans-Peter Kiem with the help of Emily Fields and Stefan Radtke at the Fred Hutch Cancer Center in Seattle (Washington, USA)
3) Statistical analyses were performed in collaboration with Alessandro Nonis (Centro Universitario di Statistica per le Scienze Biomediche, CUSSB)

Most of the studies on CD40lg-/- and hematochimeric mouse models reported in this PhD thesis have been published in a research article (on peer-reviewed scientific journal) where I am listed as a second author (Omer-Javed *et al*, 2022) and which I contributed to write together with Dr. Attya Omer-Javed and Prof. Luigi Naldini. In particular, I initially performed the *in vivo* experiments on the syngeneic mouse model under the supervision of Dr. Attya Omer-Javed, taking part in data collection and analysis. Later on, experimental planning and results interpretation on the hematochimeric mouse model were performed together with Dr. Attya Omer-Javed, while I performed the validation experiments to verify the overall replication and reproducibility of our results. I also participated in the process of statistical analysis of collected data. Eventually, I took part in the preparation and presentation of the published work. Thus, part of the text, mostly in the Results section, Figures of this thesis, Methods, and Discussion section are shared with the cognate publication.

Part of the introduction and discussion have been published in a review article where I am listed as a second author (Canarutto *et al*, 2023) and which I contributed to write together with Dr. Daniele Canarutto, Dr. Attya Omer-Javed, Dr. Samuele Ferrari and Prof. Luigi Naldini.

All sources of information are acknowledged by means of reference.

ACKNOWLEDGEMENTS

I extend my deepest gratitude to all those who have contributed to the successful completion of this doctoral thesis. This journey has been filled with challenges and triumphs, and I am indebted to all those who have been instrumental in shaping this work and my PhD path.

First and foremost, I would like to express my sincere appreciation to my Director of Studies, Professor Luigi Naldini, for his support, guidance, and mentorship throughout this research endeavor. His expertise, encouragement, and insightful feedback have been invaluable, shaping not only the direction of this thesis but also my growth as a scientist.

I am equally thankful to my Second Supervisor, Professor Vincenzo Calvanese, for his constructive feedback, patience, and expert advice. His input has greatly enriched the depth and quality of this thesis.

A special acknowledgment is reserved my lab mentor Attya Omer-Javed. Her tireless efforts, expertise, and willingness to share knowledge significantly contributed to the success of the experiments conducted during the course of this research. I cannot thank her enough for everything she taught me and for the way she helped me to grow as a researcher and as a person.

I extend my gratitude to the other present and past post-doctoral researchers in the lab, Sam, Dani, Vale, and Aurel for their collaborative spirit, insightful discussions, and invaluable assistance in various aspects of the experiments. I am also grateful to the technicians, Luisa and Chiara, for their tireless work and effort provided during these years, and all the other lab members whose contributions, both big and small, have played a crucial role in the smooth operation of the laboratory and the success of the experiments.

Heartfelt thanks goes to my fellow PhD students, Marti, Chiara, and Marco for their camaraderie, shared insights, and mutual support. Our collective journey through the ups

and downs of doctoral research has made the process not only intellectually enriching but also personally rewarding.

A special note of appreciation is extended to Professor Hans-Peter Kiem, who generously hosted me in his lab at the Fred Hutch Cancer Center in Seattle. His lab members, particularly Stefan and Emily, provided a welcoming environment and valuable assistance, contributing to the cross-disciplinary collaboration that enhanced the scope of this research.

Eventually, I would like to express my gratitude to my family and friends for their unwavering support, understanding, and inspiration throughout this academic journey. Their love and encouragement have been a constant source of motivation.

This thesis is a culmination of the collective efforts and support of these individuals, and for that, I am profoundly thankful.

ABSTRACT

In current hematopoietic stem and progenitor cell (HSPC) gene therapy, HSPCs are mobilized, genetically corrected *ex vivo*, and infused following myeloablative conditioning meant to make space the bone marrow (BM). However, the chemo/radiotherapy-based conditioning approaches used in the clinic can lead to severe acute and long-term side effects.

To address this challenge and move towards a safer, non-genotoxic conditioning regimen, we demonstrate that HSPC mobilization creates an opportunity for seamless engraftment of exogenous cells, which can effectively compete with the mobilized cells in repopulating the depleted BM. Moreover, we show that transient overexpression of the CXCR4 homing receptor, using an optimized mRNA platform, confers a competitive engraftment advantage to the transplanted cells.

In this study, we show the therapeutic efficacy in a mouse model of Hyper IgM Syndrome and in a human hematochimeric mice, showing its applicability and versatility when coupled to gene transfer and editing strategies. Additionally, transplantation of HSPCs transiently overexpressing a mobilizer-resistant CXCR4 variant in hematochimeric mice resulted in enhanced engraftment when compared to overexpression of the wild type CXCR4.

While being informative, the hematochimeric mouse model may not fully replicate the human HSPC-niche interaction. Therefore, further testing and validation of our exchange strategy in non-human primates (NHPs) are essential before considering its clinical translation. Preliminary results in the NHP model align with the observations made in human cells, indicating that CXCR4 expression can be restored during *ex vivo* culture of NHP HSPCs harvested by G-CSF and AMD3100- mediated mobilization. Moreover, transient overexpression of CXCR4 in these cells increases their migration efficiency in *in vitro* migration assays. Additionally, we demonstrated that base editing at the *CD33* locus and CXCR4 overexpression can be combined without compromising the efficiency of each procedure, providing edited cells with a migration advantage.

Overall, our findings provide proof-of-principle of a transformative strategy paving the way to broader and safer use of HSPC gene therapy.

TABLE OF CONTENTS

DECLARATION **5**

ACKNOWLEDGEMENTS **7**

ABSTRACT **9**

TABLE OF CONTENTS **11**

1 ACRONYMS AND ABBREVIATIONS **15**

2 LIST OF FIGURES AND TABLES **19**

3 INTRODUCTION **23**

3.1 HSPC biology ***23***

3.1.1 Hematopoiesis *23*

3.1.2 Bone marrow niche *26*

3.1.2.1 Cell components of the BM niche *28*

3.2 HSPC Transplantation ***31***

3.2.1 HSPC sources and collection *32*

3.2.2 HSC homing and engraftment *35*

3.2.2.1 Homing *36*

3.2.2.2 Engraftment *38*

3.2.3 Optimization of HSPC mobilization to improve yield *39*

3.3 Ex vivo manipulation for HSPC-GT ***42***

3.3.1 Gene transfer *42*

3.3.2 Nuclease-based editing *45*

3.3.3 Nickase-based editing *47*

3.3.4 Transient overexpression *50*

3.4 Conditioning ***52***

3.4.1 Myeloablative conditioning *53*

3.4.1.1 Total body irradiation *53*

3.4.1.2 Chemotherapy-based conditioning *54*

3.4.2 Non-myeloablative conditioning *55*

3.4.3 Antibody-based conditioning *56*

3.4.4 Graft-versus-host disease and immunosuppression *57*

3.5 Animal models to study HSPC-GT ***58***

3.5.1 Xenograft mouse models *58*

3.5.2 Non-human primates *60*

4 AIM OF THE WORK **63**

5 RESULTS **65**

5.1 Long-term donor chimerism is established by mobilization-based HSCT. ***65***

5.2 M-HSCT allows establishing sufficient donor chimerism to rescue the HIGM-1 phenotype ***69***

5.3 M-HSCT allows an efficient donor to recipient exchange of HSPCs within the human niche of hematochimeric mice ***76***

5.4 Transient CXCR4 overexpression increases chimerism in the humanized context, following M-HSCT ***83***

5.5 M-HSCT confers a clear advantage to gene-edited cells when paired with an engraftment enhancer ***93***

5.6 Investigating the engraftment advantage of AMD3100-resistant CXCR4 variants ***96***

5.7 Transient CXCR4 overexpression confers a migration advantage to non-human primate cells ***99***

6 DISCUSSION **107**

6.1 Limitations of the mouse model ***107***

6.2 Leveraging mRNA-based transient overexpression to confer an engraftment advantage ***108***

6.3 Enhancing mobilization to deplete the BM niche 109

6.4 Future perspectives and clinical translation 110

7 MATERIALS AND METHODS 113

7.1 Experimental models 113

7.1.1 Cell lines 113

7.1.2 Primary human CD34+ cells 113

7.1.3 Xenogeneic mouse transplantation models 113

7.1.4 Syngeneic mouse transplantation model 113

7.1.5 Non-human primates animal housing and care/Ethics Statement 114

7.1.6 Non-human Primates CD34+ cells enrichment and in vitro culture .. 115

7.2 LV vector production and titration 115

7.2.1 Transduction 116

7.3 mRNA IVT 116

7.4 Electroporation 117

7.5 Gene editing of human HSPCs and analyses 117

7.6 Adenine base editing 118

7.7 Molecular analysis 118

7.8 In vitro migration assay 119

7.9 Flow cytometry 120

7.10 Human CD34^{+} HSPC xenotransplantation experiments 121

7.11 Mobilization in vivo 121

7.12 In vivo immunization and IgG quantification 124

7.13 ELISA 125

7.14 Statistical analysis 125

REFERENCES 126

1 ACRONYMS AND ABBREVIATIONS

Acronym	Meaning
ψ or pU	Pseudouridine-5'-Triphosphate
7-AAD	7-Amino-Actinomycin D
AAV	Adeno-Associated Virus/Vector
AAVS1	Adeno-Associated Virus integration Site 1
ABE	Adenine Base Editor
ALL	Acute Lymphoblastic Leukemia
AML	Acute Myeloid Leukemia
ARCA	Anti-Reverse Cap Analog
BER	Base Excision Repair
BM	Bone Marrow
BSA	Bovine Serum Albumin
BU	Busulfan
CB or UCB	Umbilical Cord Blood
CBE	Cytosine Base Editor
CD	Cluster of Differentiation
CD40LG or CD40L	CD40 Ligand
CLP	Common Lymphoid Progenitor
CMP	Common Myeloid Progenitor
CMV	Cytomegalovirus
CRISPR	Clustered Regularly Interspaced Short Palindromic Repeats
CXCL12	CXC-Chemokine Ligand 12
CXCR4	CXC-Chemokine Receptor 4
CY	Cyclophosphamide
DBD	DNA Binding Domain
ddPCR	Digital Droplet PCR
DDR	DNA Damage Response
DPBS	Dulbecco's Phosphate-Buffered Saline

DSB	Double Stand Break
dsDNA	Double stranded DNA
EBMT	European Society for Blood and Marrow Transplantation
ELISA	Enzyme-Linked ImmunoSorbent Assay
ESE	Exon splicing enhancer
FACS	Fluorescence-Activated Cell Sorting
FBS	Fetal Bovine Serum
FLT3L	FMS-related tyrosine kinase 3 ligand
FLU	Fludarabine
G7AB	G-CSF (7 days) + AMD3100 + BIO5192
G-CSF	Granulocyte Colony-Stimualting Factor
GFP	Green Fluorescent Protein
GM-CSF	Granulocyte-Macrophage Colony-Stimulating Factor
GMP	Granulocyte-Macrophage Progenitor
GO	Gemtuzumab ozogamicin
GOI	Gene of Interest
GSE56	Genetic Suppressor Element 56
GT	Gene Therapy
GVHD	Graft versus Host Disease
HDR	Homology-Directed Repair
HEK293T	Human Embryonic Kidney 293T Cell Line
HIGM1 or X-HIGM	X-Linked Hyper-IgM Syndrome
HIV	Human Immunodeficiency Virus 1
HLA	Human Leukocyte Antigen
HPLC	High-Pressure Liquid Chromatography
HSC	Hematopoietic Stem Cell
HSCT	HSC Transplant
HSPC	Hematopoietic Stem/Progenitor Cell
i.p.	Intraperitoneal
i.v.	Intravenous
IDLV	Integrase-Defective Lentiviral Vector
IFN	Interferon

Ig	Immunoglobulin
IMDM	Iscove's Modified Dulbecco's Medium
IS	Immunosuppressive
IVT	*In Vitro* Transcription
KO	Knockout
Lin	Lineage
LT-HSC	Long-Term HSC
LTR	Long Terminal Repeat
LV	Lentiviral Vector
MAC	Myeloablative conditioning
mC	5-Methylcytidine-5'-Triphosphate
MEP	Megakaryocyte-Erythrocyte Progenitor
MFI	Mean Fluoresence Intensity
M-HSCT	Mobilization-enabled HSCT
MMP2	Matrix Metalloprotease 2
MMP9	Matrix Metalloprotease 9
MOI	Multiplicity Of Infection
moU	5-Methoxyuridine-5'-Triphosphate
mPB	Mobilized Peripheral Blood
MPP	Multipotent Progenitor
mRNA	Messenger RNA
NBSGW	NOD.Cg-Kit^{W-41J} Tyr^{+} Prkdc^{scid} Il2Rg^{tm1Wjl}/ThomJ
NGS	Next Generation Sequencing
NHEJ	Non-Homologous End Joining
NHP	Non-Human Primate
NK	Natural Killer Cell
NMAC	Non- myeloablative conditioning
NOD	Non-Obese Diabetic
NSG	NOD.Cg-Prkdc^{scid} Il2Rg^{tm1Wjl}/SzJ
NSGW41	NOD.Cg-Kit^{W41J} Prkdc^{scid} Il2Rg^{tm1Wjl}/WaskJ
PAM	Protospacer Adjacent Motif
PB	Peripheral Blood

PBMC	PB Mononuclear Cell
PCR	Polymerase Chain Reaction
PE	Prime Editor
pegRNA	Prime editing guide RNA
PGE2	Prostaglandin E2
PID	Primary Immunodeficiency
polyA	Polyadenilation Signal
qPCR	Quantitative PCR
RIC	Reduced-intensity conditioning
RNP	Ribonucleoprotein
RTC	Reduced-toxicity conditioning
s.c.	Subcutaneous
SA	Splicing Acceptor
SCF	Stem Cell Factor
SDF-1α	Stromal-Derived Factor 1α
sgRNA or gRNA	Single guide RNA
SIN	Self-inactivating
SOS/VOD	Sinusoidal obstructive syndrome/veno-occlusive disease
SR1	Stem Regenin-1
ST-HSC	Short Term-HSC
TBI	Total Body Irradiation
TNP-KLH	2,4,6, Trinitrophenyl Keyhole Limpet Hemocyanin
TPO	Thrombopoietin
TRM	Transplant-related mortality
UTR	Untranslated Region
VLA4	Very Late Antigen-4
WBC	White Blood Cells
WPRE	Woodchuck Hepatitis Virus Post-transcriptional Regulation Element
WT	Wild Type

2 LIST OF FIGURES AND TABLES

List of figures

Figure 1. Current model of lineage determination in mouse and human hematopoietic hierarchies.. 26
Figure 2. Schematic representation of the adult BM hematopoietic niche in homeostasis. 28
Figure 3. Niche-HSC molecular interactions and signaling. 30
Figure 4. HSPC homing and engraftment. 38
Figure 5. HSPC mobilization mechanisms. 41
Figure 6. Schematic representation of third generation LV constructs 44
Figure 7. DNA double strand break repair pathways 46
Figure 8. Cytosine base editing mechanism. 48
Figure 9. Adenine base editing mechanism. 48
Figure 10. Prime editing mechanism. 50
Figure 11. mRNA capping and in vitro transcription. 51
Figure 12. Mobilization-based conditioning strategy and experimental model. 65
Figure 13. HSC enrichment and mobilization efficiency assessment. 66
Figure 14. Exchange efficiency and chimerism in CD40lg recipient mice. 68
Figure 15. Assessing mobilization kinetics and efficiency. 70
Figure 16. Mobilization impact on the BM niche 72
Figure 17. Mouse-in-mouse exchange experimental design. 74
Figure 18. Chimerism and immunization. 75
Figure 19. Translating M-HSCT in humanized hematochimeric mouse model 77
Figure 20. Ex vivo cell culture promotes the recovery of key engraftment targets. 79
Figure 21. Expression kinetics of KIT and ITGA4 upon culture. 80
Figure 22. Chimerism and lineage reconstitution in peripheral blood 81
Figure 23. Chimerism and lineage composition across hematopoietic organs 82
Figure 24. Chimerism and lineage composition in the bone marrow. 83
Figure 25. mRNA optimization. 84
Figure 26. In vitro testing of optimized mRNA. 85
Figure 27. Optimize CXCR4 mRNA expression 87

Figure 28. Optimize CXCR4 isoform and in vivo testing.....88
Figure 29. Transient CXCR4 overexpression confers an engraftment advantage in vivo. 89
Figure 30. Lineage reconstitution and exchange efficiency across different organs. 91
Figure 31. Secondary transplant.....92
Figure 32. Coupling CXCR4 overexpression with HDR gene editing. 94
Figure 33. Transient CXCR4 overexpression confers HDR-edited cells an exchange advantage in different organs. 95
Figure 34. CXCR4 variants confer a migration advantage in presence of CXCR4 antagonists. 97
Figure 35. CXCR4 variant confers an engratment advantage in vivo. 98
Figure 36. NHP cells characterization.....100
Figure 37. CXCR4 overexpression kinetics in NHP CD34+ cells.....101
Figure 38. CD33 editing strategy. 102
Figure 39. Coupling CXCR4 overexpression and CD33 base editing. 104
Figure 40. Coupling CD33 editing and overexpression of CXCR4 variant.....105

List of tables

Table 1. Key cell types involved HSCs regulation in BM niches. 29
Table 2. Sources of HSPC and their characteristics. 34
Table 3. Key HSC-stroma interactions 36
Table 4. Stem Cell–Mobilizing Agents for Clinical Applications..... 39
Table 5. Estimated versus obtained chimerism following M-HSCT in Cd40lg mice 74

3 INTRODUCTION

3.1 HSPC biology

3.1.1 Hematopoiesis

Blood is one of the body's most rapidly regenerating tissues, with adults producing over one trillion (10^{12}) post-mitotic hematopoietic short-lived cells every day (Doulatov *et al*, 2012). Hematopoiesis ensures the continuous generation of blood cells throughout an individual's lifetime, serving critical functions such as immunity, oxygen transport, coagulation, and tissue remodeling (Boulais & Frenette, 2015). This intricate process primarily takes place within the bone marrow (BM), a semi-solid tissue located in the medullary cavities of long and flat bones, beginning in embryonic development and continuing into adulthood (Kobayashi *et al*, 2023).

In the early 20th century, the Russian biologist Alexander Maximov proposed the idea of a common progenitor for all blood cells (Maximow, 1909). His theory of hematopoiesis, was initially met with skepticism by many experimental hematologists, though it is widely accepted in modern hematology (Friedenstein, 1989). The aftermath of the Hiroshima and Nagasaki bombings in 1945 prompted a surge in research into the biological effects of radiation exposure – in particular neoplastic transformation – catalyzing investigations into hematopoietic stem cells (HSCs) and their response to radiation-induced damage. This tragic event motivated scientists to study the impact of radiation on the hematopoietic system, leading to significant advancements in the understanding of HSC biology (Doulatov *et al*, 2012; Hsu *et al*, 2013). Research by Till and McCulloch, focused on the characterization of stem cells starting from colony-forming units (CFUs), which are now recognized as short-lived hematopoietic progenitors (Becker *et al*, 1963; Till & McCulloch, 1961). This characterization allowed researchers to identify and study the proliferation and differentiation ability of individual cells, ultimately contributing to the understanding of the role of HSC in hematopoiesis. Another significant advancement occurred in 1959 when Donnall Thomas and his team performed the first successful BM transplant in two individuals suffering from advanced leukemia following exposure to high-dose radiation. Together, these pioneering studies

provided conclusive evidence that BM housed cells are endowed with the potential for successful engraftment and subsequent hematopoietic recovery.

Over the following decades, investigations into hematopoiesis contributed to the development of a tree-like hierarchical model, according to which, a finite pool of HSCs gives rise to more specialized progenitors, ultimately generating all differentiated blood cell lineages (Figure 1). Consequently, HSCs occupy the apex of this hematopoietic hierarchy and are characterized by three primary properties (Seita & Weissman, 2010; Gonzalez & Bernad, 2012). Firstly, they are multipotent, allowing them to produce increasingly specialized progeny through cell division, with each descendant acquiring distinct functions. Secondly, HSCs possess the ability to self-renew, dividing while preserving their fundamental stem cell identity. Lastly, these cells maintain precise homeostatic control, effectively balancing differentiation and self-renewal potential by integrating both internal and external signals.

Consistent with the conventional hierarchical model, HSCs can be categorized into three distinct subpopulations: long-term HSCs (LT-HSC), intermediate HSCs (IT-HSC), and short-term HSCs (ST-HSC), each progressively exhibiting reduced self-renewal potential and more differentiated characteristics (Benveniste *et al*, 2010; Benz *et al*, 2012). The immediate progeny of ST-HSCs are multipotent progenitors (MPPs), which, while lacking self-renewal capacity, strongly proliferate and differentiate into lineage-committed progenitors (Seita & Weissman, 2010), namely common lymphoid progenitors (CLPs) and common myeloid progenitors (CMPs). CLPs give rise to natural killer (NK) cells, and B and T lymphocytes, while CMPs further differentiate into granulocyte-macrophage progenitor cells (GMPs) and megakaryocyte-erythrocyte progenitors (MEPs). MEPs ultimately give rise to red blood cells and platelets, whereas GMPs generate monocytes, granulocytes (neutrophils, eosinophils, and basophils), and dendritic cells (Cheng *et al*, 2020).

The identification of distinct subpopulations within hematopoietic stem/progenitor cells (HSPCs) that possess self-renewal and repopulating capabilities has been crucial for advancing our understanding of HSC biology. Cytofluorimetric analyses employs antibodies conjugated with a fluorescent dye to target cell membrane-specific antigens, enabling the isolation and separation of well-defined human HSPC subsets using fluorescence-activated cell sorting (FACS). In 1984, the cell surface glycoprotein CD34,

known for facilitating cell-to-cell adhesion via L-selectin binding, emerged as a suitable phenotypic marker for HSPCs. This discovery allowed the enrichment of a diverse population of hematopoietic multi- and oligo-potent progenitor cells (Civin *et al*, 1984) with proven repopulating capacity (Berenson *et al*, 1988). Subsequently, the Lin-CD34+CD90+ marker cocktail was introduced to identify a more primitive HSPC subpopulation capable of establishing multipotent long-term cultures and ensuring sustained multilineage reconstitution *in vivo* (Baum *et al*, 1992; Weissman & Shizuru, 2008). The Lin antibody cocktail targets surface antigens expressed by various human terminally differentiated hematopoietic cells, while CD90 (Thy1) is a surface glycoprotein involved in cell-to-matrix interactions.

Further research has unveiled additional surface markers within the CD34+ cell population that enrich for more primitive human HSPCs. These markers include the pentaspan transmembrane glycoprotein CD133 (Yin *et al*, 1997), the integrin α6 (CD49f), and the endothelial protein receptor (EPCR, also known as CD201). Transplanting CD49f+ and EPCR+ human HSPCs into immunodeficient mice results in efficient and long-term multi-lineage hematopoietic system reconstitution, whereas $EPCR^{low}$ or CD49f- HSPCs contribute only to transient waves of human cell engraftment (Notta *et al*, 2011; Fares *et al*, 2017). Similarly, low or undetectable surface expression of CD38 (cyclic ADP ribose hydrolase) and CD45RA (an isoform of protein tyrosine phosphatase receptor type C) on HSPCs has been associated with more primitive phenotypes (Bhatia *et al*, 1997). Notably, some of these markers also correlate with stemness characteristics in the murine hematopoietic system, although different surface antigens are utilized in mouse studies to identify LT-HSCs (e.g., CD150 and CD48) (Kiel *et al*, 2005). Of note, the surface expression of these markers is dynamic, and may change based on culture conditions or exposure to specific factors *ex vivo*.

Recent advancements in single-cell technologies, omics studies, and mouse models unveiled a higher degree of complexity within hematopoiesis, emphasizing heterogeneity within stem and progenitor cell populations. The contemporary portrayal of the hematopoietic system integrates these novel discoveries with the classical tree-like model, presenting a hierarchical organization of highly heterogenous populations. In this perspective, differentiation is interpreted as an exceptionally flexible and dynamic

process, characterized by a *continuum* of states without strict compartmentalization (Laurenti & Göttgens, 2018).

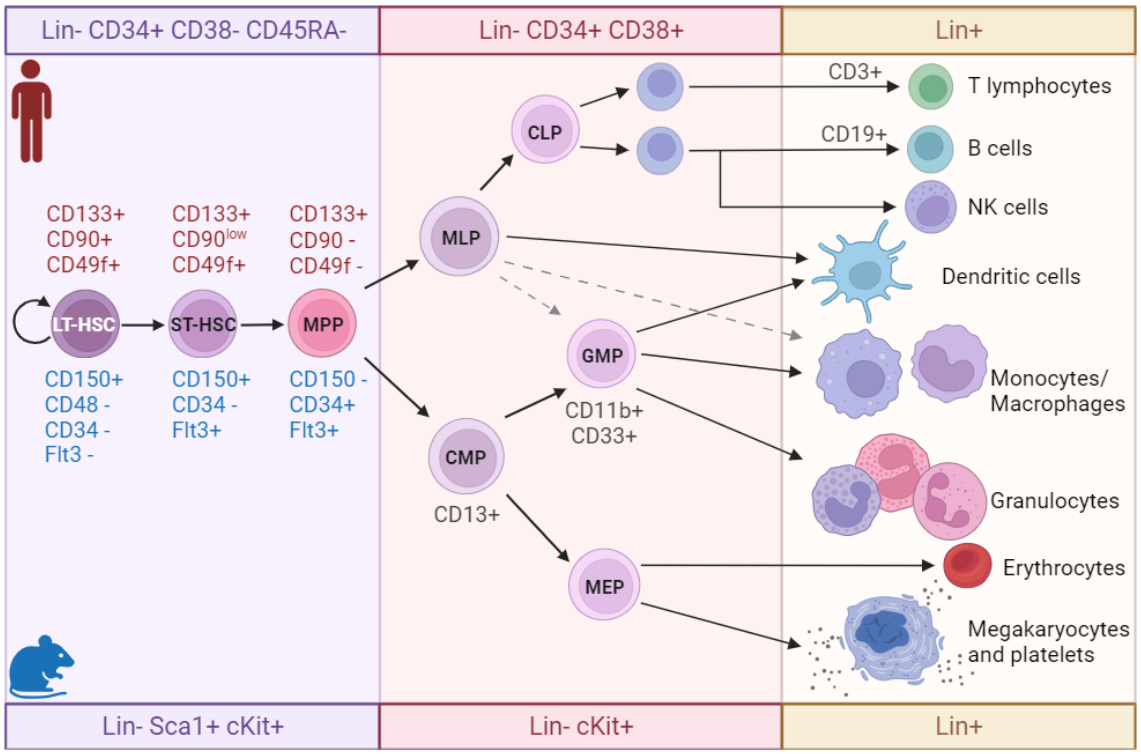


Figure 1. Hierarchical model of lineage determination in mouse and human hematopoietic hierarchies. *Markers on the top and the ones written in red are characteristic of the human hematopoietic system. Markers on the bottom and the ones written in blue are characteristic of the murine hematopoietic system. Markers in gray are shared between the two species. LT-HSC=long term HSC; ST-HSC=short term HSC; MPP=multipotent progenitors; CMP=common myeloid progenitor; CLP=common lymphoid progenitor; MLP=multilymphoid progenitor; GMP=granulocyte macrophage progenitor; MEP=megakaryocyte erythrocyte progenitor. Adapted from Doulatov S. et al., Cell Stem Cell (2012).*

3.1.2 Bone marrow niche

In the early stages of development, hematopoiesis begins in the yolk sac, a structure that surrounds the embryo at the beginning of pregnancy. As the development progresses, blood cell production migrates to the fetal liver and then eventually settles in the BM, which becomes the primary site for hematopoiesis in adults (Calvanese & Mikkola, 2023). The BM consists of a loose stroma housing blood vessels, stromal cells, and various hematopoietic cells surrounded by a meshwork of trabecular bone. Within this microenvironment numerous cell types, physical interactions, and extracellular macromolecules collaboratively create a highly regulated system to support and maintain HSCs – the hematopoietic niche (Figure 2) (Yu & Scadden, 2016). Nutrient channels

allow periosteal and feeding arteries to access the BM, branching into arterioles (De Saint-Georges & Miller, 1992; Iversen, 1997). These arterioles connect to wide-lumen vascular sinusoids, which then lead to central venous sinuses and exit through veins. Sympathetic nerves and perivascular cells are closely associated with arterioles (Morrison & Scadden, 2014). However, identifying neighboring cells that participate in the regulation of HSPCs has been challenging due to difficulties in preserving histological integrity during bone tissue sectioning and the complex immunostaining techniques required for HSC identification. Nonetheless, gaining a comprehensive understanding of the biological mechanisms governing the *in vivo* maintenance and balance of HSCs is crucial for optimizing clinical procedures aimed at *ex vivo* HSC manipulation and expansion. Therefore, extensive research has been conducted to untangle the intricate network within the BM niche.

The precise anatomical regions within the BM where HSPCs and quiescent HSCs predominantly reside remain a subject of ongoing debate, resulting in diverse and sometimes conflicting conclusions from various studies. Some indicate HSCs are found in hypoxic areas, with deeper peri-sinusoidal regions having the lowest oxygen levels, while endosteal regions are less hypoxic (Spencer *et al*, 2014), though some studies suggest proximity to arterioles (Kunisaki *et al*, 2013; Asada *et al*, 2017), others to sinusoids (Acar *et al*, 2015), and some indicate HSCs are near both (Christodoulou *et al*, 2020). Conflicting theories about HSCs locations near arterioles or sinusoids may be reconciled by studies proposing the existence of distinct HSPC populations residing in separate BM regions or that the localization of HSCs within the BM may vary based on their cell cycle status. Quiescent HSCs, for example, tend to reside near small arterioles, which are primarily found in the endosteal niche (Kunisaki *et al*, 2013), while myeloid-biased HSCs tend to interact with sinusoidal megakaryocytes and lymphoid-biased HSCs near arterioles (Itkin *et al*, 2016; Pinho *et al*, 2018). Nonetheless, it is unclear if naïve HSCs favor specific BM locations or if these locations induce lineage preferences.

Moreover, discrepancies between these studies may be attributed to various factors, including the use of different imaging technologies and the influence of HSPCs *ex vivo* manipulation, BM irradiation, and surgical or medical procedures in mouse models. For example, when gene-marked HSPCs were transplanted into recipient mice and tracked using histological and intravital microscopy techniques, there appeared to be a preference

for HSPCs to localize in the endosteal niche, situated at the border between the BM and bone (Nilsson *et al*, 2001; Lo Celso *et al*, 2009). In contrast, staining of endogenous HSCs, without any *ex vivo* manipulations, suggested a preference for perivascular niches, which are located in close proximity to the endosteum (Nombela-Arrieta & Manz, 2017).

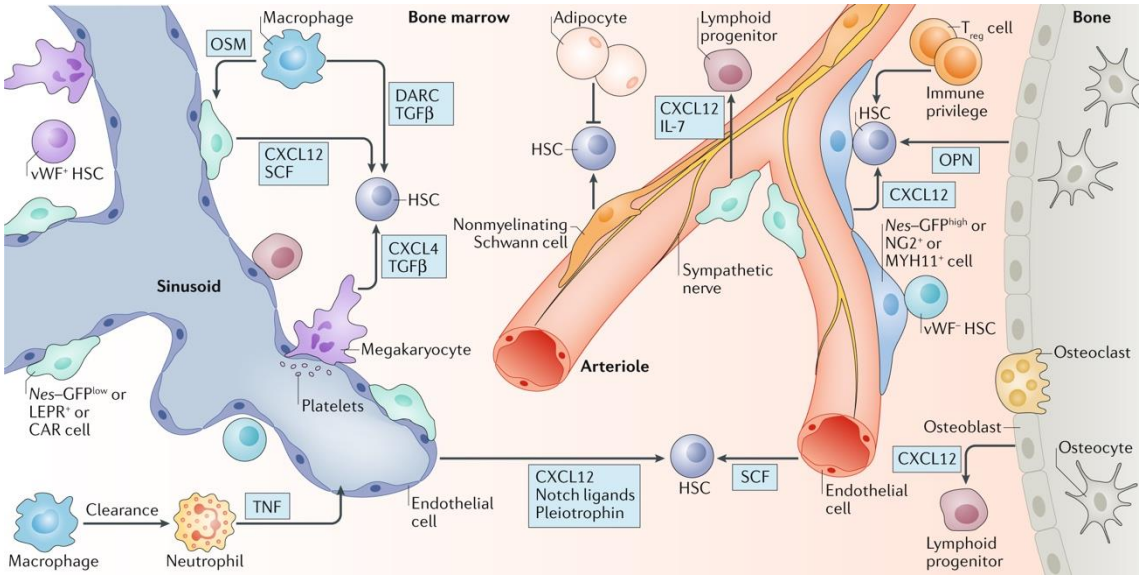


Figure 2. Schematic representation of the adult BM hematopoietic niche in homeostasis. *Schematic representation of the adult BM HSPC niche in homeostasis, showing various cell types and niche factors regulating HSPC activity. Adapted from Pinho & Frenette (2019).*

3.1.2.1 Cell components of the BM niche

The complex BM niche microenvironment involves several cell types actively contributing to HSC maintenance. In the endosteal niche, osteoblasts secrete essential components to support HSCs, such as thrombopoietin (TPO), angiopoietin (ANG-1), and CXC-chemokine ligand 12 (CXCL12 or SDF-1), while osteoclasts secrete proteases and stem cell factor (SCF) (Morrison & Scadden, 2014). In the perivascular niche, reticular cells secrete CXCL12, while endothelial cells, megakaryocytes, T cells, Schwann cells, and adipocytes contribute to the regulation of HSC homeostasis, long-term self-renewal, and quiescence (Pinho & Frenette, 2019). **Table 1** summarizes the different cell types identified in the BM niche and their role in supporting HSPCs.

Table 1. Key cell types involved HSCs regulation in BM niches.

Cells	Function	Main Molecules
Mesenchymal stem cells	Support and regulation of HSC quiescence, proliferation, differentiation	CXCL12, SCF, VCAM-1, angiopoietin-1, osteopontin
Osteoblasts	Support of HSC quiescence	Osteopontin, TPO, angiopoietin-1, N-cadherin
Endothelial cells	Support of HSC proliferation and expansion	CXCL12, SCF, Notch ligands, Del-1, E-selectin, pleiotrophin
Adipocytes	Support of HSC survival, proliferation and differentiation	CXCL12, MCP-1, SCF, CSF3, IL-8, LIF, leptin, adiponectin
Megakaryocytes	Support of HSC quiescence HSC expansion after irradiation	CXCL4, TPO, TGF-β, FGF1
Macrophages	Support of HSC quiescence HSC retention	VCAM-1, TGF-β, DARC
Treg lymphocytes	Support of HSC quiescence Protection of HSC from immune attack	IL-10, adenosine, CDC39
Sympathetic nerve fibers	HSCs mobilization	Noradrenaline
Parasympathetic nerve fibers	HSC retention in niche	Acetylcholine

Adapted from (Kandarakov et al*, 2022)*

Notably, mesenchymal stem/stromal cells (MSCs) are multipotent cells crucial for tissue repair, characterized by specific markers and the ability to differentiate into various cell types (Pittenger *et al*, 1999, 2019). Within the BM, MSCs constitute a rare perivascular population with a prominent role in supporting HSCs (Méndez-Ferrer *et al*, 2010; Greenbaum *et al*, 2013). Distinguishing subpopulations of MSCs based on marker characteristics has revealed variations in their impact on HSC functionality (Pittenger *et al*, 2019). Particularly, a population of MSCs in the perisinusoidal niche with high expression of CXCL12, SCF, and LEPR (CAR cells) has been shown to play a crucial regulatory role in preserving HSC populations (Zhou *et al*, 2014; Asada *et al*, 2017). Furthermore, the interaction between HSCs and MSCs involves complex signaling pathways, including Wnt, Notch, BMP4, as well as the beta-adrenergic receptor and norepinephrine/adrenaline, contributing to HSC self-renewal and regulation (Zhang *et al*, 2003; Morrison & Scadden, 2014). Notably, MSCs have been utilized in clinical trials to support hematopoiesis upon HSCs/MSCs co-infusion, showing faster hematopoietic

reconstitution and demonstrating their potential therapeutic application in treating hematological disorders in both autologous and allogeneic settings (Koç *et al*, 2000; Le Blanc *et al*, 2007; MacMillan *et al*, 2009). These findings collectively highlight the critical role of MSCs in supporting HSCs and maintaining the hematopoietic system, emphasizing their importance in the BM niche and regenerative medicine.

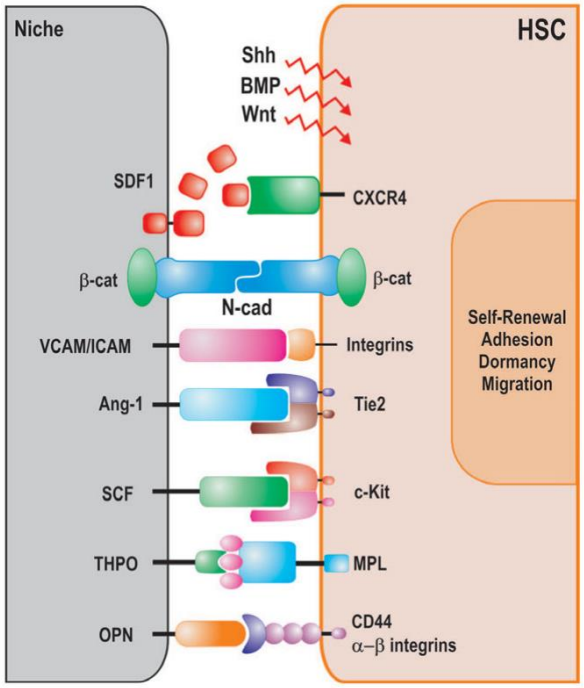


Figure 3. Niche-HSC molecular interactions and signaling.
Abbreviations: SDF1, stromal derived factor-1; CXCR-4, CXC-chemokine receptor-4; N-cad, N-cadherin; β-cat, β-catenin; VCAM, vascular cell-adhesion molecule; ICAM, intercellular adhesion molecule-4; Ang-1, angiopoietin-1; SCF, stem cell factor; THPO, thrombopoietin; OPN, osteopontin; Shh, Sonic hedgehog; BMP, bone marrow proteins; Wnt, Wingless. Adapted from Suárez-Álvarez et al*, (2012).*

Moreover, with the advent of single-cell RNA sequencing (scRNAseq) and spatial transcriptomics, a growing number of studies uncovered remarkable insights into BM stromal cell diversity and dynamics (Wolock *et al*, 2019; Baryawno *et al*, 2019; Baccin *et al*, 2020). Notably, these studies revealed distinct stromal cell subsets, endothelial sinusoidal and arteriolar cells, fibroblasts, and osteolineage and chondrocyte subsets (Wolock *et al*, 2019; Baryawno *et al*, 2019), and two new subsets of CAR cells expressing osteogenic and adipogenic gene signatures (Baccin *et al*, 2020). These investigations have thus advanced our understanding of the BM microenvironment, including its cellular dynamics and localization.

3.2 HSPC Transplantation

Hematopoietic stem cell transplantation (HSCT) is a medical procedure that involves the intravenous infusion of HSPCs to reestablish blood cell production. The process typically includes three key steps:

1. HSPC Collection: The first step involves the collection of HSC from the BM, peripheral blood, or umbilical cord blood (UCB)
2. Conditioning: This step often includes a short course of chemotherapy or total body irradiation to prepare the patient for the transplant by eliminating diseased or abnormal cells and creating space in the BM for the new stem cells
3. Infusion of Stem Cells: The harvested stem cells are then infused intravenously into the patient, where they migrate to the BM and begin producing new blood cells

HSCT encompasses three primary categories: syngeneic (utilizing HSPCs from an identical twin), allogeneic (employing HSPCs from a matched donor), or autologous (utilizing the patient's own stem cells). The choice among these transplant types depends on a variety of factors, including the patient's therapeutic needs, age, and the availability of a suitable donor (Sánchez-Guijo *et al*, 2012).

Historically, genetic differences between individuals posed a significant challenge for allogeneic HSCT, resulting in elevated mortality rates due to either graft rejection or graft-versus-host disease (GvHD), an immune reaction where donor lymphocytes attack the host's tissues (Sánchez-Guijo *et al*, 2012). The discovery of the histocompatibility complex, specifically the Human Leukocyte Antigens (HLAs), as the primary source of immunological tissue incompatibility, has significantly enhanced the safety of allogeneic HSCT (Dausset & Brecy, 1957; Dausset, 1981). Thorough HLA matching prior to transplantation, coupled with the use of immunosuppressive medications, has markedly decreased the morbidity and mortality associated with this approach (Hansen *et al*, 1980; Thomas *et al*, 1982). In the context of allogeneic HSCT for treating inherited blood disorders, the aim is to replace dysfunctional cells with healthy ones from a compatible donor. However, GvHD continues to be a substantial risk factor, constraining broader applications of allogeneic HSCT due to limitations posed by the necessity of finding a compatible donor (Sullivan, 2000). Additional challenges are posed the use of strong conditioning regimens, which are cytotoxic and can lead to severe and delayed effects in

both hematopoietic and non-hematopoietic organs, as well as delayed immune recovery. Therefore, novel approaches, such as the use of monoclonal antibodies and immunotoxins to selectively deplete HSPCs, are being investigated to reduce the genotoxicity of conditioning agents (Palchaudhuri *et al*, 2016; George *et al*, 2019; Czechowicz *et al*, 2019; Kwon *et al*, 2019; Casirati *et al*, 2023).

For patients with genetic blood disorders who lack suitable HLA-matched donors, autologous transplantation of genetically corrected HSPCs presents a promising alternative. Autologous HSCT offers several advantages, including a reduced risk of infection during immunosuppression, faster immune reconstitution, a lower risk of graft rejection, and the absence of GvHD compared to allogeneic HSCT (Sullivan, 2000; Bazinet & Popradi, 2019).

3.2.1 HSPC sources and collection

The first BM biopsy dates back to 1876 when Mosler first conducted this procedure. Subsequently, from 1929 onward, Arinkin advocated for BM aspiration as a safe and valuable approach for studying hematological diseases. Throughout history, BM aspirates have served as the primary and extensively utilized source of HSPCs.

Goodman and Hodgson pioneered the observation of HSPCs in murine peripheral blood (Goodman & Hodgson, 1962). Subsequent experiments in non-human primates (NHP) involved the cross-circulation of peripheral blood from donors with healthy marrow into irradiated syngeneic recipients to establish marrow grafts (Epstein *et al*, 1966). The development of a continuous-flow apheresis device by Judson and colleagues in 1968 further advanced the field by enabling the collection of leukocytes from peripheral blood, which was later identified to contain CFUs (Judson *et al*, 1968; McCredie *et al*, 1971). The field witnessed another major breakthrough in 1984 when Metcalf and his team discovered granulocyte colony-stimulating factor (G-CSF) and subsequently isolated and purified it (Metcalf, 1990). Administration of G-CSF stimulates neutrophils in the BM to release proteases, cleaving the molecular interactions that keep HSCs anchored to the BM stroma, ultimately promoting their egress in the peripheral blood (Greenbaum & Link, 2011). This pivotal discovery of G-CSF ushered in a new era, as it became routinely employed for HSPC mobilization in both autologous and

allogeneic transplantation studies, significantly increasing the quantity of circulating HSPCs.

In the 1980s, following the Chernobyl nuclear accident, UCB emerged as an alternative source of HSPCs with great potential. The work of Broxmeyer and colleagues culminated in the first successful UCB transplantation for the treatment of Fanconi's anemia in 1988 (Broxmeyer et al, 1989; Gluckman & Rocha, 2005). Today, data from the National Marrow Donor Program indicates that mobilized peripheral blood (mPB) has emerged as the most commonly used source of stem cells in recent years. Nevertheless, each source of HSPCs presents unique characteristics and clinical applications, as outlined in **Table 2**.

Marrow HSPCs are obtained through BM aspirates conducted on the donor. This procedure, performed under general anesthesia and sterile conditions in an operating theater, involves multiple punctures primarily in the anterior superior iliac crest areas, with the option for posterior punctures if necessary (Panch *et al*, 2017). An adult typically yields between 800 to 1200 ml of BM blood, not exceeding 15 ml per kilogram of body weight (Babic & Trigoso, 2018). Potential risks include bleeding, infection, and localized discomfort. Severe complications from this extraction method, such as pulmonary embolism and anesthesia-related issues, are exceedingly rare, occurring in less than 0.3% of cases, while mild complications, mainly associated with discomfort or pain, affect at least 10% of cases (Panch *et al*, 2017).

To harvest HSPCs from peripheral blood, stem cells need to be mobilized from the BM using drugs like G-CSF and plerixafor. Typically, in adults, G-CSF is administered for up to 6 consecutive days at doses ranging from 5 to 15 µg/kg/day (Panch *et al*, 2017). While G-CSF effectively elevates CD34+ cell levels in peripheral blood, mobilization may be insufficient in certain cases. In such instances, plerixafor (AMD3100), an antagonist of CXCR4 receptor, can be administered as a single 240 µg/kg dose at the end of a G-CSF regimen, usually given 4 to 6 hours before apheresis to enhance collection yields (Panch *et al*, 2017). For donors with unsuitable peripheral veins, such as children or dehydrated adults, central venous catheter insertion becomes necessary, often requiring hospitalization. G-CSF-based mobilization for mPB HSPCs collection may entail toxicities, including flu-like symptoms, insomnia, and bone pain associated with G-CSF, and apheresis-related complications (Pulsipher *et al*, 2014; Panch *et al*, 2017).

Table 2. Sources of HSPC and their characteristics.

	PB	BM	CB
Donor characteristics			
Transplant donor type	Haploidentical donor, MSD, MUD	Haploidentical donor, MSD, MUD	MUD
Collection risk*	Apheresis related severe adverse events ~1/1000	Surgical risk (severe adverse events) ~1/100	Postdelivery Absent/none reported
Graft characteristics			
Relative CD34 content	50×	10×	1×
Relative T cell content	100×	10×	1× (naive T cells)
Minimum cell dose for engraftment	Autologous: 2×10^6 $CD34^+$ cells/kg Allogeneic: 4×10^6 $CD34^+$ cells/kg	Same as for PB grafts	Single cord: 2.5×10^7 TNC/kg
Collection volume (mL)	~300	~1000	~100
HLA matching criteria	6/6 (MSD) 7/8 (haploidentical donor) 8/8-12/12 (MUD)	Similar to PB	4-6/6
Recipient characteristics			
Speed of engraftment	Faster	Moderate	Slower
Anti-tumor effect	Higher	Lower	Higher
Acute/chronic GvHD risk	Higher	Moderate	Lower

*PB indicates peripheral blood; MSD, matched sibling donor; MUD, matched unrelated donor; TNC, total nucleated cells. * Collection risk defined as life threatening, unexpected, or chronic disabling events. Adapted from Panch et al. (2017).*

The CD34+ cell content varies across the three primary stem cell sources, with cord blood collection having the lowest and mPB having the highest CD34+ cell counts. Moreover, all three sources contain T cells, which can potentially trigger GvHD in allogeneic transplantation, though cord blood collections typically have a smaller number of immunologically naive T cells. When comparing BM with G-CSF–mobilized PB concentrates, the latter demonstrate higher absolute counts of lymphocytes, monocytes, and dendritic cells (Panch *et al*, 2017). This variation in cellular composition contributes to differences in HLA matching requirements among the three stem cell sources, with CB

transplants having the least restrictive matching criteria. Consequently, CB transplants generally experience lower rates of acute and chronic GvHD. However, it's worth noting that CB stem cells tend to engraft more slowly due to their lower CD34+ cell numbers even though, due to the lower immunogenic potential, it is possible to pool cells from different donors to increase the number of infused HSCs (Schönberger *et al*, 2004).

G-CSF administration before BM collection is believed to enrich the population of more primitive HSPCs within the marrow while mobilizing myeloid-biased progenitors and T cells into the PB (Deotare *et al*, 2015). This dual effect aims to enhance engraftment while reducing the risk of GvHD in G-CSF–primed marrow. Studies comparing G-CSF–primed BM to non-primed BM in the context of HLA-matched allogeneic transplants have shown that primed BM exhibit faster engraftment and similar or lower rates of GvHD (Di Bartolomeo *et al*, 2013). When comparing G-CSF–primed BM to G-CSF–mPB, reported outcomes suggest that patients receiving PB grafts experience comparable or slightly improved engraftment but have higher rates of GvHD. However, overall survival does not significantly differ between the two groups (Di Bartolomeo *et al*, 2013). Nevertheless, it is important to consider that G-CSF–primed BM collections come with combined side effects related to G-CSF administration and the hazards associated with the biopsy procedure, including general anesthesia, mechanical injury, and anemia (Panch *et al*, 2017).

While previous efforts to incorporate HLA-haploidentical BM or G-CSF–mobilized mPB in transplantation protocols often faced challenges (such as elevated GvHD rates, post-transplant infections, and graft failure), recent advancements in graft engineering and immune suppression therapies have significantly enhanced the success rate and adoption of haploidentical donor transplants. Nevertheless, the demand for technical expertise in graft manipulation techniques may result in added costs for the routine utilization of haploidentical grafts, thus further limiting its applications.

3.2.2 HSC homing and engraftment

HSPCs express surface receptors capable of binding molecules released by or expressed on the surface of the other cells present in the BM niche. Notably, CXC-chemokine receptor 4 (CXCR4) is a surface receptor on HSPCs that binds to CXCL12.

This interaction is essential for HSC maintenance, BM homing, and mobilization (Ara *et al*, 2003). **Table 3** summarizes the key regulators in HSC retention in the BM niche.

HSPCs can exit the BM (mobilization) by loosening cell-to-cell and cell-to-extracellular matrix contacts and downregulating CXCL12/CXCR4 signaling, allowing them to pass through the BM-blood barrier and enter the blood stream. Conversely, they can return to the BM (homing) following chemotactic molecular gradients (as CXCL12). Interestingly, CXCR4 expression undergoes diurnal regulation, being downregulated during the daytime and upregulated at night, possibly due to sympathetic nervous system regulation of the circadian rhythm, resulting in physiological HSC recirculation (Méndez-Ferrer *et al*, 2008). This process likely sustains a stem cell pool in peripheral BM locations and facilitates responses to organ damage and infections (Ratajczak *et al*, 2018).

Table 3. Key HSC-stroma interactions

Molecule	HSC Receptor	Producing Cells	Regulatory Function
CXCL12	CXCR4	MSCs, ECs, ADs	HSC maintenance, homing and niche retention
SCF	KIT	MSCs, ECs, ADs	HSC survival, homing, maintenance and proliferation
TGF-β	TGFBR1	MKs	HSC quiescence
Osteopontin	CD44	OBs, MSCs	Suppression of HSC proliferation and expansion
Angiopoietin 1	TIE2	OBs, MSCs	HSC maintenance and quiescence
VCAM-1	VLA4	MSCs, Mϕ	HSC homing
TPO	MPL	MKs, OBs	HSC quiescence, maintenance and proliferation
Jagged-1	NOTCH	MSCs, ECs, OBs	HSC maintenance, expansion and self-renewal
EGF	EGFR	ECs	HSCs survival and maintenance

HSCs—hematopoietic stem cells, MSCs—mesenchymal stem/stromal cells, ECs—endothelial cells, ADs—adipocytes, MKs—megakaryocytes, OBs—osteoblasts, Mϕ—macrophages. Adapted from Suárez-Álvarez et al*, (2012).*

3.2.2.1 Homing

HSCT involves intravenous infusion of HSPCs into preconditioned recipients via central line, with limited use of intraosseous HSPC infusion in clinical practice. Initially,

transplanted HSPCs widely disperse throughout organs and blood circulation, but the predominant engraftment and hematopoiesis occur within the BM (Liesveld *et al*, 2020). This transition from circulation to BM, termed "homing", is a somewhat inefficient process, with only about 2% of HSPCs detected in the BM 24 hours post-HSCT (Kang & Chao, 2012).

The homing of HSPCs is a highly coordinated process that involves interactions between HSPCs, endothelial cells, and the microenvironment of the BM niche. This process begins with the initial binding of HSPCs to endothelial selectins and VCAM-1, which triggers rolling and subsequent adhesion to the endothelial cells (Perlin *et al*, 2017). These interactions are reinforced by VLA-4 (α4β1)/VCAM-1 and LFA-1(αLβ2)/ICAM-1 interactions, facilitating HSPC transendothelial migration towards BM niches (Liesveld *et al*, 2020). Matrix metalloproteinases (MMP)-2 and MMP-9 play essential roles in degrading the basement membrane, further facilitating transendothelial and subendothelial HSPC migration (Lapidot *et al*, 2005). Ultimately, ligands found on stromal cells and the niche's extracellular matrix interact with HSPC integrins, anchoring HSPCs within the niche (Liesveld *et al*, 2020).

In particular, the interaction between CXCR4 - expressed on the surface of HSPCs - and its ligand CXCL12 - expressed by stromal cells and secreted in the BM niche microenvironment – plays a pivotal role in the homing process (Peled *et al*, 1999). After TBI, the levels of CXCL12 within the marrow niche environment significantly rise, creating a CXCL12 gradient between the marrow niche and the bloodstream (Lapidot *et al*, 2005). This gradient serves as a powerful attractant for HSPCs, drawing them out of the sinusoidal vessels and guiding them toward the marrow niches. Moreover, CXCL12 acts not only as a chemoattractant for HSPC migration but it also enhances homing through several intricate mechanisms. For example, CXCL12/CXCR4 interaction enhances the adhesion of HSPCs to endothelial ligands, such as VCAM-1 and ICAM-1, via VLA-4, VLA-5, and LFA-1, facilitating firm attachment of HSPCs to endothelial cells (Kang & Chao, 2012). Moreover, CXCL12 upregulates the levels of MMP-2 and MMP-9, promoting the degradation of the basement membrane, thereby facilitating HSPCs transendothelial migration (Kang & Chao, 2012).

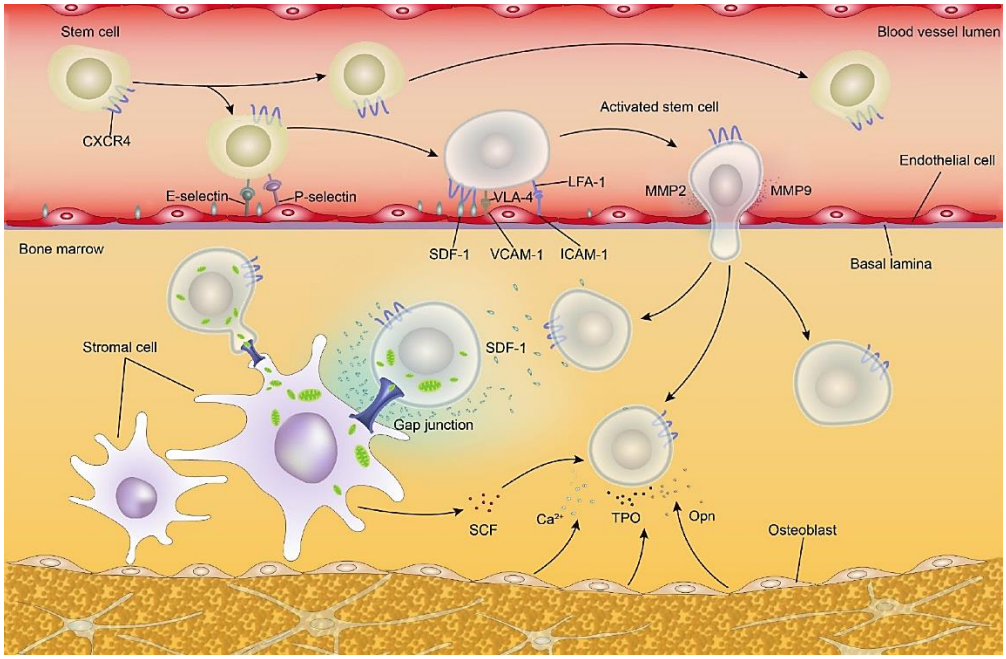


Figure 4. HSPC homing and engraftment. *The interaction between stromal cells in the recipient's bone marrow and HSPCs from the donor significantly contributes to the process of HSPC homing and engraftment. Key factors involved include calcium (Ca2+), C-X-C chemokine receptor 4 (CXCR4), intercellular adhesion molecule-1 (ICAM-1), lymphocyte function-associated antigen-1 (LFA-1), matrix metalloproteinase 2 (MMP-2), matrix metalloproteinase 9 (MMP-9), osteopontin (Opn), stem cell factor (SCF), stromal-derived factor-1 (SDF-1), thrombopoietin (TPO), vascular cell adhesion molecule-1 (VCAM-1), and very late antigen 4 (VLA-4). Adapted from Chen* et al*, 2023.*

3.2.2.2 Engraftment

Once HSPCs have successfully homed to marrow niches, they initiate a series of crucial processes, including self-renewal, expansion, and differentiation, ultimately leading to the reestablishment of hematopoiesis, a phenomenon referred to as HSC engraftment. Various elements within the BM microenvironment, including MSC, endothelial cells, osteoblasts, and osteoclasts, engage with HSPCs through diverse mechanisms, impacting self-renewal, quiescence, or survival (Kang & Chao, 2012). Maintaining a quiescent HSC population post-HSCT is vital for successful engraftment and hematopoiesis reconstitution. Several niche factors collaborate to achieve this, with the CXCL12/CXCR4 interaction taking a prominent role in HSPC survival and BM maintenance (Broxmeyer, 2012). At low concentrations, CXCL12 collaborates with other cytokines to support HSPC survival and proliferation (Lee *et al*, 2002; Kang & Chao, 2012). Conversely, at high concentrations, CXCL12 induces quiescence in primitive HSCs, thus preserving the HSC pool (Cashman *et al*, 2002; Tzeng *et al*, 2011).

The precise mechanisms by which CXCL12 maintains HSC quiescence are still under investigation, but recent studies suggest the involvement of crosstalk between CXCL12 and transforming growth factor-β (TGF-β) in balancing HSPC quiescence and proliferation (Chabanon *et al*, 2008). In summary, the CXCL12/CXCR4 interaction exerts multifaceted effects on HSPCs, influencing their migration, homing, retention, and the equilibrium between quiescence and proliferation.

3.2.3 Optimization of HSPC mobilization to improve yield

The use of recombinant human G-CSF, such as filgrastim or lenograstim, effectively stimulates granulocyte expansion, activating enzymes such as neutrophil elastases and matrix metalloproteinases, which disrupt the CXCL12/CXCR4 axis, thus facilitating stem cell egress (Altuntaş & Korkmaz, 2017).

Another mobilization option involves plerixafor (AMD3100), a small molecule that inhibits the binding of CXCL12 to CXCR4, thereby facilitating HSPC mobilization (Matthys *et al*, 2001). Moreover, while G-CSF alone is effective in only around two-thirds of cases, the combination of G-CSF and plerixafor has shown a synergistic effect, increasing CD34+ cell levels in peripheral blood up to 10-fold beyond baseline levels (DiPersio *et al*, 2009). As a result, plerixafor is currently authorized for combination with G-CSF when mPB collections with G-CSF alone fail to meet the minimum CD34+ cell dose requirements for autologous transplants. Since the mobilization regimen significantly impacts mPB concentrate yields and HSPC characteristics, numerous mobilization agents have undergone clinical evaluation and approval, including granulocyte-macrophage colony-stimulating factor (GM-CSF), stem cell factor (SCF), and plerixafor, with others still in pre-clinical development. Each of these agents exhibits distinct mechanisms of action, clinical indications, and side effect profiles, as delineated in **Table 4**.

Table 4. Stem Cell–Mobilizing Agents for Clinical Applications.

Drug	Mechanism of Action	Clinical Indications	Side Effects	Caveats
G-CSF	CXCL12 downregulation, release of proteases	PB or BM-HSPC mobilization	Bone pain, insomnia, flu-like symptoms	Cumbersome 5-day dosing regimen

Drug	Mechanism of Action	Clinical Indications	Side Effects	Caveats
Plerixafor	Reversible antagonist of CXCR4/CXCL12	Synergistic mobilizing agent with G-CSF	Mild: Injection site reaction, diarrhea	Ineffective as stand-alone agent
GM-CSF	Similar to G-CSF	Same as G-CSF, mobilization lower than G-CSF	Fever, hypertension, skin rash	Mobilizes more macrophages, monocytes
SCF	c-KIT downregulation*	Synergistic use with G-CSF	Diffuse erythema, injection site reaction	Approved for clinical use only in Canada and New Zealand

*GM-CSF indicates granulocyte-macrophage colony-stimulating factor; SCF, stem cell factor. * Mechanism of action of SCF is unclear, it is believed to be related possibly to c-KIT receptor downregulation. Adapted from Panch* et al *(2017).*

Comparative analyses of HSPC phenotypes mobilized using G-CSF alone versus the combination of G-CSF and plerixafor have shown that G-CSF alone tends to result in HSCs with a myeloid bias, while the addition of plerixafor to G-CSF-mobilized HSPCs demonstrates a higher prevalence of T, B, and mast cell features, as evidenced by gene expression profiling (Lidonnici *et al*, 2017). Although generally well-tolerated, the cost-effectiveness of plerixafor in routine clinical use is still under evaluation, and ongoing research aims to determine its optimal dosage and safety in healthy allogeneic donors. In contrast, GM-CSF and SCF exhibited less favorable collection and side effect profiles, limiting their widespread clinical utilization.

Since the effectiveness of G-CSF-mediated stem cell mobilization is influenced by a variety of patient- and donor-related factors, including age, race, and sex, ongoing research into BM niche pathways remains essential to enhance HSPC mobilization and advance the quality and clinical outcomes of transplantation procedures. For instance, the potential use of natalizumab, an α4-blocking antibody currently used to treat Crohn's disease and multiple sclerosis, has shown promise in the mobilization of HSPCs in murine and non-human primate models when administered independently or alongside either G-CSF or SCF (Craddock *et al*, 1997; Bonig *et al*, 2008). Subsequent clinical investigations in multiple sclerosis' patients corroborated its ability to efficiently mobilize CD34+ cells in humans (Zohren *et al*, 2008; Jing *et al*, 2010). However, its association with potentially life-threatening conditions as progressive multifocal leukoencephalopathy has precluded its clinical use for mobilization (Bloomgren *et al*, 2012). Addressing the concerns arising

from natalizumab-induced prolonged α4 inhibition, researchers have developed BIO5192, an exceptionally potent and selective small molecule antagonist targeting α4β1. This compound has been shown to effectively mobilize HSPCs, either as a standalone treatment or in combination with G-CSF and/or AMD3100, resulting in a remarkable 30-fold increase in murine HSPC mobilization over basal levels and without the prolonged leukocytosis that poses a risk of progressive multifocal leukoencephalopathy (Ramirez *et al*, 2009).

A different approach leverages on the chemokine Gro-β or its truncated form, which binds to the CXCR2 receptor, stimulating neutrophils to release proteases, thus rapidly mobilizing a more primitive HSPC subset when compared to G-CSF-mobilized HSCs (Fukuda *et al*, 2007). However, the effectiveness of HSC mobilization using Gro-β has been found to depend on MMP-9 and shows variable outcomes among different mouse strains, although Hoggatt and colleagues showed increased mPB CD34+ cells in a placebo-controlled tolerability trial in healthy subjects (Hoggatt *et al*, 2018). Interestingly, Gro-β showed a synergistic activity with plerixafor, leading to rapid increase in the circulation of HSPCs without the requirement of G-CSF in mice (Hoggatt *et al*, 2018).

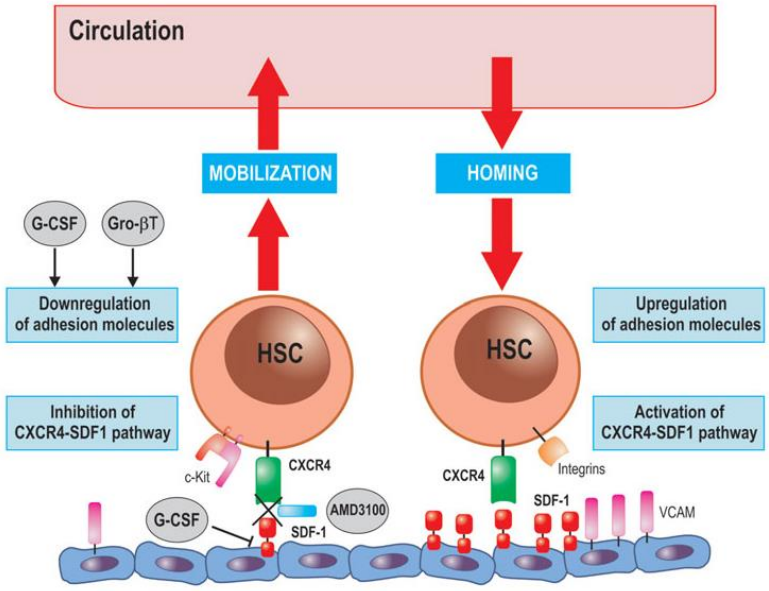


Figure 5. HSPC mobilization mechanisms.
HSC mobilization involves the down-regulation of adhesion molecules and chemokine receptors, directing cells into the bloodstream. Cytokines, including G-CSF and Gro-B, induce the release of proteolytic enzymes that downregulate adhesion molecules and inactivate SDF-1. AMD3100 selectively blocks SDF-1

binding to CXCR4, facilitating rapid HSC mobilization. Adapted from Suárez-Álvarez et al, (2012).

3.3 *Ex vivo* manipulation for HSPC-GT

Hematopoietic stem/progenitor cell gene therapy (HSPC-GT) is a cutting-edge therapeutic approach that harnesses the potential of hematopoietic stem cells to treat a wide range of genetic and non-malignant diseases, offering promising avenues for disease management and potential cures. This approach is based on genetic manipulation of the patient's cells to correct the disease-causing mutation, with genetic modifications usually accomplished by delivering exogenous nucleic acids into human cells (Verma & Weitzman, 2005). To do so, non-viral delivery platforms employ chemical or physical techniques such as chemical transfection, electroporation, or nanoparticle-based methods to facilitate the entry of genetic material across the cell's plasma membrane. While non-viral systems generally offer cost-effectiveness advantages over viral platforms, their efficacy and potential toxicity require meticulous evaluation, contingent on the specific application (Ramamoorth, 2015). In contrast, viral platforms own a specialized machinery evolved for host cell infection, thus typically exhibiting superior delivery efficiency compared to non-viral delivery methods, although they are associated with a higher risk of immunogenicity, mutagenesis, and carcinogenesis (Ferrari *et al*, 2023).

3.3.1 Gene transfer

Viral vectors exhibit diverse capabilities in terms of integrating their genetic material into host cells, influenced by their viral origin. Non-integrating vectors, like Adenoviral vectors (AdVs) (Wold & Toth, 2013) and adeno-associated vectors (AAVs) (McCarty et al, 2004), have limited integration efficiency, predominantly maintaining their genetic material in episomal form, which is gradually diluted during host cell proliferation. Conversely, integrating vectors, such as retroviral vectors (RVs) and lentiviral vectors (LVs), persist through cell divisions by reverse transcribing their RNA genome and integrating the DNA provirus into the host genome, making them well-suited for stable gene expression over time. Nevertheless, retroviral systems derived from the gammaretrovirus Murine Leukemia Virus showed limitations in transducing human HSCs due to their quiescent nature, characterized by reduced cell cycle activity during steady-state hematopoiesis (Cheshier *et al*, 1999; Passegué *et al*, 2005; Pietras *et al*,

2011). Consequently, HSCs required *ex vivo* culture for several days with multiple cytokines to induce cycling, potentially leading to a loss of self-renewal capacity. In contrast, lentiviral vectors emerged as a valuable alternative, as they efficiently transduce non-dividing cells, since they traverse nuclear pores by recruiting host cell proteins (Naldini *et al*, 1996; Miyoshi *et al*, 1998; Case *et al*, 1999).

To harness the full potential of LVs as carriers for gene therapy, extensive vector engineering aimed to preserve infectivity while removing non-essential genomic elements related to viral replication or pathogenicity. *Cis*-acting genomic viral elements are non-coding sequences that influence various processes, including nearby gene transcription and reverse transcription, replication, packaging, and provirus integration. In particular, efforts focused on the segregation of *cis*-acting sequences into distinct constructs (Follenzi & Naldini, 2001), that are co-transfected into producer cell lines to efficiently assemble viral particles, subsequently harvested and purified. In current vector constructs for viral vector production, viral proteins are expressed from plasmids devoid of packaging sequences. A separate transfer vector carries the packaging signal (Ailles & Naldini, 2002) and incorporates the gene of interest (GOI) alongside necessary regulatory elements, replacing viral genes.

To minimize the risk of generating replication-competent viruses, homologies between the transfer vector and packaging constructs are minimized. In the envelope construct, a strong Cytomegalovirus (CMV) promoter and a polyadenylation signal (polyA) take the place of viral long terminal repeats (LTRs), controlling the expression of the vesicular stomatitis virus glycoprotein (VSV.G), which confers a wide tropism for the LV (Follenzi & Naldini, 2001). The packaging construct houses the *gag* and *pol* genes, under CMV promoter control, alongside a polyA signal, and in third generation vectors another distinct construct is dedicated to encoding the *rev* gene (Ailles & Naldini, 2002). In modern self-inactivating (SIN) transfer vectors, essential components include modified LTRs lacking the U3 region, leading to LTR transcriptional inactivation, necessitating an unrelated promoter, like the Rous Sarcoma Virus (RSV) promoter, at the 5' end of the transfer vector plasmid for robust Tat-independent LV genome synthesis (Ailles & Naldini, 2002). U3 deletion significantly enhances LV biosafety by reducing the risk of oncogene activation due to the LTR enhancer's effects on neighboring genes. Additionally, SIN LVs exhibit a lower potential for vector mobilization and

recombination with wild-type viruses than non-SIN vectors (Bukovsky et al., 1999). Third generation improved SIN transfer vectors also feature the woodchuck hepatitis virus post-transcriptional regulatory element (WPRE) for improved post-transcriptional transgene expression via enhanced polyadenylation, and the central polypurine tract sequence (cPPT), facilitating nuclear translocation of the vector genome (Vigna & Naldini, 2000).

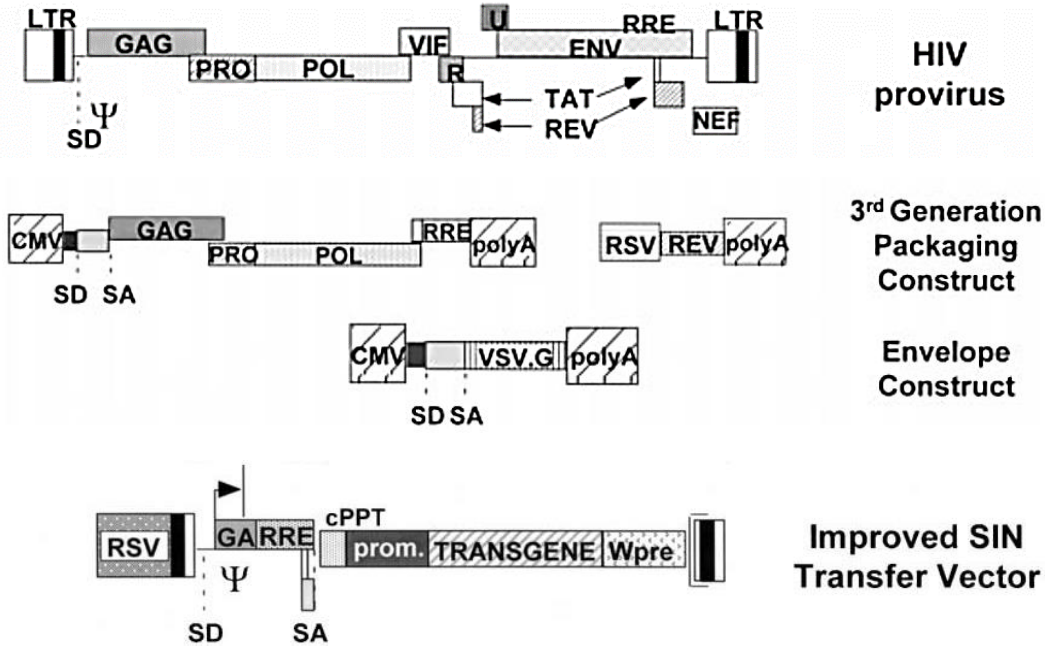


Figure 6. Schematic representation of third generation LV constructs
The envelope construct (Env) contains the CMV promoter, splicing donor (SD) and splicing acceptor (SA) sites, Vesicular Stomatitis Virus Glycoprotein (VSV.G), and a polyadenylation signal (polyA). The first packaging construct (Packaging-1) includes the CMV promoter, SD and SA sites, gag and pol genes, and a polyA signal. The second packaging construct (Packaging-2) encodes the rev gene under the control of the Rous Sarcoma Virus (RSV) promoter. The self-inactivating (SIN) transfer vector comprises the RSV promoter, 5' SIN long terminal repeat (LTR), SD and SA sites flanking the packaging signal (ψ), central polypurine tract (cPPT), transgene cassette (GOI), Woodchuck Hepatitis Virus Posttranscriptional Regulatory Element (WPRE), and 3' SIN LTR (Vigna & Naldini, 2000).

Adeno-associated viruses (AAVs) are a class of non-integrating single-stranded DNA viruses, which require helper viruses for replication and carry a genome of around 4.8 kb within a protein capsid. This genome includes three vital genes: *Rep* (responsible for replication), *Cap* (encoding capsid proteins), and *aap* (involved in assembly) (Li & Samulski, 2020). Key to their utility as delivery vectors is their tissue tropism, with twelve human AAV serotypes identified, each displaying distinct tissue preferences and with

engineered hybrid capsids to further broaden their potential applications. Although primarily non-integrating, AAVs can sporadically integrate, albeit with low efficiency, into specific genomic sites, such as the AAV integration site 1 (AAVS1) locus, particularly well-documented for AAV2 (Kotin *et al*, 1990; Samulski *et al*, 1991).

Recombinant AAVs (rAAVs) serve as versatile delivery vectors by preserving the 5' and 3' ITRs while replacing viral genes with a gene of interest controlled by an external promoter (Li & Samulski, 2020). As the viral counterpart, these engineered rAAVs persist as episomes in host cell nuclei. Consequently, transgenes delivered by rAAVs typically remain separate from the host DNA and gradually diminish with cell division, though random integration of rAAVs into cell genomes has been reported (Colella *et al*, 2018).

3.3.2 Nuclease-based editing

In recent decades, the field of gene therapy has seen significant advancements with the introduction of various programmable chimeric molecules for precise gene editing. Designer nucleases, including Zinc Finger (ZFN) (Urnov *et al*, 2005), Transcriptional Activator-Like Effector (TALEN) (Christian *et al*, 2010), and CRISPR-Cas nucleases (Jinek *et al*, 2012), are composed of a customizable DNA binding domain, which can be a protein domain or a guide RNA (gRNA), coupled with a catalytically active domain. They are designed to recognize specific target sequences and to induce DNA double-strand breaks (DSBs) upon successful binding. The resulting DNA DSBs activate various DNA repair pathways, leading to the permanent modification of the target site (Scully *et al*, 2019).

The repair of DNA after a DSB typically involves processes like non-homologous end joining (NHEJ) and microhomology-mediated end-joining (MMEJ), which can introduce small nucleotide insertions and deletions (indels) at the target site. This often disrupts the recognition by the DNA binding domain, achieving the desired genetic modification. Cells in the S/G2 cycle phases may employ high-fidelity homology-directed repair (HDR) when provided with a DNA template containing sequences homologous to the cut site (Ferrari *et al*, 2023). HDR allows for the precise integration of a new sequence into the genome, overcoming the limitations of integrating vectors. To facilitate HDR editing, exogenous DNA templates encoding for the corrective sequence must be supplied. This is achieved through the use of single-stranded or double-stranded DNA (ss/dsDNA)

oligonucleotides (Shy *et al*, 2023) or viral vectors like Integrase-Defective LV (IDLV) or Adeno-Associated viral Vectors (AAV), depending on the size of the intended edit (Genovese *et al*, 2014; Ferrari *et al*, 2022).

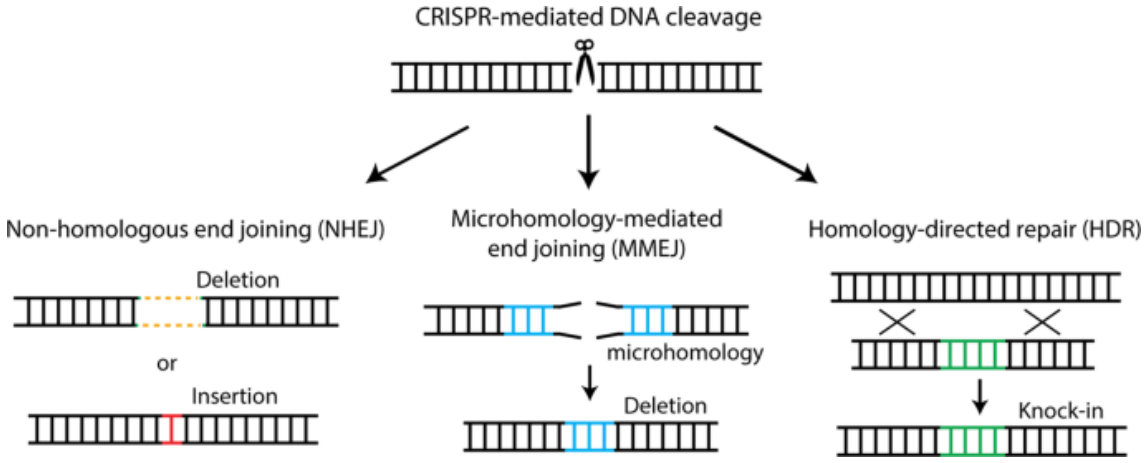


Figure 7. DNA double strand break repair pathways
Upon encountering a double-strand break (DSB) in DNA, cells employ different repair mechanisms. Homology-directed repair (HDR) utilizes a template, often a sister chromatid, to precisely restore the sequence. Microhomology-mediated end joining (MMEJ) involves rejoining broken ends that share short homologous sequences, resulting in small deletions. Non-homologous end joining (NHEJ) rejoins broken ends without requiring sequence homology, frequently leading to insertions or deletions. Adapted from Jang et al*, (2020).*

Eukaryotic cells have evolved a sophisticated mechanism, known as the DNA damage response (DDR), to address double-strand breaks (DSBs) that can be caused by various factors like exposure to radiation or chemicals (Scully *et al*, 2019). The DDR system involves multiple pathways that ultimately converge on the tumor suppressor protein p53. Activation of p53 plays a pivotal role in determining the cell's fate, whether it will survive, differentiate, undergo senescence, or apoptosis (Scully *et al*, 2019). Similarly, the introduction of a small number of nuclease-induced DSBs in HSPCs triggers a p53-dependent DDR, which diminishes their potential for reconstitution and reduces clonal diversity (Schiroli *et al*, 2019). Increasing DSBs, especially with less specific nucleases, results in an overwhelming DDR, triggering inflammation, cell cycle arrest, and apoptosis, thus significantly impairing HSPC clonogenic capacity. To address these challenges in therapeutic genome editing, optimizing nuclease specificity and temporarily inhibiting p53 has proven to minimize DDR induction and mitigate its consequences (Schiroli *et al*, 2019; Ferrari *et al*, 2020).

Advancements in designer nuclease technology and their refined delivery methods have empowered the precise and efficient editing of multiple target sites within human HSPCs (Wu *et al*, 2019; Demirci *et al*, 2020). However, the challenging task of integrating lengthy therapeutic sequences via homology-directed repair (HDR) is exacerbated by the limited cell cycling and slow progression typically observed in long-term repopulating HSCs. Despite significant efforts to enhance HDR efficiency through various means such as optimizing culture conditions (Genovese *et al*, 2014; Lattanzi *et al*, 2021; Charlesworth *et al*, 2022), promoting cell-cycle progression (Lomova *et al*, 2019; Ferrari *et al*, 2020; Shin *et al*, 2020), and selecting optimal delivery vehicles for the DNA template, efficient HDR editing remains challenging (Shy *et al*, 2023; Genovese *et al*, 2014; Schiroli *et al*, 2019; Ferrari *et al*, 2022). Conversely, strategies based on NHEJ-mediated mechanisms have demonstrated consistent and reproducible effectiveness in recent clinical trials targeting hemoglobinopathies. Notably, the first CRISPR-based therapy for the treatment of sickle-cell disease and β-thalassemia has recently been approved for clinical application, and others are anticipated to obtain regulatory approval in the near future (Frangoul *et al*, 2021; Wong, 2023).

3.3.3 Nickase-based editing

Base editors (BEs) and prime editors (PEs) represent newer genome engineering tools, consisting of a modified Cas-derived DNA binding domain, fused to enzymatic domains like deaminases (base editing) or reverse transcriptases (prime editing) (Anzalone *et al*, 2020). Importantly, BEs and PEs offer the advantage of eliminating the need for DNA double-strand breaks (DSBs) and cell-cycle phase restrictions.

BE are constructed by modifying the Cas nuclease to reduce its activity, and then fusing it with a DNA deaminase enzyme. When this modified Cas nuclease binds to the target DNA, it forms a structure called an R loop, which exposes specific nucleotides to the DNA deaminase enzyme's activity. Cytosine base editors (CBEs) employ cytidine deaminases to transform cytosines into uracils, which are read as thymines by DNA polymerases. This effectively converts C•G base pairs into T•A base pairs (Komor *et al*, 2016). However, these uracil intermediates can be removed by Uracil DNA N-glycosylase, leading to the restoration of the original sequence through the base excision repair pathway. To improve the efficiency and accuracy of editing, CBEs include uracil

glycosylase inhibitor proteins (UGIs), which elevate the presence of uracil at the target locus (Anzalone *et al*, 2020).

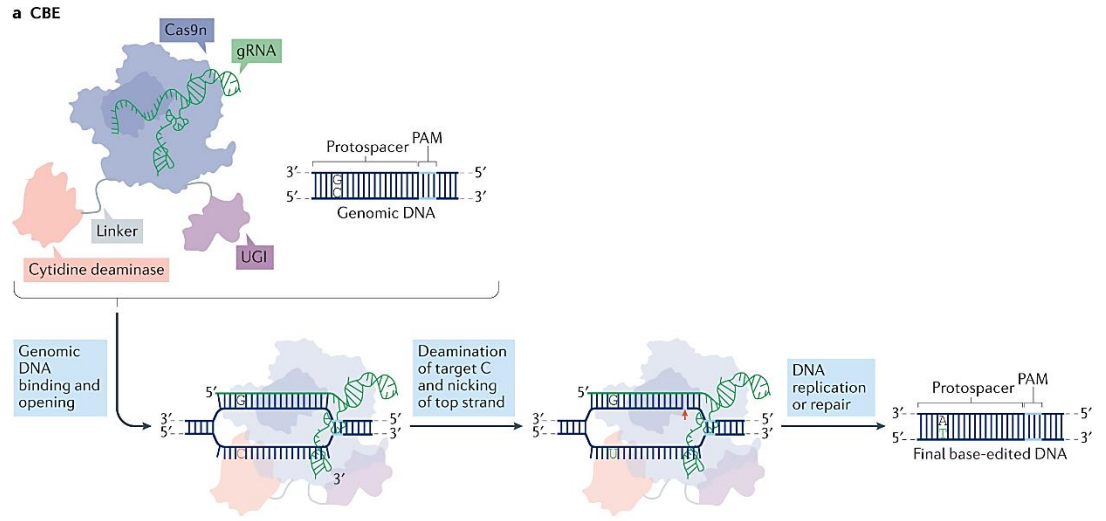


Figure 8. Cytosine base editing mechanism.
Cytosine base editing involves the targeted conversion of cytosine (C) to uracil (U) within the DNA sequence. The cytosine deaminase induces a C-to-U conversion, creating a U-G mismatch. Cellular repair mechanisms then replace the mismatched base with thymine (T), resulting in the final edited DNA sequence. To prevent unintended base excision repair, the uracil glycosylase inhibitor (UGI) inhibits the removal of the uracil base. Adapted from Porto et al*, (2020).*

Conversely, adenine base editors (ABEs) use the *Escherichia coli* adenosine deaminase TadA to convert adenosines into inosines, which are read as guanines by the repair machinery, converting A•T pairs to G•C (Gaudelli *et al*, 2020). The most recent ABEs, such as ABE8e, use a modified TadA domain generated by directed evolution to increase efficiency while decreasing bystander editing (Richter *et al*, 2020).

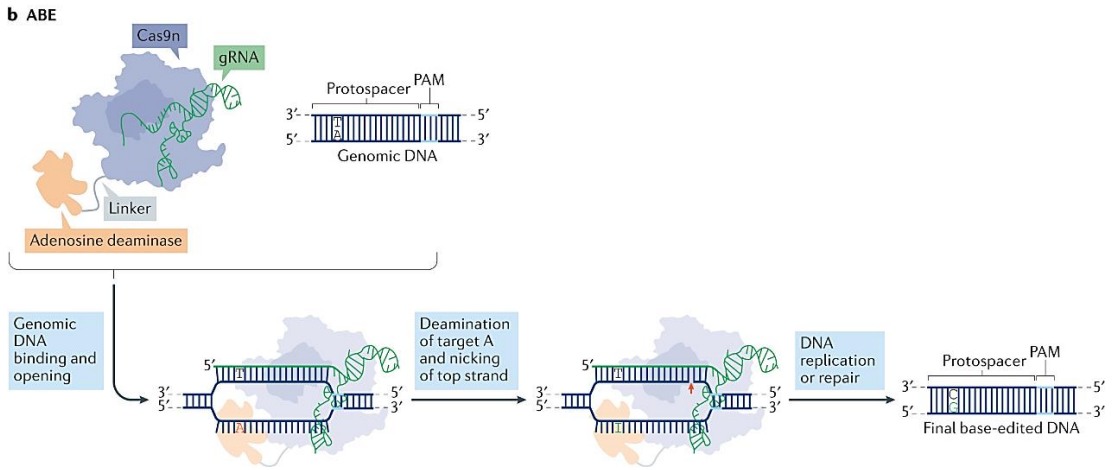


Figure 9. Adenine base editing mechanism.

During adenine base editing, adenosine deaminase domain induces the formation of an inosine (I) intermediate, which is recognized as guanine by DNA repair mechanisms eventually results in the A-to-G replacement. Adapted from Porto et al*, (2020).*

To enhance the efficiency of base editing, many base editors employ a Cas nickase, rather than a dCas DNA-binding protein. This Cas nickase induces a nick in the non-deaminated DNA strand, triggering cellular repair using the deaminated strand as a template for resynthesis (Anzalone *et al*, 2020). This approach ensures that both target DNA strands undergo editing, resulting in a stable conversion of the target base pair. Furthermore, refinements, including linker optimization, integration of a nuclear localization sequence, and codon optimization, have significantly elevated editing efficiencies in mammalian cells and *in vivo* (Anzalone *et al*, 2020; Liu *et al*, 2022).

In various genome editing applications, especially those focused on correcting or introducing specific mutations in mammalian genomes, precise alterations such as point mutations, or small insertions and deletions are required. While base editors introduce transition point mutations without causing DSBs, they currently lack the ability to create transversion point mutations (e.g. C•G-to-G•C, C•G-to-A•T, T•A-to-G•C, and T•A-to-A•T,), and precise insertions or deletions. A more recent genome editing technology called prime editing overcomes these limitations by allowing the introduction of all 12 possible types of point mutations, as well as small insertions and deletions. Prime editors are fusion proteins that combine three elements: i) a nickase Cas9 domain; ii) an engineered prime editing gRNA (pegRNA), which specifies the target site in its spacer sequence and encodes the desired edit in a overhang at the 3′ end; iii) and a reverse transcriptase domain that that converts the pegRNA sequence into a DNA edit (Anzalone *et al*, 2019). While there is promise in prime editing (PE), its efficacy in primary cells remains modest and exhibits considerable variability among distinct genomic loci and cell types (Kim *et al*, 2021). Multiple approaches have been devised to enhance its efficiency, including the utilization of a modified prime-editing protein, refining the design of prime-editing guide RNA, manipulating the mismatch repair pathway, and optimizing the delivery strategy (Nelson *et al*, 2022; Zhao *et al*, 2023). On the other hand, this technology remains limited to short-range edits and correction of individual mutations.

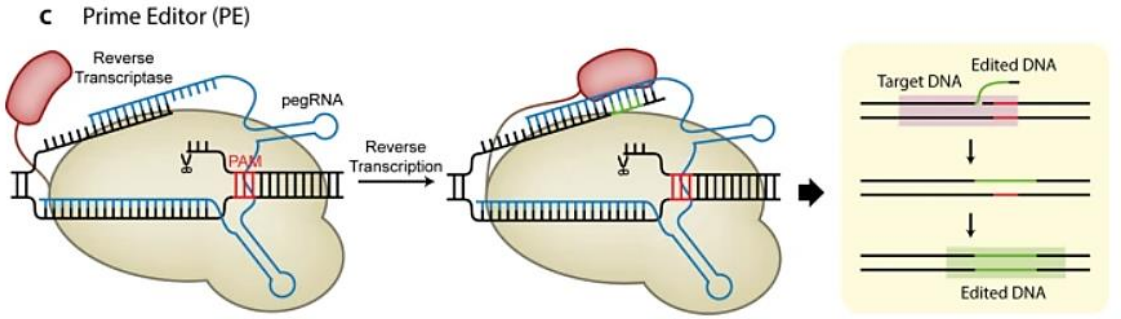


Figure 10. Prime editing mechanism.
The pegRNA directs the nCas9-RT complex to the target site, where the reverse transcriptase synthesizes a new DNA strand with the desired edit. The newly synthesized strand then replaces the original strand, resulting in the precise incorporation of the edit. Adapted from (Anzalone et al*, 2020)*

3.3.4 Transient overexpression

The rapid advancements within the realm of mRNA engineering and non-viral mRNA delivery have yielded a multitude of strategies to confront the complex issues associated with the clinical utilization of mRNA. Challenges encompassing mRNA translatability, stability, and the potential for immunostimulation can be effectively addressed through the integration of innovative mRNA designs. Furthermore, mRNA delivery systems have emerged as a viable solution to tackle some of the intricacies related to mRNA transportation (Huang *et al*, 2022). A functional approach to designing these delivery systems necessitates the protection of mRNA molecules against nuclease-driven degradation, successful navigation through various biological barriers, and the efficient transport of mRNA into the cytoplasm, ultimately ensuring robust protein expression.

Synthetic *in vitro* transcribed (IVT) mRNAs closely resemble naturally occurring mature eukaryotic mRNAs and comprise five key elements: i) a 5' cap, ii) a 5' untranslated region (UTR), iii) an open reading frame (ORF) encoding the protein of interest, iv) a 3' UTR, and v) and a poly(A) tail (Tusup *et al*, 2019). Optimizing these components can enhance translation efficiency and mRNA stability. For instance, employing poly(A) tails longer than 100–150 nucleotides can enhance mRNA stability and improve the efficiency of translation initiation by interacting with poly(A) binding proteins (Passmore & Coller, 2022). Moreover, the design of the 5′ cap offers an alternative approach to mitigate undesirable immunological responses triggered by mRNAs. The primary cap, known as Cap 0, consists of a 7-methylguanosine (m7G) nucleotide linked to the RNA through a 5'-5'-triphosphate bridge (Ramanathan *et al*, 2016). Commonly, this is further modified

to Cap 1, where the first mRNA base undergoes an additional 2' methylation. Cap 1 offers advantages such as increased mRNA stability and enhanced recruitment of the eukaryotic initiation factor 4E (eIF4E), facilitating translation initiation (Ramanathan *et al*, 2016). Two main methods are employed for capping mRNAs *in vitro*: co-transcriptional capping and post-transcriptional capping. Co-transcriptional capping incorporates cap analogs, anti-reverse cap analogs (ARCA), or Cap trinucleotides (CleanCap from Trilink) into the transcription process to ensure the desired cap structure from the start (Henderson *et al*, 2021). In contrast, post-transcriptional capping uses enzymes like the vaccinia virus capping enzyme to add or modify caps after transcription. The choice of capping method depends on experimental requirements and the desired mRNA properties.

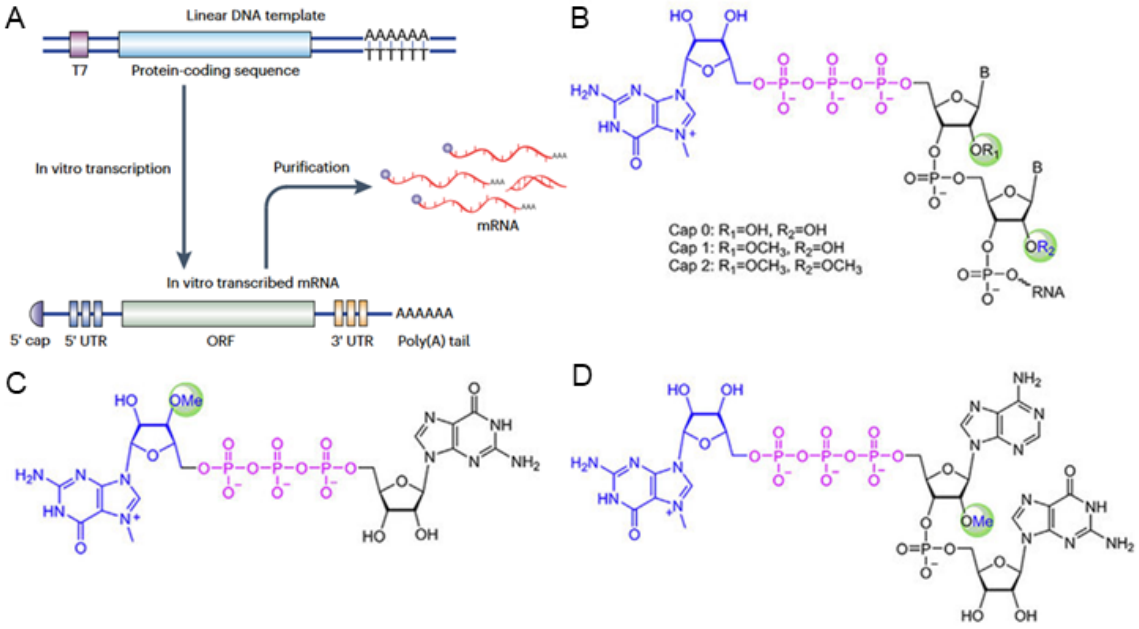


Figure 11. mRNA capping and* in vitro *transcription.
A) In vitro *transcription pipeline from DNA template to mRNA.* ***B)*** *Eukaryotic cap structures and their categorization into Cap 0, Cap 1, and Cap 2 based on the presence of 2'-O-methyl groups at residues R1 and R2.* ***C)*** *The structure of an ARCA Cap0 Dimer.* ***D)*** *The structure of CleanCap AG Cap1 Trimer. Adapted from Ramanathan* et al*, (2016)*

In the clinical application, the effective use of mRNA for therapeutic purposes hinges on two critical objectives: achieving robust mRNA translation within target cells and mitigating unwanted immune responses. Therapeutic mRNA synthesis employs *in vitro* transcription within a cell-free system, in which an RNA polymerase like T3, T7, or SP6 initiates mRNA production starting from a linear DNA template derived from PCR or digested plasmid (Tusup *et al*, 2019). Afterward, conventional laboratory-scale

purification methods are utilized, though they often fall short in completely eliminating impurities like double-stranded RNA and RNA fragments, which can lead to reduced therapeutic efficacy and unintended biological reactions. Therefore, additional steps of purification are often required for clinical-grade mRNA synthesis. Moreover, exogenous mRNA possesses immunostimulatory potential that poses a significant hurdle to clinical translation (Rohner *et al*, 2022). Pattern recognition receptors (PRRs) detect exogenous mRNA, akin to viral RNA, triggering an immune response. Activation of these PRRs leads to the production of type I interferons (IFNs) and proinflammatory cytokines, ultimately hindering mRNA translation (Tusup *et al*, 2019). Notably, pioneering work by Karkikó and Weissman on nucleoside modifications enabled clinical translation in the context of mRNA-based vaccination and was recently awarded with the Nobel Prize (Karikó *et al*, 2005; Anderson *et al*, 2010).

Another critical point for mRNA therapeutics is the delivery – either *ex vivo* or *in vivo* – which is also tangled with efficiency, toxicity and biodistribution issues. Today, the introduction of recombinant proteins or gene editors into HSPCs *ex vivo* is mainly accomplished through electroporation, which allows the delivery of either IVT mRNAs encoding for the gene editors or pre-assembled ribonucleoprotein complexes (RNPs) into HSPCs. However, electroporation is associated with high stress levels and can induce p53 activation, thus limiting prolonged and repeated action (Schiroli *et al*, 2019; Ferrari *et al*, 2022). To address these limitations, alternative delivery methods are emerging, including polymer-based nanoparticles (El Kharrag *et al*, 2021) or lipid nanoparticles (LNPs) that encapsulate RNA or RNPs (Rohner *et al*, 2022; Vavassori *et al*, 2023). These approaches hold the potential for reduced toxicity and enhanced flexibility in delivering genome editors to HSPCs both *ex vivo* and *in vivo*.

3.4 Conditioning

Conditioning is employed to create space within the niche for the engraftment of donor HSPCs. These conditioning regimens are customized to address distinct goals, including anti-tumoral effects, immune suppression, central nervous system penetration, and the required level of myeloablation for effective chimerism, depending on the specific disease. The extent to which the niche is vacated correlates with the conditioning regimen intensity. With fully myeloablative conditioning, most resident cells are eliminated from

the niche, facilitating substantial engraftment of infused cells. In contrast, with milder conditioning, not all resident cells are removed, leading to a competitive process between endogenous and infused HSPCs for engraftment.

While chemotherapy is essential for preparing the BM niche for HSC infusion, it also inadvertently harms the stromal cells within the niche. This damage can potentially impair the BM's ability to efficiently attract and host the transplanted HSCs. Furthermore, the molecular signals generated by localized BM injury, alongside with reduced production and release of blood cells, can stimulate HSC proliferation and expedite hematopoietic reconstitution. Nevertheless, it is crucial to recognize that these cytotoxic regimens lack specificity, ultimately leading to a spectrum of short- and long-term off-target side effects, including symptoms like nausea, vomiting, secondary tumors, multi-organ damage, and infertility. The impact of conditioning regimens can significantly differ based on their intensity and mechanism of action, categorizing them as either myeloablative or non-myeloablative, depending on whether they completely or partially eliminate resident HSPCs.

3.4.1 Myeloablative conditioning

3.4.1.1 Total body irradiation

Total body irradiation (TBI) occupies a pivotal role within myeloablative conditioning (MAC) regimens, particularly in the context of HSCT. Historically, TBI, when combined with cyclophosphamide, has stood as the gold standard conditioning regimen for patients afflicted with acute leukemia prior to embarking on the HSCT journey. Conventionally, a dose of 12 Gy TBI has been the established norm (Thomas *et al*, 1982). While there has been exploration into higher TBI doses, reaching up to 14.25 Gy, the advantages were counterbalanced by heightened toxicity and an escalation in transplant-related mortality (Clift *et al*, 1990). TBI serves a dual purpose, offering both myeloablative (MA) and immunosuppressive properties, thereby ensuring the successful engraftment of HSCs. This therapeutic modality achieves uniform dose distribution throughout the entire body, encompassing anatomical sanctuaries like the central nervous system. Over time, the standard protocol has evolved to involve fractionating the 12 Gy TBI into six doses of 2 Gy, administered twice daily over a 3-day period (Thomas *et al*, 1982). Recent insights from the European Society for Blood and Marrow Transplantation (EBMT) have

illuminated that the modality of dose fractionation and its delivery rate have emerged as critical determinants affecting both therapeutic efficacy and associated toxicity (Belkacemi *et al*, 2018). TBI complications encompass a spectrum, ranging from mucositis and interstitial pneumonia to sinusoidal obstruction syndrome/veno-occlusive disease (SOS/VOD), hemorrhagic cystitis, and the emergence of long-term side effects such as growth retardation, endocrine disruptions, cataracts, and secondary malignancies.

3.4.1.2 Chemotherapy-based conditioning

MAC regimens, widely employed in both autologous (auto-) and allogeneic (allo-) HSCT, are characterized by their reliance on high-dose chemotherapy and predominantly based on alkylating agents. These regimens are notable for their ability to induce profound and prolonged cytopenia, often spanning up to 21 days, necessitating the infusion of stem cell grafts to expedite hematopoietic recovery (Bacigalupo *et al*, 2009). Among the historically prominent MAC regimens, busulfan/cyclophosphamide (BU/CY) serves as an archetype of chemotherapy-based conditioning. As early as 1987, the Johns Hopkins group developed this protocol with the goal of reducing long-term radiation-induced toxicities and simplifying HSCT planning, especially in medical facilities lacking access to specialized instruments (Tutschka *et al*, 1987). Over the years, numerous studies demonstrated the comparability of BU/CY and CY/TBI regimens in the context of allo-HSCT for the treatment of ALL (Mohty *et al*, 2010) and AML (Nagler *et al*, 2013). The introduction of intravenous BU, characterized by a more predictable pharmacokinetics, enabled a more precise control of plasma levels, thereby reducing the necessity for plasma testing and dose adjustments. This significant advancement substantially reduced BU-associated SOS/VOD and transplant-related mortality (Nagler *et al*, 2013).

In the pursuit of further diminishing regimen-related toxicity, certain MAC regimens replaced cyclophosphamide with fludarabine (FLU), a nucleoside analog known for its noteworthy immunosuppressive properties and synergistic effects with alkylating agents due to its inhibitory impact on DNA repair mechanisms. The combination of BU and FLU exhibited a more favorable toxicity profile while maintaining comparable efficacy. In a recent study comparing BU/FLU to BU/CY, a significant reduction in transplant-related mortality was observed in the BU/FLU arm, without discernible difference in relapse incidence (Rambaldi *et al*, 2015). Additionally, recent endeavors have incorporated other

alkylators such as clofarabine (Chevallier *et al*, 2012) and treosulfan (Eder *et al*, 2017) into MAC protocols for ALL and AML, aiming to mitigate the relapse incidence while achieving outcomes comparable to TBI-based conditioning regimens.

3.4.2 Non-myeloablative conditioning

In the past two decades, non-myeloablative and reduced-intensity conditioning (RIC) regimens have gained substantial recognition and acceptance in the field of HSCT. Their primary objective is to alleviate organ toxicity and reduce transplant-related mortality, thereby broadening the accessibility of HSCT to elderly and medically frail patients who would otherwise not qualify for conventional myeloablative conditioning (Slavin et al., 1998). Furthermore, a category of regimens referred to as reduced-toxicity conditioning has been developed. These regimens are characterized by the use of fludarabine and less myeloablative alkylating agents, aiming to facilitate the safe administration of high-dose therapy. To systematically classify conditioning regimen intensity, an expert panel endeavored to predict the duration and reversibility of cytopenia following HSCT (Bacigalupo *et al*, 2009). Based on this classification, MAC has been defined as a regimen that induces mostly irreversible cytopenia, while non-myeloablative regimens result in minimal cytopenia. RIC regimens, in contrast, lead to profound cytopenia although it may not always be irreversible. Effective RIC creates sufficient room for donor stem cells to engraft and commence their function. Nevertheless, the use of lower doses in RIC regimens increases the likelihood of incomplete stem cell replacement when contrasted with MAC.

The overall outcome comparison between these low-intensity conditioning protocols and MAC hinges on the net effect of opposing factors. These factors include a reduction in transplant-related mortality and an increase in the relapse incidence, ultimately resulting in similar rates of leukemia-free survival and overall survival. Patient age, comorbidities, and disease status at the time of transplantation are pivotal determinants of prognosis. reduced-toxicity conditioning regimens generally offer more potent activity while minimizing toxicity, making them better suited for patients who are ineligible for myeloablative conditioning (Shimoni *et al*, 2018). Within this category, novel conditioning protocols have emerged, although a consensus on their classification has yet to be reached. These regimens incorporate agents such as clofarabine and thiotepa, with

the TBF regimen (thiotepa, busulfan, fludarabine) standing out as particularly noteworthy (Saraceni *et al*, 2018).

3.4.3 Antibody-based conditioning

The remarkable specificity of monoclonal antibodies has been extensively explored for the purpose of selectively eliminating specific cell populations. In this context, non-genotoxic conditioning aims to create space within the BM niche without resorting to conventional chemotherapy regimens, selectively removing host HSCs. Instead, it employs safer drugs that specifically target HSPCs while sparing non-hematopoietic cells. For instance, the ubiquitous CD45 marker plays a pivotal role in immune cell function, with mutations having severe implications, including severe combined immunodeficiency (SCID). Antibody-drug conjugates (ADCs) targeting CD45 have demonstrated the ability to deplete the white blood cell compartment (Palchaudhuri *et al*, 2016). When administered to mice before HSCT, this approach led to hematopoietic reconstitution comparable to TBI but with fewer side effects. Furthermore, it facilitated faster T-cell repopulation, potentially by protecting the thymic stroma from radiation damage (Palchaudhuri *et al*, 2016).

Another strategy focuses on targeting the c-KIT receptor (CD117), whose expression is restricted to HSPCs and that plays a vital role for HSPC function. Antibody-mediated blocking of c-KIT, owing to its significance in HSPC retention and maintenance, can effectively deplete murine HSPCs *in vivo*, allowing for the establishment of donor chimerism levels of up to 90% after HSCT (Czechowicz *et al*, 2007). Similar outcomes have been replicated in non-human primates (NHPs) and are currently being evaluated in humans, particularly within the context of HSCT for severe combined immunodeficiencies (NCT02963064) (Kwon *et al*, 2019). When coupled with a toxin like saporin, anti-c-KIT antibodies exhibit increased efficacy, resulting in over 99% depletion of host HSPCs and facilitating rapid and efficient engraftment of donor HSCs (Czechowicz *et al*, 2019). However, a patient treated with a c-KIT antibody-conjugated with amanitin toxin tragically experienced severe adverse effects leading to death, resulting in the discontinuation of the clinical trial and highlighting the need for further validation.

Recently, Casirati and colleagues introduced an intriguing approach for the treatment of AML. They devised a method to modify epitopes on donor HSPCs employed in BM transplantation, rendering them selectively resistant to chimeric antigen receptor T cells (CAR-T) or monoclonal antibodies, all the while preserving the function and regulation of essential proteins (Casirati *et al*, 2023). This innovation facilitates the targeting of crucial leukemia-survival genes, reducing the risk of immune escape by the tumor. Leveraging epitope mapping and library screenings, they pinpointed amino acid alterations that disrupt the binding of therapeutic monoclonal antibodies directed against KIT. These modifications were seamlessly integrated into CD34+ HSPCs via a base-editing technique, ensuring engraftment and the potential for multilineage differentiation (Casirati *et al*, 2023), although raising concerns about the immunogenic potential that still need to be investigated.

As the fine-tuning of pharmacokinetics and pharmacodynamics for ADC and testing of base editing in HSPCs progress to ensure safe and effective clinical application, the scope of their utilization in HSCT conditioning may expand to encompass a wider array of medical indications.

3.4.4 Graft-versus-host disease and immunosuppression

Graft-versus-host disease stands as the most life-threatening complication following allo-HSCT. This condition arises when recipient T cells perceive the host's tissues as foreign entities. Despite a history spanning 50 years and nearly half a million procedures conducted worldwide, GvHD continues to pose the most difficult challenge for healthcare professionals in their daily practice. In total, approximately 30–50% of patients undergoing allo-HSCT will experience acute GvHD, with around 15% developing severe forms (grades III–IV) (Jacobsohn & Vogelsang, 2007). Notably, the prior occurrence of acute GvHD is the primary risk factor for the subsequent development of chronic GvHD.

The utilization of immunosuppressive strategies preempts the onset of acute GvHD since the prevention of chronic GvHD essentially hinges on the effective mitigation of the acute phase. These agents include frequently used drugs like sirolimus, tacrolimus, cyclosporine, abatacept, and mycophenolate mofetil, all of which inhibit T cell activation (Santos *et al*, 1983). Several of these agents have demonstrated efficacy in preclinical and clinical studies aimed at preventing and suppressing immune responses to foreign

transgenes. For instance, post-transplant administration of cyclosporine in dogs infused with GFP-transduced HSPCs, effectively prevented the development of immune reactions against transgene products (Beagles *et al*, 2005). Similarly, the addition of Sirolimus (inhibitor of mammalian target of rapamycin - mTOR) and Abatacept (CTLA4-Ig) to busulfan conditioning allowed the engraftment of GFP-transduced cells in rhesus macaques (Uchida *et al*, 2019).

While immunosuppressive drugs were able to temporarily prevent the development of immune responses in unprimed hosts, they proved ineffective in averting immune responses in animals with preexisting anti-transgene immunity (Berger *et al*, 2001). These findings have implications for gene therapy targeting HSCs, particularly in disorders where patients may have preexisting immunity to the transgenic protein due to enzyme replacement therapy (Drysdale *et al*, 2020). Furthermore, in studies where immune responses to foreign transgenes were successfully suppressed using immunosuppressive drugs, occasional responses emerged upon discontinuation of drug administration (Uchida *et al*, 2019; Drysdale *et al*, 2020). Consequently, conventional immunosuppressive regimens may not be adequate for inducing long-term tolerance to certain transgenes, although adjustments in drug dosage and duration could potentially achieve this objective.

3.5 Animal models to study HSPC-GT

3.5.1 Xenograft mouse models

In 1988, John Dick's team pioneered the transplantation of human BM-derived hematopoietic cells into C.B-17 SCID mice, establishing the first hematochimeric mouse model for human hematopoiesis (Kamel-Reid & Dick, 1988). However, human cell engraftment was short-lived and limited to a few myeloid progenitors. Infusing human interleukin 3 (IL-3), granulocyte-macrophage colony-stimulating factor (GM-CSF), and SCF cytokines into C.B-17 SCID mice with human BM-derived cells resulted in lymphoid and myeloid reconstitution by "immature human cells" (Lapidot *et al*, 1992). Yet, engraftment remained transient due to functional host NK cells, macrophages, and granulocytes.

Enhanced human engraftment was achieved by breeding C.B-17 SCID mice with non-obese diabetic (NOD) mice (Shultz *et al*, 1995), which lacked functional NK cells, macrophages, had an impaired complement system and a Signal Regulatory Protein α (SIRP1α) variant cross-reacting with the human Cluster of Differentiation 47 (CD47) molecule, thus inhibiting phagocytosis of human cells. Despite improved chimerism in the NOD/SCID model, challenges included limited human B/T cell maturation and a high incidence of thymic lymphoma, hindering long-term studies. Crossing mice homozygous for interleukin-2 receptor γ-chain (*IL2rg*) gene mutations with NOD/Shi-SCID or NOD/LtSz-SCID mice yielded NOG or NSG mice, respectively. NOG and NSG mice completely lack murine B, T, and NK cells, supporting long-term human cell engraftment (Goyama *et al*, 2015). NSG mice are now the primary immunodeficient model for human HSPC xenotransplantation.

Nevertheless, obstacles emerge as a result of the suboptimal interaction between human receptors on HSCs and murine cytokines in the BM niche, and the aging process in mice, causing declining human engraftment after six months in NSG mice. Strategies to address this include: (i) Supplementing mice with human recombinant proteins; (ii) *In vivo* lentiviral gene delivery of human cytokines; (iii) Hydrodynamic injection of plasmid DNA encoding human cytokines (Rongvaux *et al*, 2013); (iv) Transgenic mice expressing human cytokines SCF, GM-CSF, and IL-3 (NSGS mice) (Wunderlich *et al*, 2018); (v) Replacing murine cytokine genes with human counterparts (MISTRG mice), which also express human SIRP1α (Rongvaux *et al*, 2014).

Regardless of the mouse strain used, sub-lethal irradiation is typically required to create space in the recipient mice's BM for robust human cell engraftment. However, employing irradiation in the NSG model poses a risk of organ and tissue damage, including the BM microenvironment. In contrast, the NSGW41 (non-irradiated *NOD.Cg-Kit^{W41J} Prkdc^{scid} Il2rg^{tm1Wjl}*, Cosgun *et al*, 2014) and NBSGW (nonirradiated *NOD.Cg-Kit^{W41J} Tyr^{+} Prkdc^{scid} Il2rg^{tm1Wjl}*, McIntosh *et al*, 2015) mouse models, generated by crossing NSG mice with C57BL/6 mice harboring a hypomorphic mutant *c-Kit* allele (W41), achieve human cell chimerism levels comparable to NSG mice without the necessity for irradiation. As previously mentioned, c-Kit is crucial for normal hematopoiesis, and viable mutants closely resemble aplastic anemia (Geissler et al., 1981). Therefore, mouse hosts with *c-Kit* mutations confer a competitive advantage for

wild-type donor cells, enabling the engraftment of hematopoietic stem cells (HSCs) with reduced or no irradiation (Waskow *et al*, 2009; Cosgun *et al*, 2014). Additionally, these models facilitate robust multilineage engraftment of human hematopoietic cells and the production of human erythroid cells, expanding opportunities for investigating the functionality of hematopoietic stem and progenitor cells (HSPCs) *in vivo* (McIntosh *et al*, 2015). Notably, recent studies indicate that NBSGW mice outperform NSG mice as engrafters for specific samples (as in myelodysplasic syndrome cells, Schmitt *et al*, 2022), opening up possibilities for specialized research applications such as patient-derived xenograft models.

3.5.2 Non-human primates

Although mice offered an invaluable starting point as small animal models to establish preliminary proof-of-concepts, they still have considerable limitations in reproducing the nuances of human BM biology, homing of modified stem cells, engraftment capability and kinetics, and immune-mediated complications after transplantation. This leaves substantial knowledge gaps around safety, efficacy, and long-term outcomes that pose risks when progressing rapidly to clinical trials without sufficient animal model data.

In contrast, non-human primates (NHPs) like rhesus (*Macaca mulatta*) and pigtail (*Macaca nemestrina*) macaques have proven invaluable as preclinical models to enable translation of HSC gene therapies to the clinic. Both species offer close homology to human physiology, providing more predictive data on safety and efficacy compared to rodents alone. Rhesus macaques have a long history stretching back to the 1990s as foundational models to establish gene transfer methods into HSCs (Kohn *et al*, 1987; Dunbar *et al*, 1996; Lozier *et al*, 1999). Their larger size can also be advantageous for certain research procedures. However, rhesus also harbor limitations including viral infections like Herpes B that can confound results, high cost, limited availability, and more challenging animal handling (Abee, 2012). In contrast, the emerging pigtail macaque model offers favorable characteristics as an alternative species for HSC gene therapy development. Pigtails are smaller and easier to handle, lacking problematic viruses complicating some rhesus studies (Abee, 2012). Additionally, pigtails possess specific mutations in TRIM5α that allow HIV infection, making them uniquely valuable models for HIV cure research and gene transfer studies based on lentiviral infection

(Trobridge *et al*, 2008). However, pigtails have not yet been characterized to the same extensive degree as rhesus across broad areas of genomics, virology, and previous gene therapy experiments.

Collectively, NHPs remain critical for fine-tuning HSC gene therapies to maximize safety and avoid pitfalls before reaching human patients. Their close mimicry of the critical aspects of human hematopoiesis and HSC transplant, enable more comprehensive evaluation and enhancement of gene therapies preclinically. Similarities span the cell types comprising primate and human BM, proliferation kinetics, cytokine profiles in the stem cell niche, and orchestration of engraftment of donor cells by the adaptive immune system (Shepherd *et al*, 2007; Radtke *et al*, 2016). These characteristics underpin the utility of NHPs to illuminate the intricacies of homing, sustained repopulation, lineage-specific differentiation, and *in vivo* selection of gene-edited HSC clones.

The ability to closely evaluate multi-lineage engraftment, kinetics, duration, safety, and efficacy of gene-modified grafts in macaques builds greater confidence than mice alone for clinical translation. Testing different vector constructs, conditioning intensities, donor sources, cell doses, immunosuppressive combinations, and other variables allows customization and process improvements to maximize engraftment success and avoid adverse outcomes like graft failure or excessive toxicity. Potential obstacles may also emerge, such as impacts of pre-existing anti-vector immunity on transduction efficacy. Interestingly, a recent work by Abraham et al. explored the impacts of different conditioning regimens on engraftment and clonal dynamics of gene-modified HSCs in NHP. Three primates received autologous CD34+ cells genetically modified *ex vivo* with barcodes after busulfan conditioning, and barcode tracking over 2 years showed substantially lower engraftment compared to historical data on TBI conditioning (Abraham *et al*, 2023). Notably, the clonal kinetics differed, with fluctuating waves of clones that took longer to stabilize versus early fixed clonal patterns after TBI (Abraham *et al*, 2023). These results highlight that conditioning intensity significantly influences levels and longevity of gene-modified HSC engraftment. Moreover, this busulfan-induced longitudinal clonal evolution mirrored previous clinical findings (Biasco *et al*, 2016), corroborating the value of NHPs to model patient outcomes and thus suggesting that detailed testing in macaques can address unanswered questions from mouse experiments, providing pivotal data to guide successful design of human clinical trials.

Nevertheless, limitations persist in directly extrapolating NHP outcomes to humans, including subtle differences in immune function, animal-to-animal variability, and logistical barriers to BM access. Though overall, macaques currently represent the most practical and powerful animal model option for accurately modeling human HSC gene therapy to the greatest degree possible at the preclinical stage. Their use critically de-risks the path to clinical translation and improves the likelihood of safety and efficacy when these curative therapies reach patients.

4 AIM OF THE WORK

The demands for HSPC transplantation are expected to escalate in tandem with the aging global population, with advances in gene therapy, and with the exploration of HSC-GT in new therapeutic indications. Yet, the adverse effects of myeloablative conditioning represent one of the main limitations, resulting in stromal cells damage, localized inflammation, and impairment of BM capacity for optimal recruitment and retention of the infused HSCs (Bacigalupo *et al*, 2009; Carreras *et al*, 2019). Moreover, since these cytotoxic regimens lack specificity, they give rise to a range of short- and long-term off-target adverse effects, thus reducing safety and limiting a broader application of HSC-GT (Gyurkocza & Sandmaier, 2014). However, when the conditioning is milder, engraftment becomes a competitive process between endogenous and infused HSPCs (Socie *et al*, 1995; Walters *et al*, 2001; Andreani *et al*, 2011; Magnani *et al*, 2020).

Here we aim to develop a non-genotoxic conditioning protocol by exploiting transient overexpression of engraftment enhancers that would lower the burden of HSCT, ultimately broadening the applicability of HSPC-GT to a plethora of diseases.

To achieve this aim, we will:

1. Develop in mice a robust HSPC mobilization protocol as conditioning strategy to vacate BM niches and allow engraftment of donor cells.
2. Validate the therapeutic potential of mobilization-based conditioning for the treatment of Hyper IgM syndrome by HSCT in the mouse model.
3. Translate these principles to human CD34+ cells assayed in the human hematochimeric mouse model.
4. Optimize a platform for mRNA *in vitro* transcription to allow a robust but transient overexpression of CXCR4 and other engraftment enhancers in donor cells.
5. Combine the transient overexpression of CXCR4 with gene and base editing.
6. Investigate the potential further advantages conferred by transient overexpression of mobilizer-resistant CXCR4 variants.
7. Translate our strategy in the clinically relevant non-human primate animal model.

5 RESULTS

5.1 Long-term donor chimerism is established by mobilization-based HSCT

We posited that mobilization regimens, which induce the egress of resident HSPCs from the BM, might also create space for newly transplanted cells. Hence, transplanting HSPCs at the peak of mobilization could allow competition with mobilized recipient cells for BM niche repopulation, establishing donor chimerism (Figure 12A). We evaluated two mobilization regimens in mice, one resembling a clinically approved protocol using G-CSF and AMD3100 (G7A) and the other including BIO5192 (G7AB). C57BL/6J CD45.2 mice received G-CSF via a subcutaneous pump for a week along with AMD3100 with or without BIO5192 intraperitoneally on days 6 and 7 (Figure 12B).

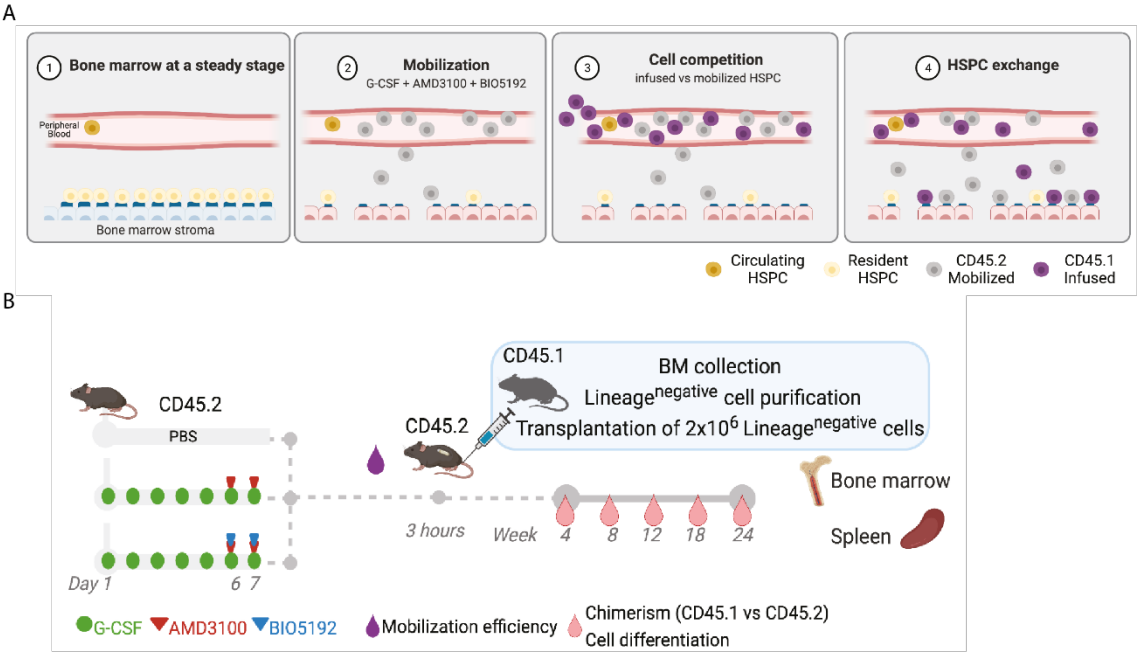


Figure 12. Mobilization-based conditioning strategy and experimental model. *A) Schematic of the M-HSCT strategy, illustrating the proposed exchange between mobilized recipient CD45.2 (in gray) and donor CD45.1 cells (in purple).* ***B)*** *Schematic of the M-HSCT protocol. Recipient CD45.2 mice were mobilized with G-CSF (green dots) and AMD3100 (red triangle), with and without BIO5192 (blue triangle) (G7A; G7AB), and subsequently transplanted with CD45.1 2 x10^6 Lin$^-$ cells, collected from the BM.*

Mobilization was assessed 3 hours post-AMD3100 injection, revealing a 6-fold increase in WBC counts, an 8-fold increase in progenitors (Lin-Sca1+Kit+ [LSK]), and a 200-fold increase in the HSC-enriched fraction (LSK CD150+CD48- [SLAM HSC]) in circulation (Figure 13A, C), compared to non-mobilized control mice (Sham). BIO5192 augmentation led to higher mobilization of WBC, LSK, and SLAM HSC, resulting in an additional 2-fold increase in SLAM HSC over G7A levels (Figure 13C), concordantly with what was also reported previously (Ramirez *et al*, 2009). To assess if this level of mobilization and subsequent BM niche availability were adequate for donor cell engraftment, $2x10^6$ CD45.1 lineage-negative (Lin-) cells, purified from BM, were transplanted into CD45.2 congenic recipients following the final AMD3100 or AMD3100/BIO5192 injection (Figures 12B and 13B-D).

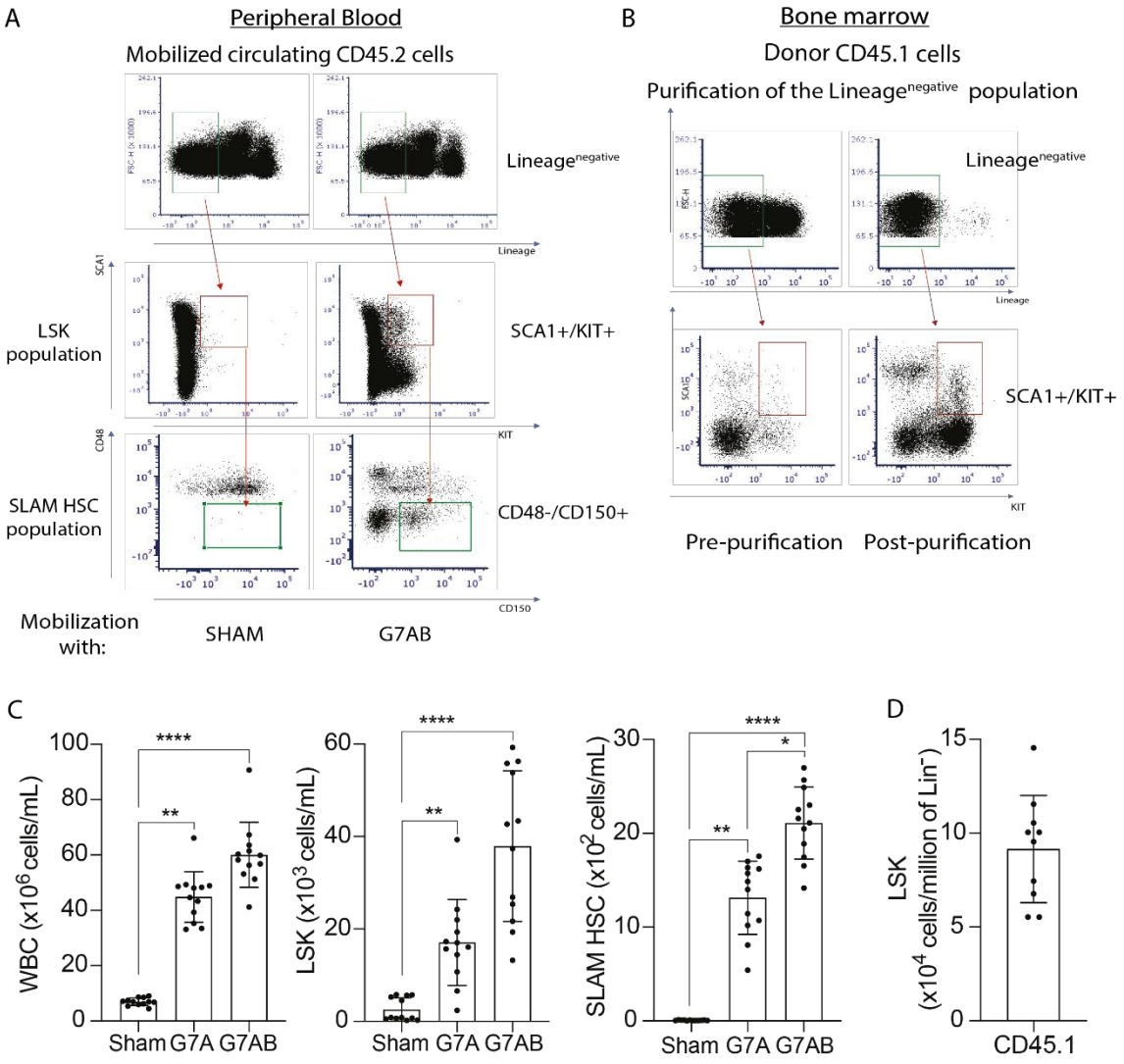


Figure 13. HSC enrichment and mobilization efficiency assessment.

A) *Representative plots showing the gating strategy used to characterize LSK and SLAM HSC circulating in the peripheral blood, stained for lineage markers, SCA1, KIT, CD48, and CD150.* ***B)*** *Representative plots showing the gating strategy used to characterize the donor cells, extracted from the BM, stained for lineage markers, SCA1, KIT, pre-, and post-purification of lineage negative cells.* ***C)*** *Counts of mobilized WBC (left panel), LSK (middle panel), and SLAM HSC (right panel) per mL in the PB in non-mobilized (Sham) and G7A and G7AB mobilized mice.* ***D)*** *Counts of LSK cells per million of Lin^- CD45.1 donor cells, collected from the BM. The results are mean ± SEM, with n ≥ 10 biological replicates. In all the analyses, p less than 0.05 were considered significant (*p < 0.05, **p < 0.01, ***p < 0.001, ****p < 0.0001. ''ns'' means non-significance).*

Donor chimerism reached a median of 20% following the G-CSF/AMD3100 mobilization protocol and increased to 30% with the addition of BIO5192. This chimerism remained stable for up to 24 weeks (Figure 14A), while non-mobilized control mice showed minimal donor chimerism (<1%). The myeloid and lymphoid proportions were similar between mobilized and non-mobilized control mice (Figure 14B, left panel). Initially, donor cells displayed a myeloid-biased output in the weeks after engraftment, likely due to early repopulation by short-term progenitors (Figure 14B, right panel). However, by the experiment's end, lineage composition became similar between donor and recipient cells (Figure 14B). Chimerism was maintained across differentiated cell subsets, including T cells (CD4 and CD8), B cells (CD19), and myeloid cells (CD11b) in the peripheral blood (PB) (Figure 14C), BM (Figure 14D), including within LSK and SLAM HSC (Figure 14E), and spleen (Figure 14F). Moreover, lineage distribution exhibited similarities between recipient and donor-origin cells in BM (Figure 14G). These findings validate the engraftment of donor long-term multilineage HSPCs, establishing the proof of principle for a low-burden HSCT. This approach involves the exchange of resident and donor HSPCs during mobilization without genotoxic conditioning, referred to hereafter as mobilization-based HSCT (M-HSCT).

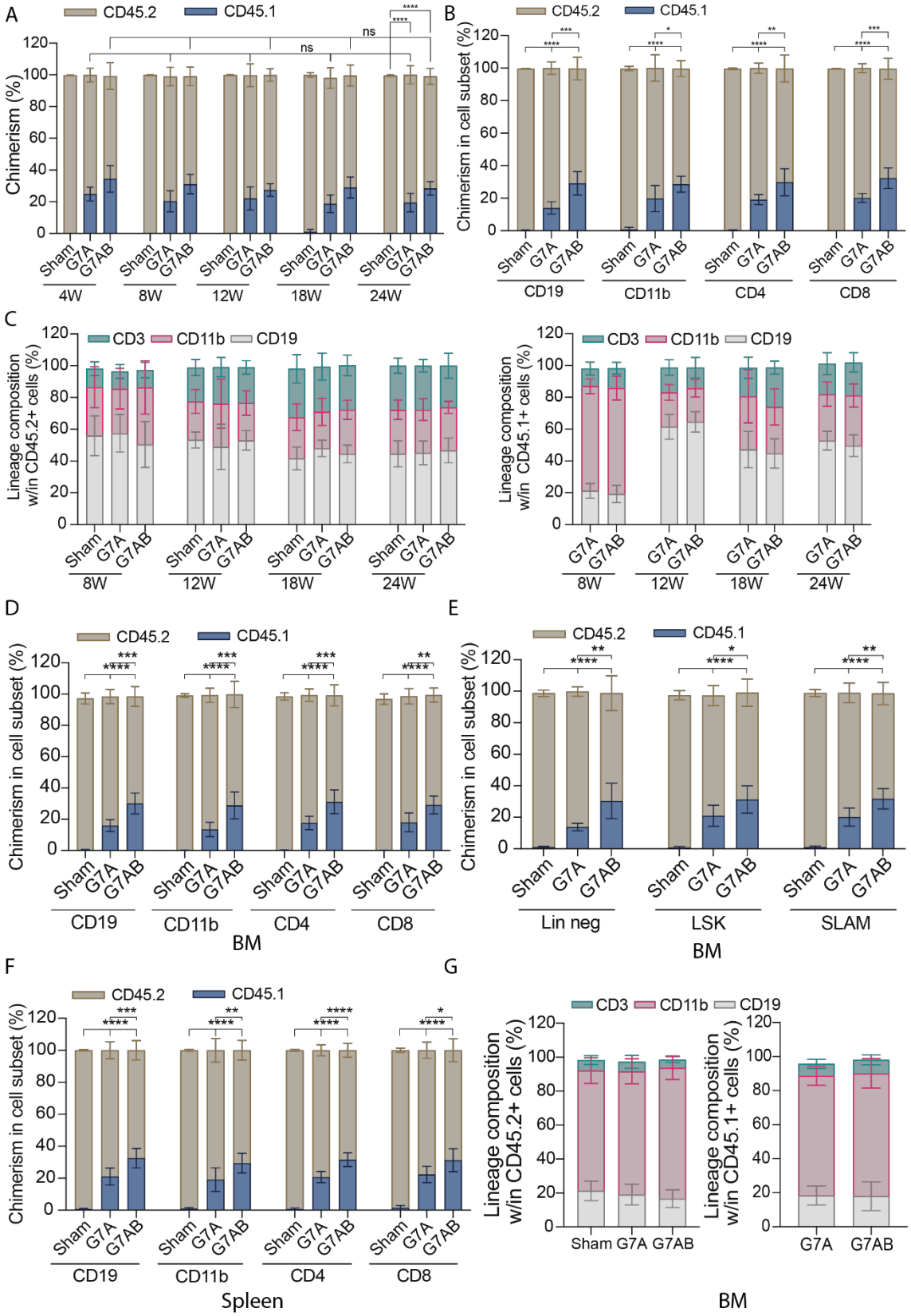


Figure 14. Exchange efficiency and chimerism in CD40lg recipient mice.
A) *Long-term follow-up of the donor CD45.1 (blue) and recipient CD45.2 (ocher) chimerism observed within total CD45+ cells in PB after transplanting 2 x10^6 Lin-*

cells post-mobilization in recipient CD45.2 mice. ***B)*** *The reconstitution of myeloid and lymphoid lineages over time of the recipient CD45.2+ cells (left panel) and CD45.1+ cells (right panel) in the PB of recipient CD45.2 mice.* ***C-F)*** *Chimerism of CD45.1 cells was observed within CD19+ B cells, CD11b+ myeloid cells, CD4+ T helper cells, and CD8+ T cytotoxic cells in the PB (C) and BM (D), within the Lin-, LSK, and SLAM HSC (E) and spleen (F).* ***G-H)*** *Myeloid and lymphoid lineage composition of CD45.2+ cells (left panel) and CD45.1+ cells (right panel) in the BM (G) and spleen (H) of CD45.2 mice. The results are mean ± SEM, with n ≥ 10 biological replicates. In all the analyses, p less than 0.05 were considered significant (*p < 0.05, **p < 0.01, ***p < 0.001, ****p < 0.0001. ''ns'' means non-significance).*

5.2 M-HSCT allows establishing sufficient donor chimerism to rescue the HIGM-1 phenotype

To explore the therapeutic potential of M-HSCT, we employed $Cd40lg^{-/-}$ mice, a model faithfully representing the phenotype of human primary combined immunodeficiency hyper IgM syndrome 1 (HIGM-1; Renshaw *et al*, 1994). This is a rare primary immunodeficiency disorder characterized by low serum concentrations of IgG, IgA, and IgE antibodies. It is caused by a mutation in the CD40LG gene, leading to impaired T-cell activation of B cells and subsequent defective antibody class switching. Given the potential negative impact of G-CSF treatment on the BM niche (Greenbaum & Link, 2011; Lévesque *et al*, 2003a, 2003b; Petit *et al*, 2002), we investigated various mobilization protocols differing in G-CSF presence, dose, duration, and combinations with other drugs (Figure 15A). Altering G-CSF dosage or treatment duration, or excluding it, significantly reduced LSK and SLAM HSC mobilization. Analysis of peripheral blood (PB) showed peak mobilization of WBC, LSK, and SLAM HSC approximately 3 hours after AMD3100 or AMD3100/BIO5192 injection (Figures 15B-D). The addition of AMD3100 to standard G-CSF treatment increased mobilized LSK levels threefold, with BIO5192 further enhancing this fivefold (Figure 15C). Notably, $Cd40lg^{-/-}$ mice exhibited mobilization levels similar to WT mice (Figure 15E).

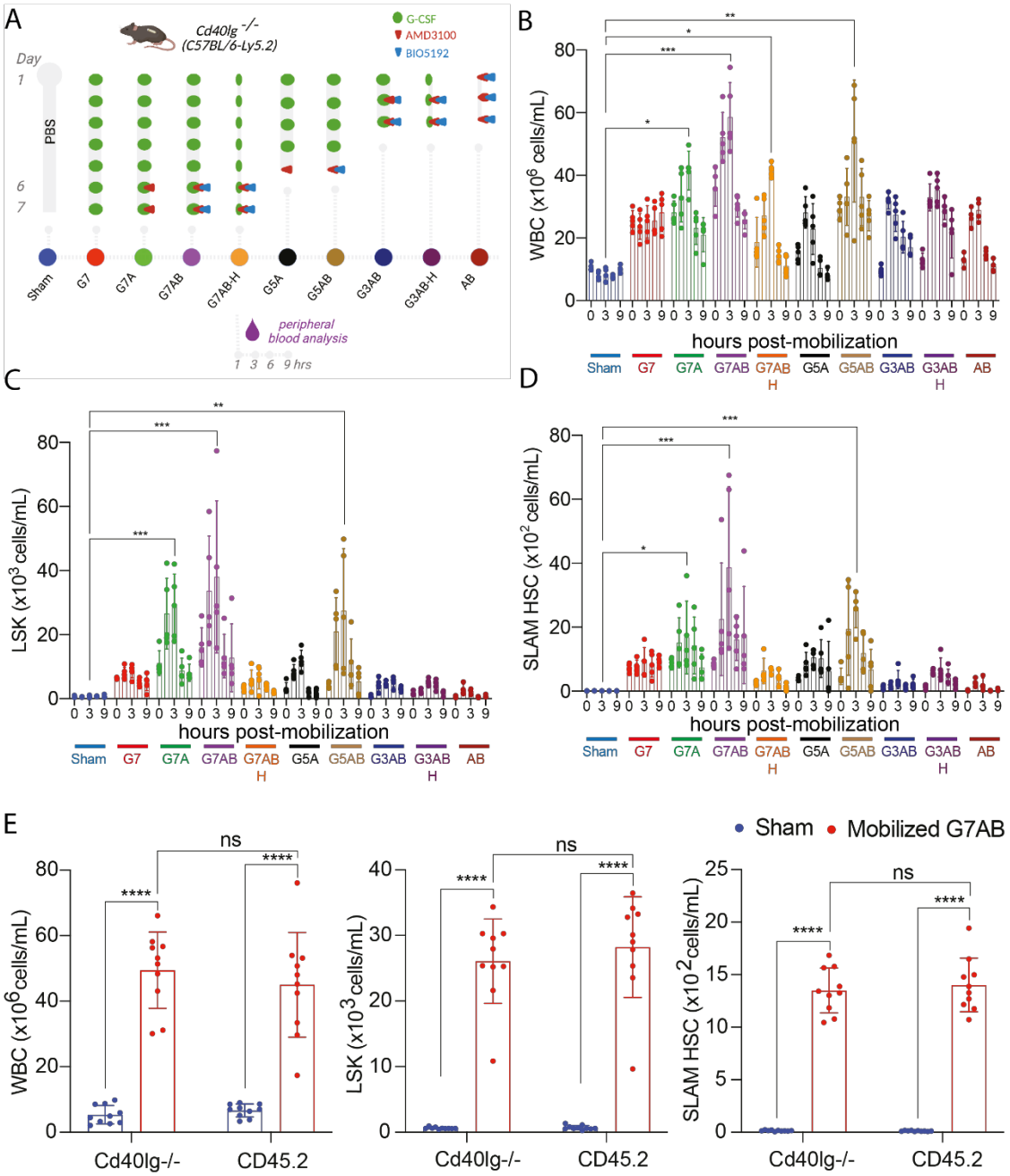


Figure 15. Assessing mobilization kinetics and efficiency.
A) *Schematic of different mobilization protocols tested and the times of analysis in Cd40lg-/- mice.* ***B-D)*** *Counts of mobilized WBC (B), LSK (C), and SLAM HSC (D) per mL in the PB of Cd40lg-/- mice treated with PBS (Sham), G-CSF for 7 days (G7), G-CSF for 7 days and AMD3100 (G7A), G-CSF for 7 days, AMD3100 and BIO5192 (G7AB), half-dose of G-CSF for 7 days, AMD3100 and BIO5192 (G7AB-H), G-CSF for 5 days and AMD3100 (G5A), G-CSF for 5 days, AMD3100 and BIO5192 (G5AB), G-CSF for 3 days, AMD3100 and BIO5192 (G3AB), half-dose of G-CSF for 3 days, AMD3100 and BIO5192 (G3AB-H), and only AMD3100 and BIO5192 (AB) at 0, 1, 3, 6, and 9 h after the last injection of A or AB.* ***E)*** *Counts of mobilized WBC (left panel), LSK (middle panel), and SLAM HSC (right panel) cells per mL in the PB of Cd40lg-/- mice and CD45.2 mice, after mobilization with PBS*

*(Sham) or mobilized with G7AB. A mixed-effect model (REML), followed by a post hoc analysis with Sidak's test. The results are mean ± SEM, with n ≥ 5 biological replicates for the kinetic experiments, except for the AB group (n = 4), and with n ≥ 9 biological replicates for the Cd40lg-/- M-HSCT experiments. In all the analyses, p less than 0.05 were considered significant (*p < 0.05, **p < 0.01, ***p < 0.001, ****p < 0.0001. ''ns'' means non-significance).*

While AMD3100/BIO5192 treatment had limited effects on blood neutrophil and monocyte counts, G-CSF treatment substantially increased them (Figures 16A–16D). G-CSF treatment elevated MMP9, a myeloid cell-released protease, and decreased CXCL12, a chemokine critical for HSPC homing and retention, in BM stroma, indicating extracellular matrix remodeling (Figures 16D-16E), consistent with previous reports (Greenbaum & Link, 2011). Interestingly, comparing CXCR4 expression on circulating SLAM HSC with or without G-CSF mobilization revealed lower expression in the former, suggesting induced cleavage of the molecule (Figure 16F). Comparison of SLAM HSC numbers in the lower limb BM between untreated and mobilized mice at the peak of mobilization indicated a 55% decrease in the latter (Figure 16G; left panel). However, only 75% of these cells were accounted for in the PB (Figure 16G; right panel), implying that some of the egressed cells became trapped in other organs, such as the spleen.

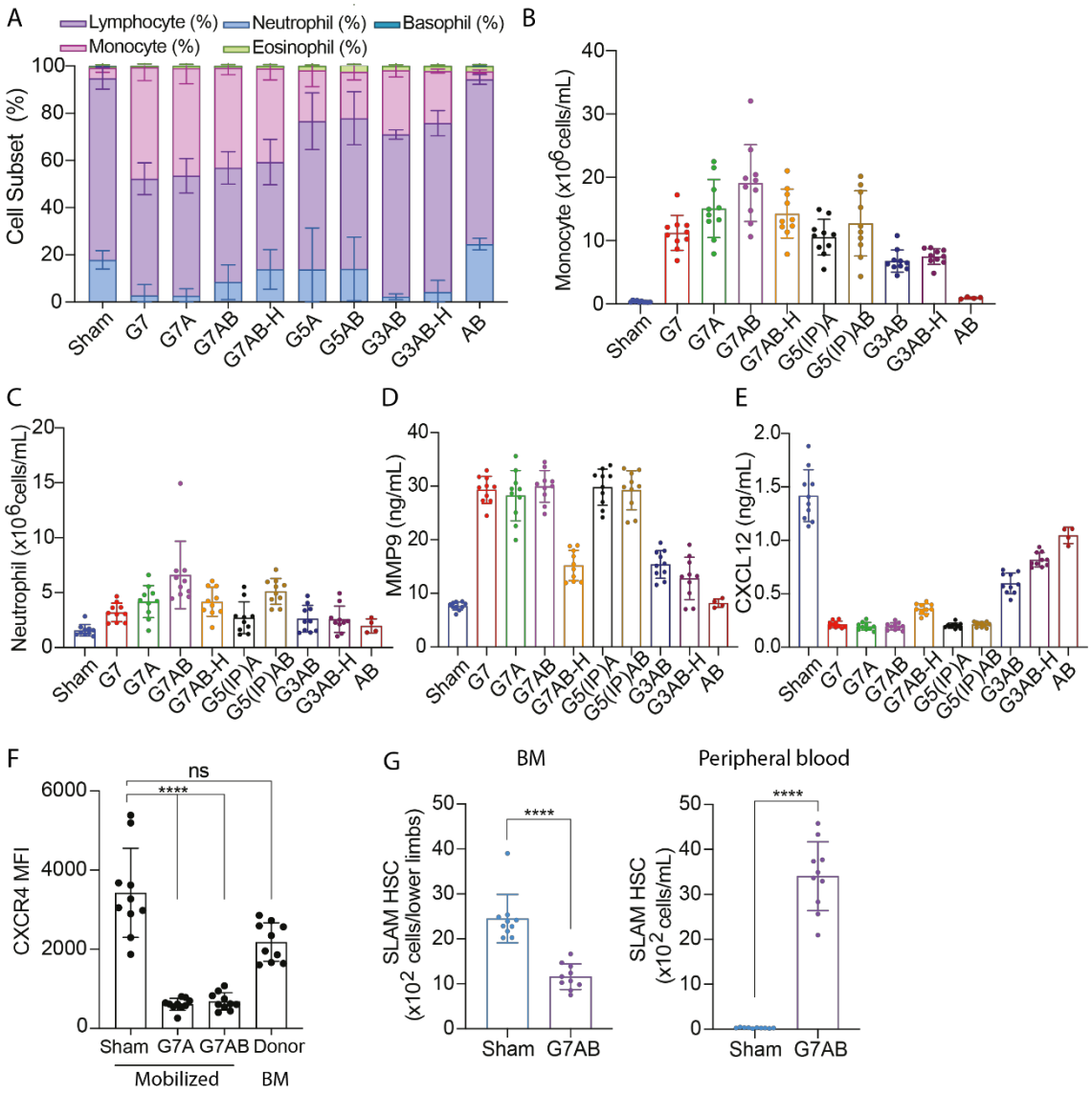


Figure 16. Mobilization impact on the BM niche

A) *The percentage of neutrophils, lymphocytes, monocytes, eosinophils, and basophils in the PB after different mobilization protocols.* ***B-C)*** *Counts of mobilized monocytes (B) and neutrophils (C) per mL in the PB after different mobilization protocols.* ***D-E)*** *MMP9 (E) and CXCL12 (F) concentration in the BM extracellular extracts of Cd40lg-/- mice mobilized with protocols described above.* ***F)*** *CXCR4 MFI on circulating LSK after treatments with PBS, G7A, G7AB, and on donor cells purified from untreated bone marrow. A Kruskal-Wallis test, followed by a post hoc analysis with Dunn's test.* ***G)*** *Total counts of SLAM HSC in the lower limbs (left panel) and in the PB per mL (right panel) of Cd40lg-/- mice treated with PBS or mobilized with G7AB. The results are mean ± SEM, with n ≥ 5 biological replicates for the kinetic experiments, except for the AB group (n = 4), and with n ≥ 9 biological replicates for the Cd40lg-/- M-HSCT experiments. In all the analyses, p less than 0.05 were considered significant (*p < 0.05, **p < 0.01, ***p < 0.001, ****p < 0.0001. ''ns'' means non-significance).*

Given the lower efficiency and increased harm of current editing protocols for mouse cells compared to their human counterparts (Schiroli *et al*, 2017), we transplanted $2x10^6$ WT CD45.1 Lin- cells, purified from BM, as a surrogate for autologous gene-corrected cells. These were transplanted into Cd40lg-/- recipients at the peak of mobilization following the G-CSF, AMD3100, and BIO5192 regimen (Figure 17). A stable chimerism of approximately 30% WT cells was achieved across all lineages and differentiated cells in the PB (Figure 18A-B), spleen (Figure 18C), and BM (Figures 18D-E) of transplanted mice. By the study conclusion, cellular subsets exhibited comparability between recipient and donor cells and between the non-mobilized (Sham) and mobilized group (G7AB) in the PB (Figure 18F), BM (Figure 18G), and spleen (Figure 18H). Interestingly, the achieved chimerism exceeded our initial estimate of approximately 20%, which was based on the data in Figure 16G and the following assumptions: (1) uniform mobilization occurred throughout the entire mouse BM, (2) the lower limbs accounted for 20% of BM (Nombela-Arrieta & Manz, 2017), and (3) mobilized and infused cells competed equally (Table 5; column G7AB). This discrepancy suggests an advantage for donor BM-harvested cells not exposed to the mobilization process, potentially due to their higher CXCR4 expression (Figure 16F) in the presence of limited CXCL12, highlighting a favorable engraftment window for donor HSPCs immediately following mobilization. To explore niche repopulation dynamics during mobilization, we transplanted $2x10^6$ WT CD45.1 Lin- cells, purified from the BM, following various mobilization protocols. We observed that, despite infusing the same number of cells, chimerism decreased with reduced mobilization efficiency. Even when we infused seven times more donor cells than mobilized ones, chimerism remained low, suggesting that residual non-mobilized cells were likely limiting the exchange by occupying the niche (Table 5; Figure 18I). Conversely, when we varied the number of transplanted cells below the saturating dose in mice mobilized with the same protocol, we observed dose-dependent engraftment (Figure 18J). We then immunized the mice with a thymus-dependent antigen (trinitrophenyl-keyhole limpet hemocyanin, TNP-KLH) and assessed whether immunoglobulin (IgG) class switching was restored through transplantation. While non-mobilized Cd40lg-/- mice produced nearly undetectable levels of antigen-specific IgGs, M-HSCT-treated mice exhibited a significant improvement in switched-antibody responses to primary and recall vaccinations, although these levels remained below those

of control WT mice (Figure 18K). Partial rescue of immune function in transplanted mice was further demonstrated by the presence of splenic germinal B cells, whereas non-mobilized mice failed to engage B cells in germinal center formation (Figure 18L). Overall, these findings highlight the potential of M-HSCT to rescue the humoral immune response in HIGM-1 mice without the need for a conditioning regimen.

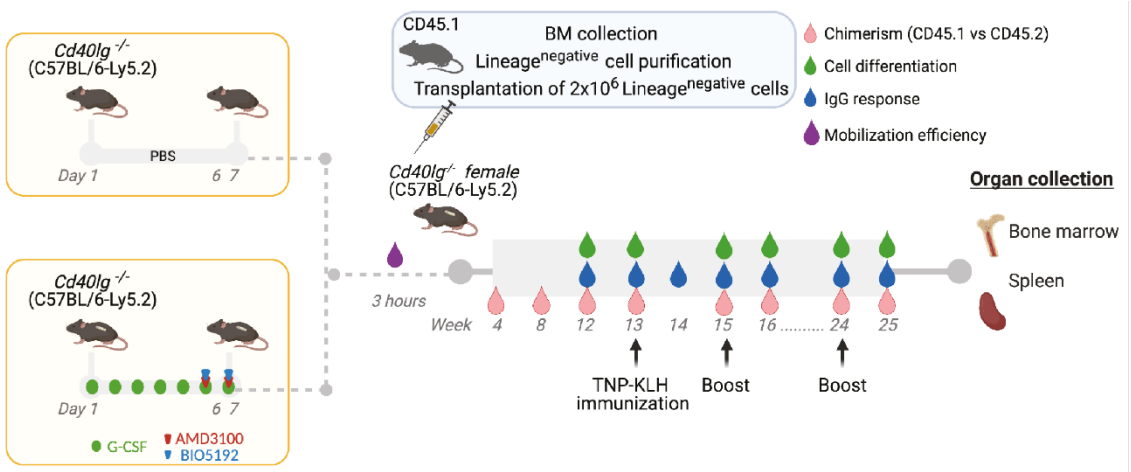


Figure 17. Mouse-in-mouse exchange experimental design.
Schematic of the M-HSCT protocol applied to Cd40lg-/- mice. The recipient Cd40lg-/- mice were mobilized with G-CSF (green dots), AMD3100 (red triangle), and BIO5192 (blue triangle) (G7AB), and subsequently transplanted with 2 x10⁶ WT CD45.1 Lin- cells, collected from the BM.

Table 5. Estimated versus obtained chimerism following M-HSCT in Cd40lg-/- mice

Treatment	Mobilized SLAM HSCs (mL)	Estimated mobilized SLAM HSCs/mouse (V blood = 1.5 mL)	Percentage of estimated BM vacancy	Total SLAM HSCs transplanted (from BM purified 2 × 10^6 Lin^-)	Ratio recipient to donor	Percentage of estimated chimerism	Percentage of obtained chimerism
Sham	10	15	0	4,000	1:0.00375	0	N/A
G7	900	1,350	11	4,000	1:0.33	8	N/A
G7A	1,700	2,550	20	4,000	1:0.64	12	19
G7AB	3,500	5,250	42	4,000	1:1.31	18	30
G7AB-H	600	900	7	4,000	1:0.23	6	9
G5(IP)A	1,000	1,500	12	4,000	1:0.38	9	N/A
G5(IP)AB	2,500	3,750	30	4,000	1:0.94	15	N/A
G3AB	600	900	7	4,000	1:0.23	6	8
G3AB-H	350	525	4	4,000	1:0.13	4	5
AB	300	450	4	4,000	1:0.11	3	N/A

Estimation is based on the following theories: (1) mobilization occurred to the same extent throughout all the mouse BM, (2) the lower limbs account for 20% of it, and (3) the mobilized and infused cells compete equally (with n ≧ 5).

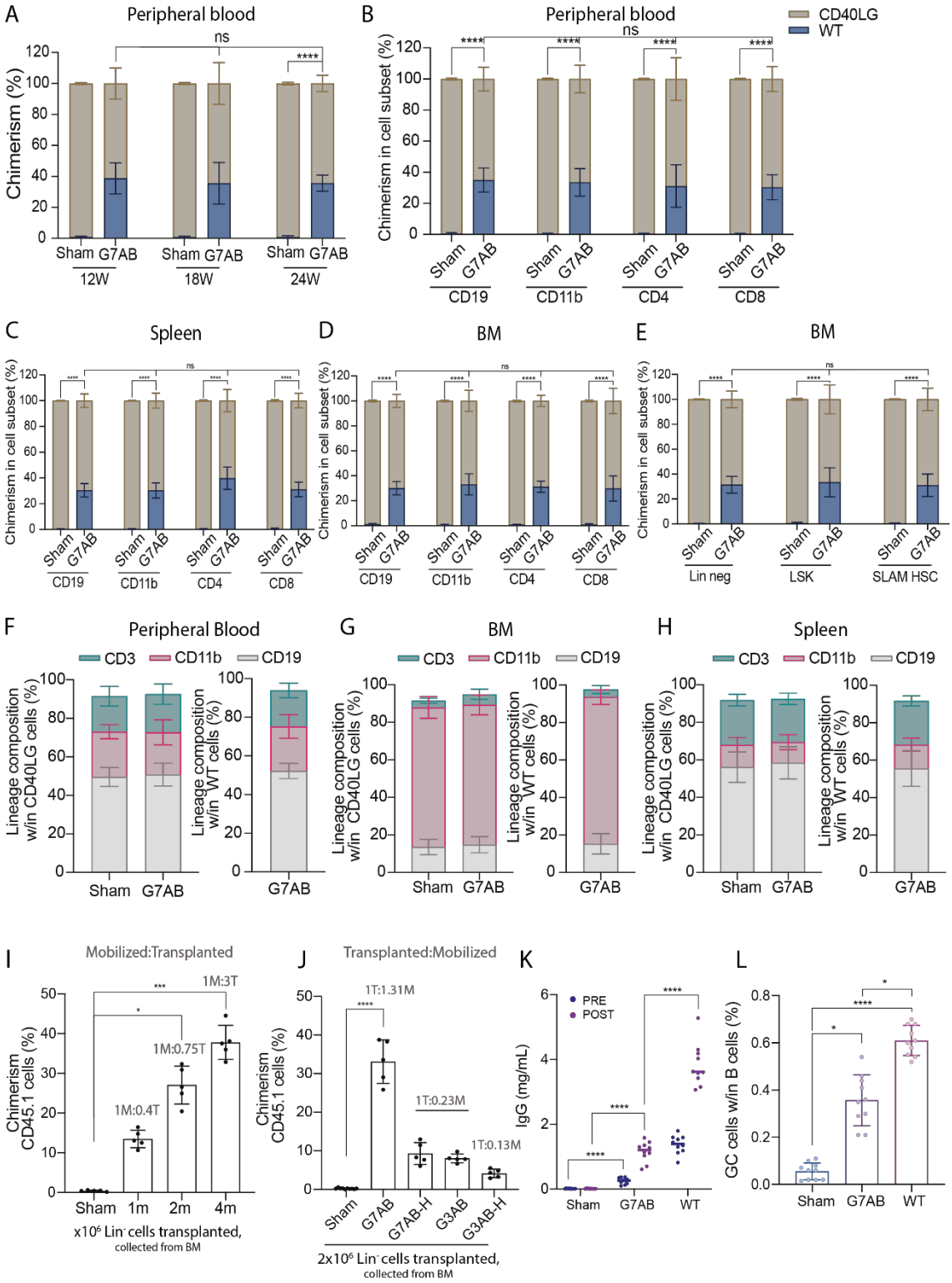


Figure 18. Chimerism and immunization.

A) *Schematic of the M-HSCT protocol applied to Cd40lg-/- mice. The recipient Cd40lg-/- mice were mobilized with G-CSF (green dots), AMD3100 (red triangle), and BIO5192 (blue triangle) (G7AB), and subsequently transplanted with 2 x10⁶ WT CD45.1 Lin- cells, collected from the BM.* ***B)*** *Long-term follow-up of the donor WT (blue) and recipient Cd40lg-/- (ocher) chimerism observed within total CD45+ cells in PB after transplanting 2 x10⁶ Lin- cells (collected from the BM) post*

mobilization in recipient Cd40lg-/- mice. ***C-F)*** *Chimerism of WT cells was observed within CD19+, CD11b+, CD4+, and CD8+ cells in the PB (C), spleen (D), and BM (E) and within Lin-, LSK, and SLAM HSC in the BM (F). A mixed-effects model (REML), followed by a post hoc analysis with Tukey's test (between groups) or by post hoc analysis with Dunnett's test (within groups).* ***G-I)*** *Myeloid and lymphoid lineage composition of Cd40lg-/- (left panel) and WT (right panel) cells in the PB (G), BM (H), and spleen (I) of Cd40lg-/- mice after M-HSCT.* ***J)*** *TNP-KLH-specific IgG concentration in sera collected 7 days before (pre) and after (post) TNP-KLH vaccination of Cd40lg-/- mice after M-HSCT.* ***K)*** *The percentage of PNA+GL7+ splenic germinal centers B cells within the spleen of Cd40lg-/- mice after TNP-KLH vaccination of Cd40lg-/- mice treated by M-HSCT.* ***L)*** *Chimerism of CD45.1 cells at 20 weeks, following different M-HSCT protocol, subsequently transplanted with 2 3 106 WT CD45.1 Lin- cells, collected from the BM.* ***M)*** *Chimerism of CD45.1 cells at 20 weeks, following mobilization with G7AB and subsequently transplanted with different cell doses (WT CD45.1 Lin- cells, collected from the BM). The results are mean ± SEM, with n ≥ 5 biological replicates for the kinetic experiments, except for the AB group (n = 4), and with n ≥ 9 biological replicates for the Cd40lg-/- M-HSCT experiments. In all the analyses, p less than 0.05 were considered significant (*p < 0.05, **p < 0.01, ***p < 0.001, ****p < 0.0001. ''ns'' means non-significance).*

5.3 M-HSCT allows an efficient donor to recipient exchange of HSPCs within the human niche of hematochimeric mice

To explore the applicability of M-HSCT in humans, we utilized NSGW41 mice with a mutant kit receptor to reduce competition with human HSPCs. We established an *in vivo* model of human HSPC mobilization by transplanting NSGW41 mice with $3x10^5$ CD34+ cells derived from G-CSF mobilized peripheral blood (mPB). After confirming hematopoietic engraftment (Figure 19A), we treated the mice with the optimized mobilization protocol (G7AB). This resulted in a significant increase in WBC counts, both murine (LSK) and human (CD34+CD38-) progenitors (Figure 19C). Notably, human CD34+CD38- cells peaked in the peripheral blood 3 hours after the final mobilizer administration, suggesting this as the optimal time for transplanting human donor cells. Correspondingly, we observed up to a 65% reduction in human CD34+CD38- cells in the BM of mobilized mice, which was mirrored by an increase of these cells in the peripheral blood, accounting for 60% of the egressed cells (Figure 19B).

We proceeded to assess CD34+CD38- cell exchange post-mobilization by transplanting the outgrowth of $1x10^5$ CD34+ cells counted on day 1 post-thawing (Figure 19D). Prior to infusion, mPB cells from the same donor were transduced with GFP-expressing LV, enabling the distinction of these cells from the previously engrafted and resident cells (Figure 19E). This culture step, simulating an LV-based gene replacement

protocol for therapeutic purposes, resulted in an increased expression of CXCR4, which is involved in HSPC homing and retention, countering the effects of thawing and prior *in vivo* exposure to G-CSF (Figure 19F).

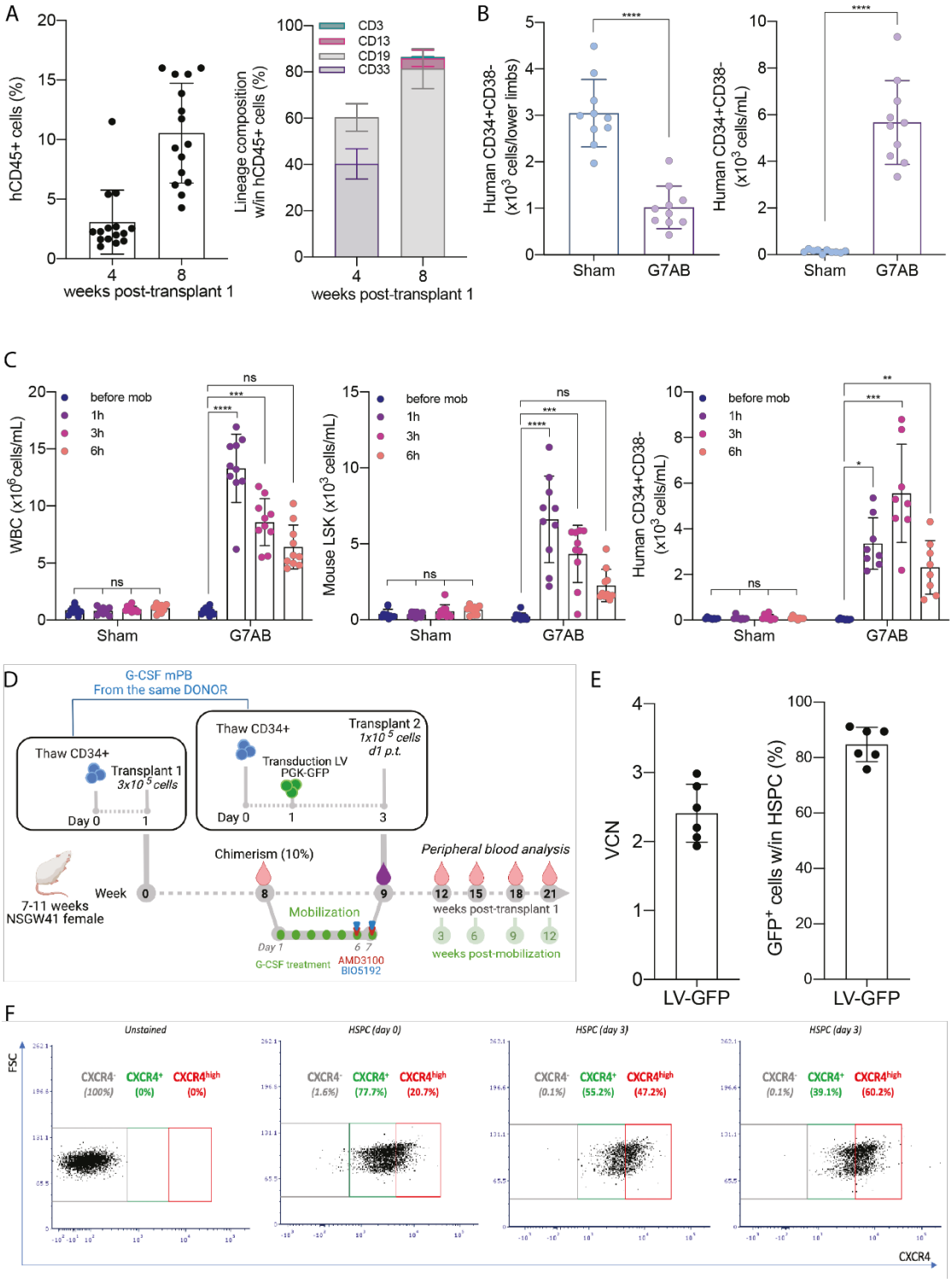


Figure 19. Translating M-HSCT in humanized hematochimeric mouse model
A) *The percentage of human chimerism (CD45+; left panel) and lymphoid/myeloid cell composition within the human CD45+ population (right panel) over time in*

NSGW41 mice, following the first transplant of human CD34+ cells. ***B)*** *Total counts of CD34+ CD38 cells in the lower limbs (left panel) and the PB per mL (right panel) of humanized NSGW41 mice non-mobilized (Sham) or mobilized (G7AB).* ***C)*** *Counts of mobilized WBC (left panel), LSK cells (middle panel), and human CD34+ CD38 cells (right panel) per mL in the PB of humanized NSGW41 mice nonmobilized or mobilized with G7AB at 0, 1, 3, and 6 h after the last injection of AMD3100 and BIO5192.* ***D)*** *Schematic illustration of competitive transplantation, after G7AB mobilization, between human resident cells and newly transplanted CD34+ G-CSF mPB GFP-transduced cells in NSGW41 mice.* ***E)*** *Vector copy number (VCN) in HSPCs population (CD34+CD133+CD90+) (left panel) and the percentage of GFP+ cells measured within CD34+ cells (right panel), in vitro, after transduction.* ***F)*** *Representative plots showing the gating strategy used to characterize the* $CXCR4^{high}$ *population in the HSPC (CD34+CD133+CD90+) population.* ***G)*** $CXCR4^{high}$ *MFI over time after thawing, stained with an antibody targeting the N terminus epitope of CXCR4, on the HSPC population (CD34+CD133+CD90+) mobilized with G-CSF. The longitudinal comparisons, performed by a mixed-effect model (REML), followed by a post hoc analysis with Dunnett's test. The results are mean ± SEM, with n ≥ 5, with 3 different donors. In all the analyses, p less than 0.05 were considered significant (*p < 0.05, **p < 0.01, ***p < 0.001, ****p < 0.0001. ''ns'' means non-significance).*

Interestingly, the mobilized cells exhibited an increasing CXCR4 mean fluorescence intensity (MFI) upon culture when using an N terminus-directed antibody, consistent with reported N-terminal cleavage of the molecule upon G-CSF exposure and subsequent restoration of full-size molecule expression in culture (Figures 20A-C) (Lévesque *et al*, 2003a, 2003b). Moreover, cultured cells exhibited higher migration efficiency in *in vitro* transwell migration assay (Figure 20D). Notably, the same culture-mediated recovery effect, was observed also for KIT and ITGA4, which are both known to sustain HSC proliferation and homing (Figure 21A-B).

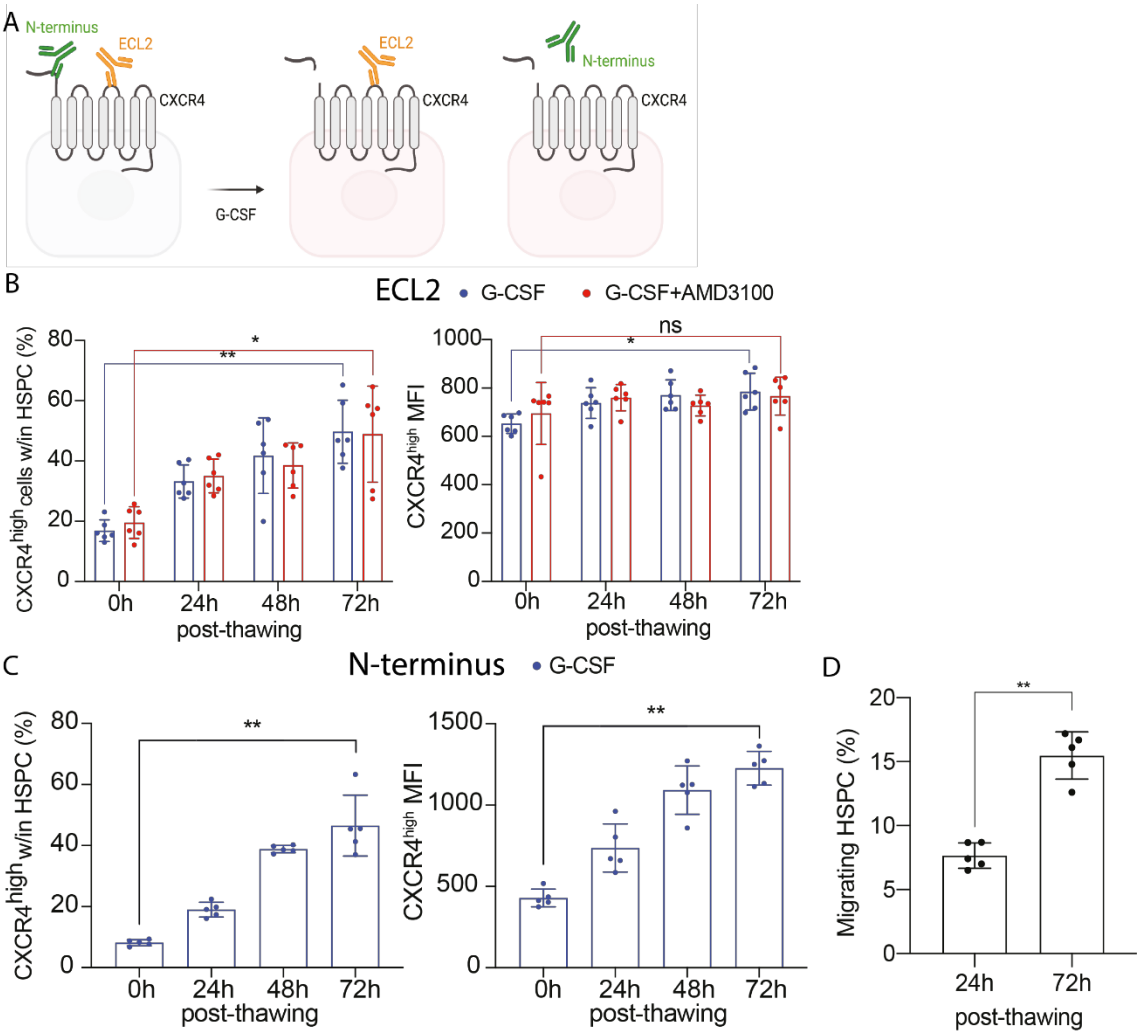


Figure 20. Ex vivo cell culture promotes the recovery of key engraftment targets. ***A)*** *Scheme of CXCR4 cleavage following G-CSF mobilization and related antibodies localization.* ***B)*** *The percentage of CXCR4^{high} cells (left panel) and MFI (right panel) over time after thawing, stained with an antibody targeting the ECL2 epitope of CXCR4, on the HSPC population mobilized with G-CSF or G-CSF/AMD3100.* ***C)*** *The percentage of CXCR4high cells (left panel) and MFI (right panel) over time after thawing, stained with an antibody targeting the N terminus epitope of CXCR4, on the HSPC population mobilized with G-CSF.* ***D)*** *The percentage of migrating HSPCs, performed at 24 and 72 h post thawing, previously collected with G-CSF. A Kruskal-Wallis test was performed, followed by a post hoc analysis with Dunn's test. The longitudinal comparisons, performed by a mixed-effect model (REML), followed by a post hoc analysis with Dunnett's test. The results are mean ± SEM, with n ≥ 5, with 3 different donors. In all the analyses, p less than 0.05 were considered significant (*p < 0.05, **p < 0.01, ***p < 0.001, ****p < 0.0001. ''ns'' means non-significance).*

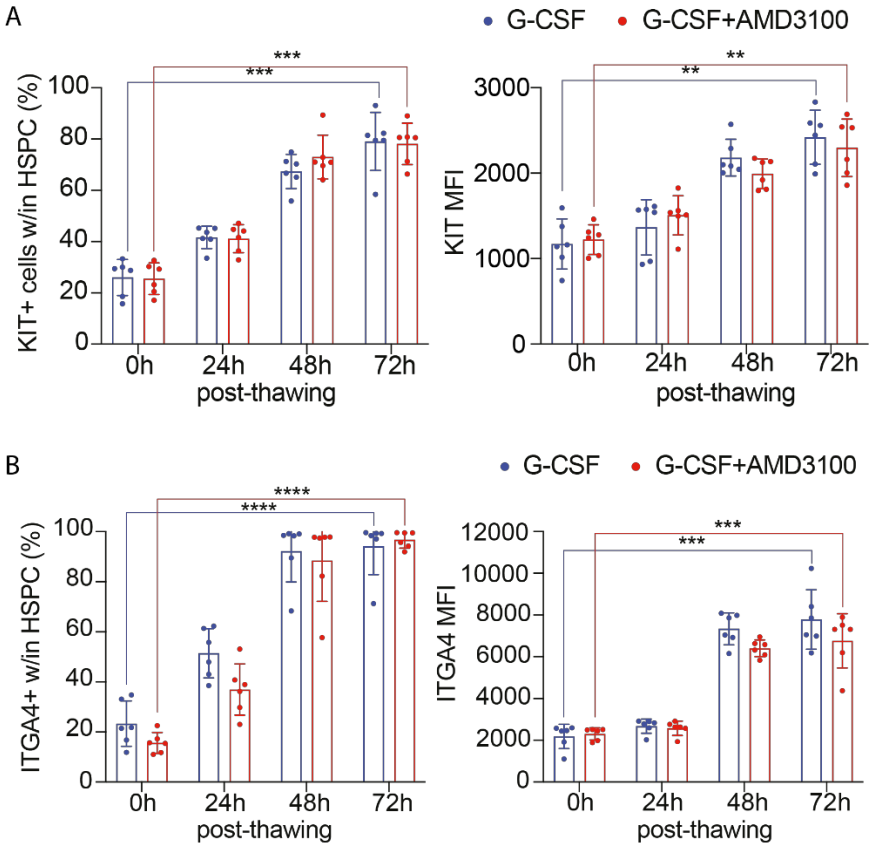


Figure 21. Expression kinetics of KIT and ITGA4 upon culture.
A) *The percentage of KIT+ cells (left panel) and MFI (right panel) over time after thawing, on the HSPC population mobilized with G-CSF or G-CSF/AMD3100.* ***B)*** *The percentage of ITGA4+ cells (left panel) and MFI (right panel) over time after thawing, on the HSPC population mobilized with G-CSF or G-CSF/AMD3100.*

The size of the human graft continued to increase over time in non-mobilized mice but comprised only a low percentage of GFP+ cells (<1%) even at late time points, indicating no engraftment of the newly infused cells in the absence of mobilization (Figure 21B-C). Conversely, mice receiving mobilization treatment initially experienced a decrease in the human graft, followed by a rescue accompanied by an increasing fraction of GFP+ cells, implying that these cells effectively competed with the mobilized ones. By the end of the experiment, GFP+ cells constituted a median of 30% of the human graft and were present in all human lineages found in the blood of mobilized mice (CD19+ B cells, CD13+ myeloid cells, and CD3+ T cells), whereas they were nearly absent in non-mobilized mice (Figures 21D). Lineage composition was similar between mobilized and non-mobilized mice (Figure 21E, left panel). Intriguingly, GFP+ cells initially exhibited a myeloid-biased output during the first weeks after transplantation, akin to newly engrafting progenitors in the C57BL/6J mouse model described earlier (Figure 21E, right panel).

However, GFP+ cells were subsequently found in all detectable lineages in the following weeks, approaching the lineage distribution of the total human graft by the experiment's conclusion (Figure 21E).

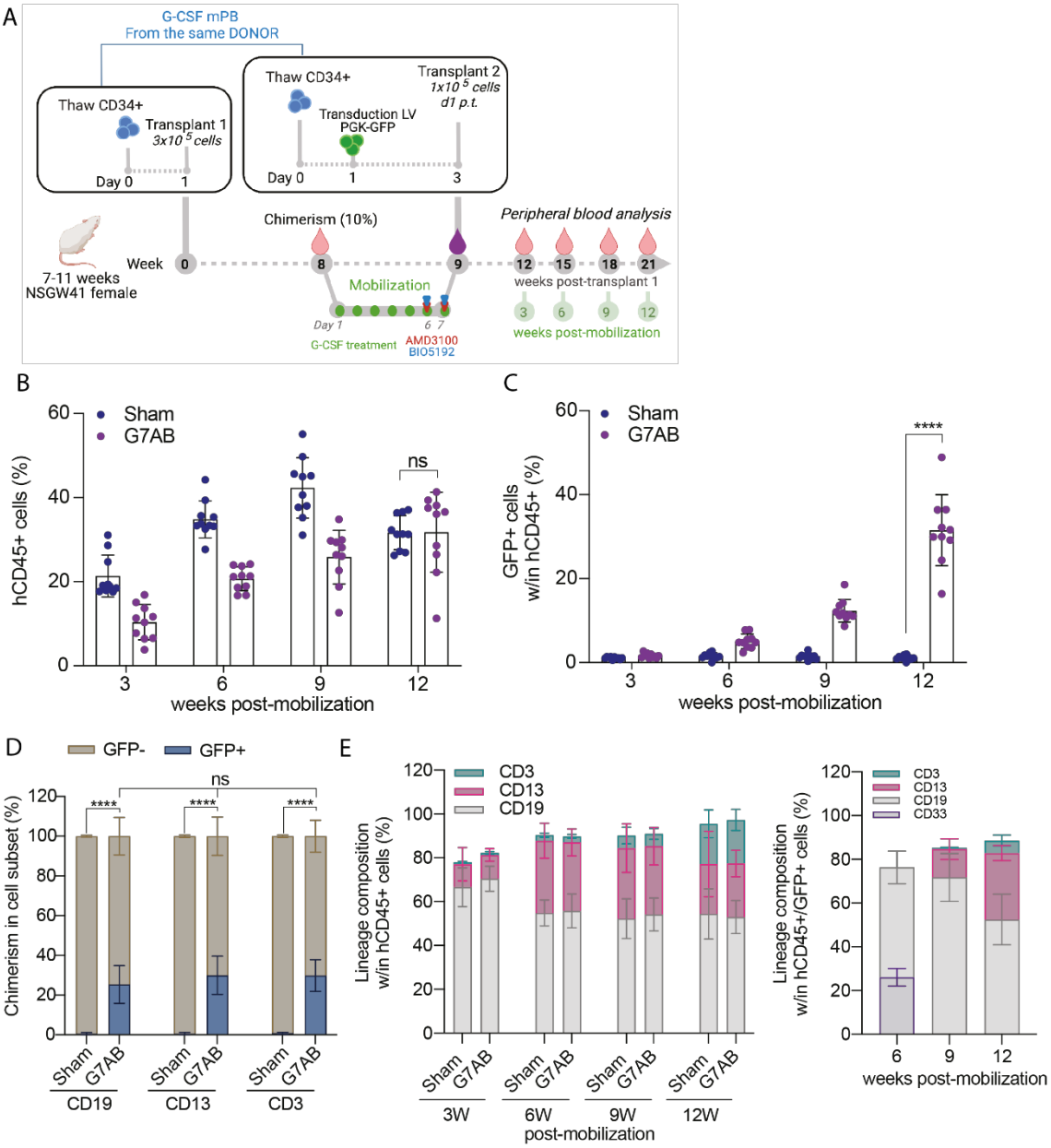


Figure 22. Chimerism and lineage reconstitution in peripheral blood
A) *Schematic illustration of competitive transplantation, after G7AB mobilization, between human resident cells and newly transplanted CD34+ G-CSF mPB GFP- transduced cells in NSGW41 mice.* ***B-C)*** *Long-term follow-up of human CD45+ (B) and GFP+/CD45+(C) cells chimerism in PB after M-HSCT in NSGW41 mice.* ***D)*** *Chimerism of GFP+ cells was observed within CD19+, CD13+, and CD3+ cells at the end of the experiment in PB after M-HSCT.* ***E)*** *The reconstitution of myeloid and lymphoid lineages over time of human CD45+ (left panel) and CD45+/GFP+ cells (right panel) in the PB after M-HSCT. The results are mean ± SEM, with n ≥ 9 biological replicates. In all the analyses, p less than 0.05 were considered*

*significant (*p < 0.05, **p < 0.01, ***p < 0.001, ****p < 0.0001. ''ns'' means non-significance).*

In the BM, spleen, and thymus, the levels of the human graft were comparable between mobilized and non-mobilized mice, while GFP+ cells reached up to 30% in mobilized mice (Figures 23A-B). In contrast, non-mobilized mice had GFP+ engraftment below 1%. The lineage distribution between the total human graft and GFP+ cells remained consistent across all organs (Figures 23C-F and 24A-B), demonstrating similar levels of chimerism across all cell subsets, including the most primitive progenitors (HSPCs: CD34+CD38-CD90+; Figure 24C-D). These findings provide strong support for the notion that partial chimerism of *ex vivo* modified HSPCs can be achieved for human hematopoiesis through M-HSCT without the need for prior conditioning.

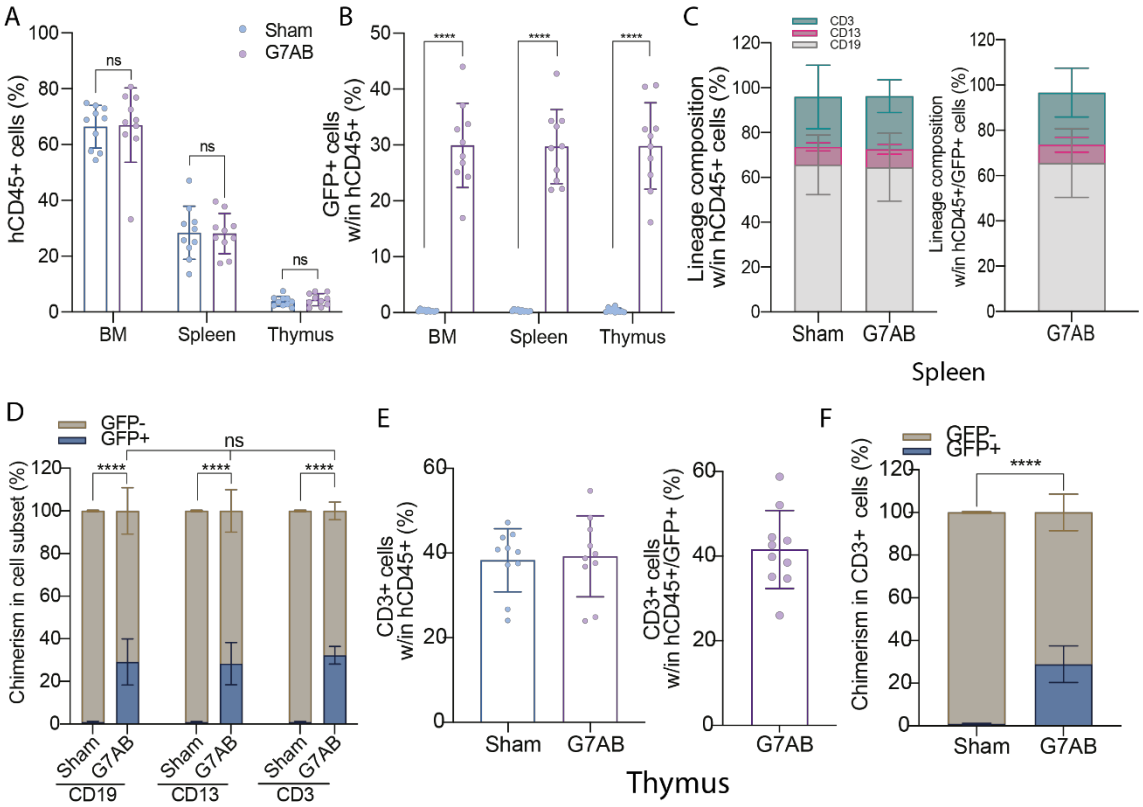


Figure 23. Chimerism and lineage composition across hematopoietic organs
A-B) *Human CD45+ (A) and GFP+/CD45+ (B) cells chimerism in the BM, spleen, and thymus after M-HSCT.* ***C)*** *Myeloid and lymphoid lineage composition of human CD45+ cells (left panel) and CD45+/GFP+ cells (right panel) in the spleen of NSGW41 mice after M-HSCT.* ***D)*** *Chimerism of GFP+ cells was observed within CD19+, CD13+, and CD3+ cells in the spleen after M-HSCT.* ***E)*** *The percentage of T cells within human CD45+ (left panel) and CD45+/GFP+ cells (right panel) in the thymus after M-HSCT.* ***F)*** *Chimerism of GFP+ cells was observed within T cells in the thymus after M-HSCT.*

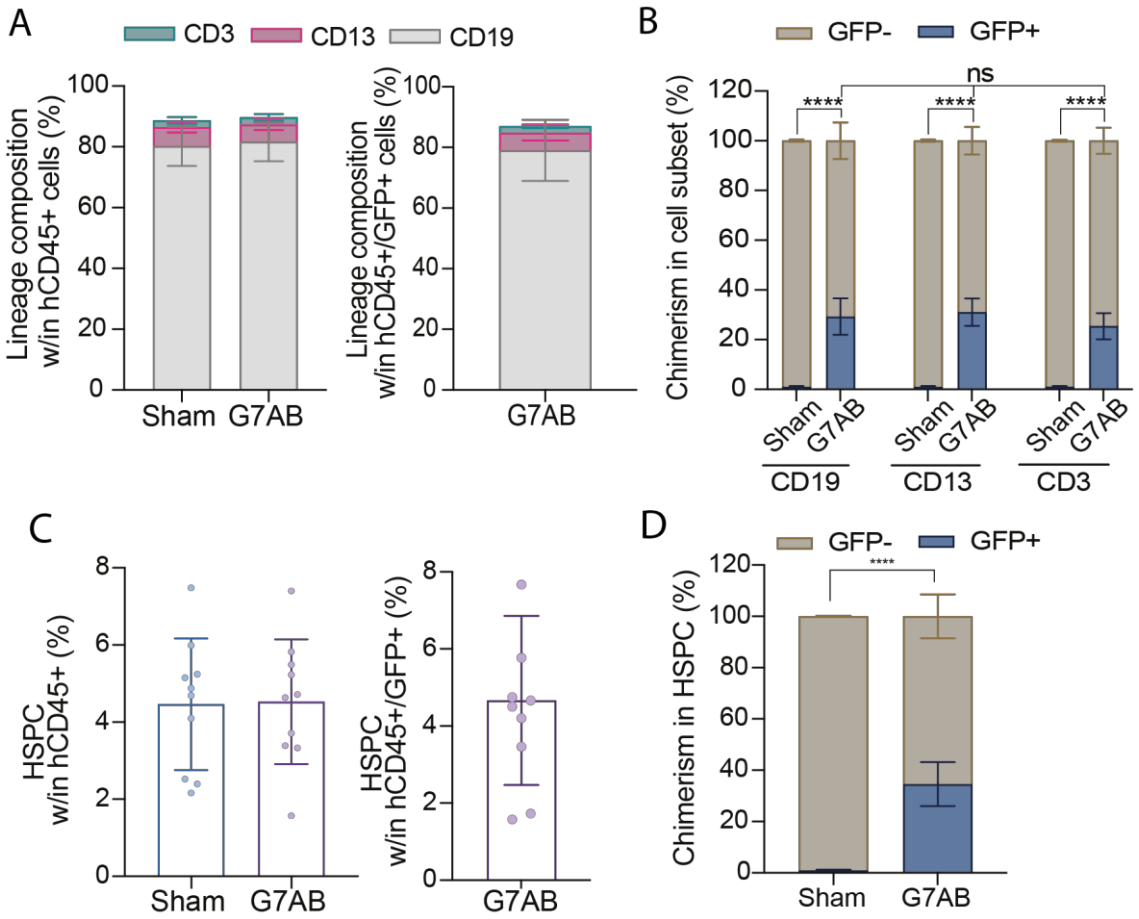


Figure 24. Chimerism and lineage composition in the bone marrow.
A) Myeloid and lymphoid lineage composition of human CD45+ (left panel) and CD45+/GFP+ cells (right panel) in the BM of NSGW41 mice after M-HSCT. ***B)*** *Chimerism of GFP+ cells was observed within CD19+, CD13+, and CD3+ cells in the BM after M-HSCT.* ***C)*** *The percentage of HSPCs (CD34+ CD38- CD90+) in human CD45+ (left panel) and CD45+/GFP+ cells (right panel) in the BM after M-HSCT.* ***D)*** *Chimerism of GFP+ cells was observed within HSPCs in the BM after M-HSCT. The results are mean ± SEM, with n ≥ 9 biological replicates. In all the analyses, p less than 0.05 were considered significant (*p < 0.05, **p < 0.01, ***p < 0.001, ****p < 0.0001. ''ns'' means non-significance).*

5.4 Transient CXCR4 overexpression increases chimerism in the humanized context, following M-HSCT

To enhance HSPC engraftment, we leveraged the transient overexpression of CXCR4. We optimized an *in vitro* transcription (IVT) platform, exploring various 5' and 3' UTR sequences, poly-adenylation tail lengths, and capping methods (Figure 25). Our optimized construct, pVAXi, included an AG CleanCap, an Eif4 aptamer at the 5' UTR, a WPRE sequence at the 3' UTR, and a 150-bp polyA tail. During mRNA synthesis,

modified uridine (pseudouridine) was incorporated, followed by high-performance liquid chromatography (HPLC) purification to mitigate an interferon response in the electroporated cells (Figure 26).

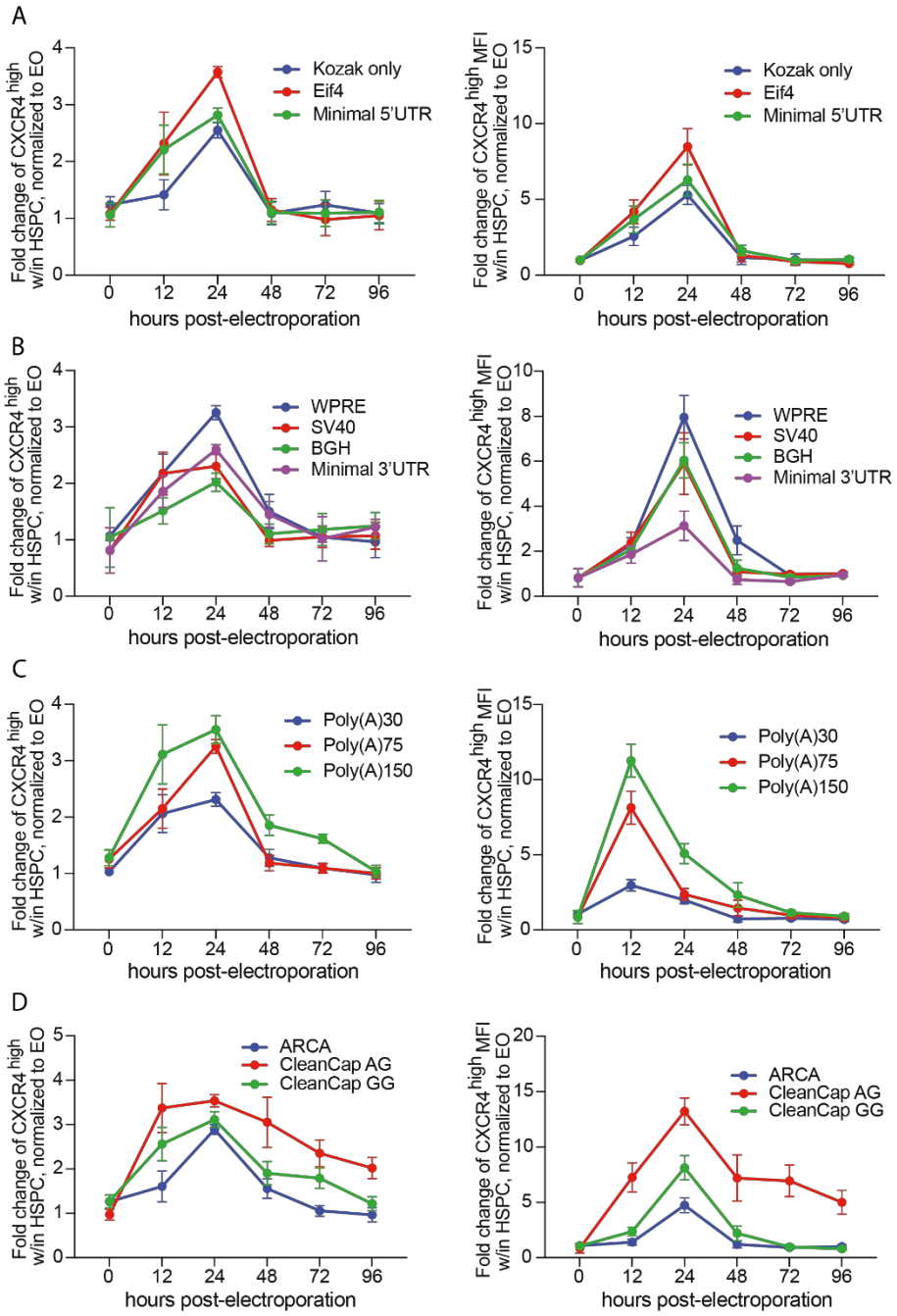


Figure 25. mRNA optimization.
A-D) *Fold change of CXCR4high cells (left panel) and CXCR4high MFI (right panel) in HSPCs (CD34+CD133+CD90+) electroporated with CXCR4 mRNA differing for the 50 UTR sequence (A), the 30 UTR sequence (B), the polyA tail length (C), and the mRNA capping (D), normalized to electroporated-only (EO) cells. The results are mean ± SEM, with n ≥ 5 for data collected in vitro (3 different donors). In all the analyses, p less than 0.05 were considered significant (*p < 0.05, **p < 0.01, ***p < 0.001, ****p < 0.0001. ''ns'' means non-significance).*

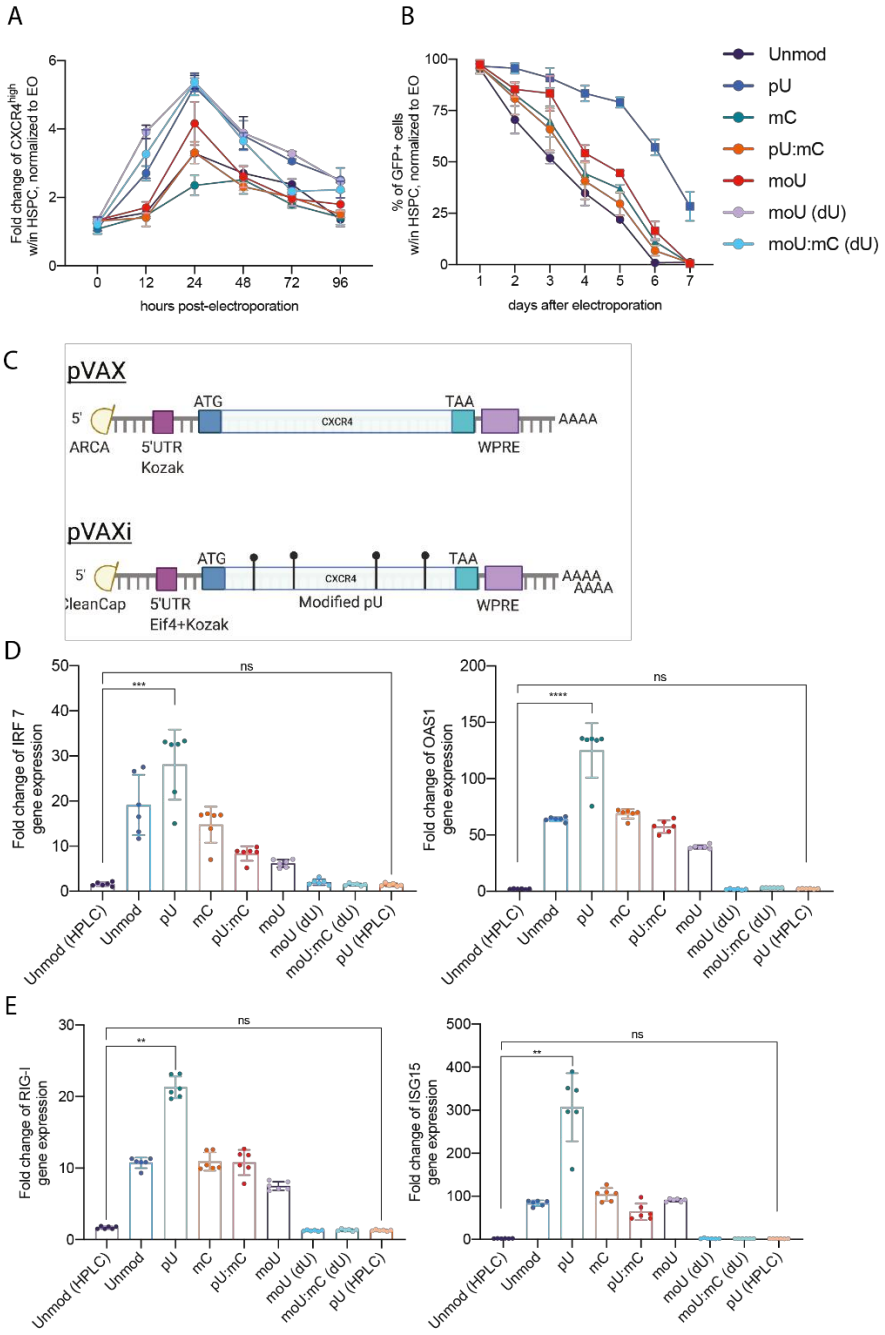


Figure 26. In vitro testing of optimized mRNA.
A) Fold change of CXCR4high cells in HSPCs electroporated with CXCR4 mRNA differing for nucleotides used during mRNA synthesis, normalized to EO cells. ***B)*** *The percentage of GFP+ cells in HSPCs, electroporated with GFP mRNA differing for nucleotides used for the mRNA synthesis, normalized to EO cells.* ***C)*** *Schematic of the pVAX CXCR4 mRNA and improved pVAXi CXCR4 mRNA.* ***D)*** *Fold change of IRF7, OAS1, RIG-I, and ISG15 gene expression, in cells electroporated with CXCR4 mRNA differing for nucleotides used during mRNA synthesis, normalized to EO cells.*

Electroporation of CXCR4 mRNA resulted in an increase in cells expressing CXCR4 and its MFI in both the bulk CD34+ population and primitive HSPCs (CD34+CD38-CD90+) for up to 3 days (Figures 27A–D). Transwell migration assays demonstrated that HSPCs overexpressing CXCR4, including the more primitive subset, migrated more effectively towards CXCL12 compared to control cells electroporated with GFP mRNA (Figures 27E-F and 27I). Notably, CXCR4 overexpression rapidly reaches a plateau with this improved platform, though higher concentrations impact on the overall HSC population (Figures 27G-J). We also tested two CXCR4 isoforms and found that isoform 1, which differed by 9 amino acids at the N terminus, elicited a stronger response to CXCL12 and was used in subsequent experiments (Figures 28A–C).

To assess the impact of CXCR4 overexpression on engraftment, we conducted experiments in immunodeficient NOD-SCID-IL2Rg-deficient (NSG) mice. Cells transiently overexpressing CXCR4 yielded a larger human graft in the peripheral blood, reaching a median of 45% human chimerism compared to 35% in cells overexpressing control GFP (Figure 28D). Lineage distribution was similar between both groups in the peripheral blood, bone marrow, spleen, and thymus (Figures 28E-F). Remarkably, bone marrow analysis showed an increased representation of the most primitive fraction of human HSPCs in mice transplanted with CXCR4 overexpressing cells (Figure 28G).

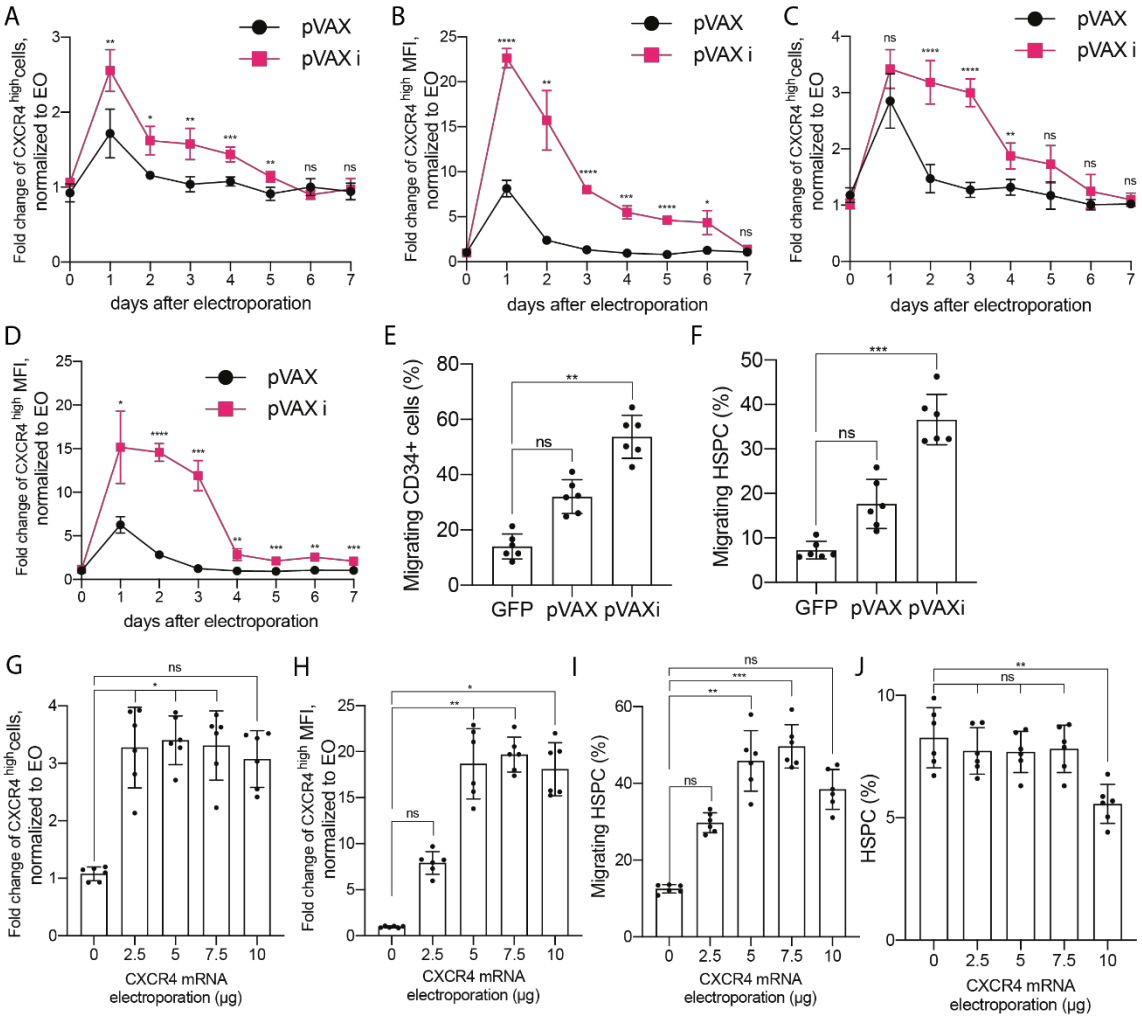


Figure 27. Optimize CXCR4 mRNA expression

A-B) *Fold change of CXCR4high cells (A) and CXCR4high MFI (B) in bulk CD34+ cells, electroporated with CXCR4 mRNA (pVAX) or optimized CXCR4 mRNA (pVAXi), normalized to electroporated-only (EO) cells.* ***C-D)*** *Fold change of CXCR4high cells (C) and CXCR4high MFI (D) in CD34+CD133+CD90+ HSPCs, electroporated with CXCR4 mRNA or optimized CXCR4 mRNA, normalized to EO cells.* ***E-F)*** *The percentage of migrating bulk CD34+ cells (E) and HSPCs (F), electroporated with GFP, CXCR4, or optimized CXCR4 mRNA.* ***J-K)*** *Fold change of CXCR4high cells (J) and CXCR4high MFI (K) in HSPCs, electroporated with different quantities of CXCR4 mRNA, normalized to EO cells.* ***L)*** *The percentage of migrating HSPCs, electroporated with different quantities of CXCR4 mRNA.* ***N)*** *The percentage of HSPCs (CD34+CD133+CD90+) in CD34+ cells electroporated with different quantities of CXCR4 mRNA. A Kruskal-Wallis test, followed by a post hoc analysis with Dunn's test. The results are mean ± SEM, with n ≥ 10 biological replicates for data collected in vivo, n ≥ 4 biological replicates for secondary transplant experiments, and n ≥ 5 for data collected in vitro (3 biological replicates and 2 technical replicates). In all the analyses, p less than 0.05 were considered significant (*p < 0.05, **p < 0.01, ***p < 0.001, ****p < 0.0001. ''ns'' means non-significance).*

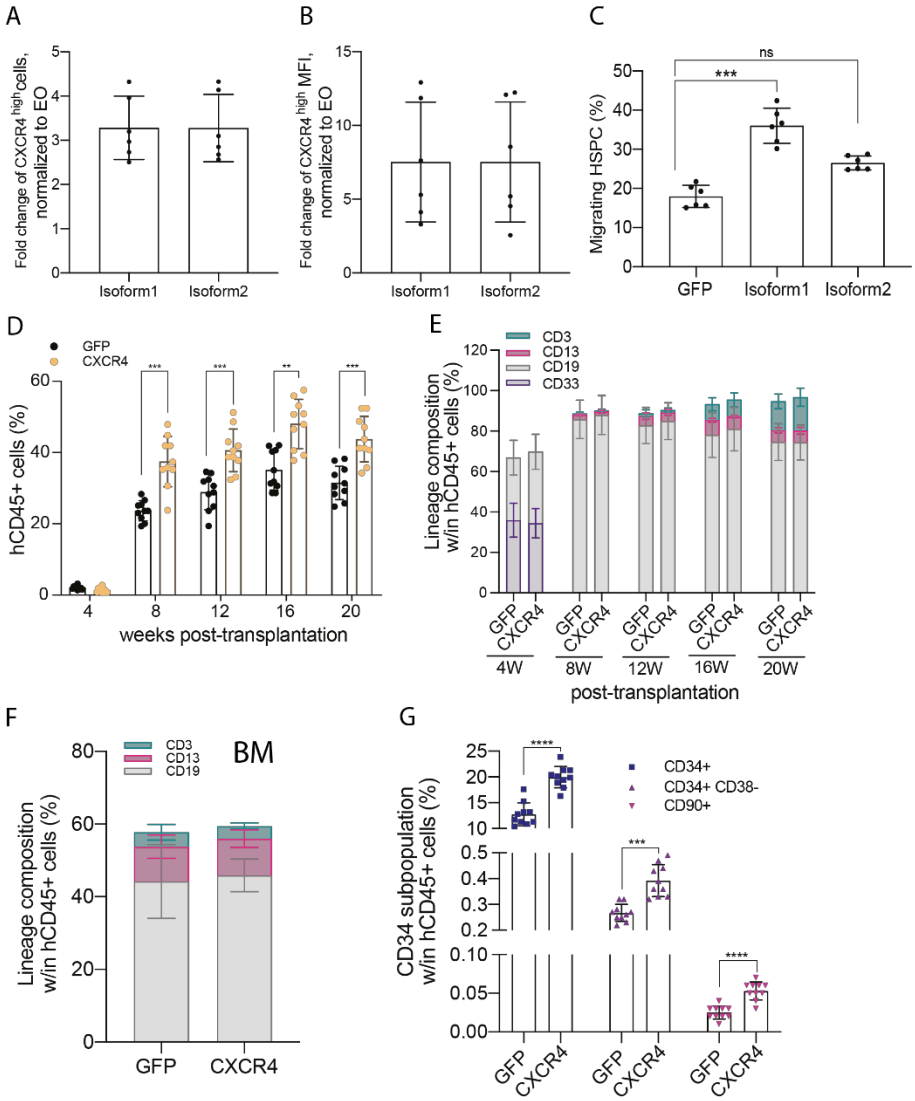


Figure 28. Optimize CXCR4 isoform and in vivo testing.
A-B) *Fold change of CXCR4high cells (A) and CXCR4high MFI (B) in HSPCs, electroporated with CXCR4 isoform1 or isoform2 mRNA, normalized to EO cells.* ***C)*** *The percentage of migrating HSPCs, electroporated with GFP, CXCR4 isoform1, or isoform2 mRNA.* ***D)*** *Long-term follow-up of human CD45+ in the PB of NSG mice, following the transplantation of CD34+ cells electroporated with GFP or CXCR4 mRNA.* ***E)*** *The reconstitution of myeloid and lymphoid lineages over time within total CD45+ cells in the PB of NSG mice, transplanted with CD34+ cells electroporated with GFP or CXCR4 mRNA.* ***F)*** *Myeloid and lymphoid cell composition of human CD45+ cells in the BM of NSG mice, transplanted with CD34+ cells electroporated with GFP or CXCR4 mRNA.* ***G)*** *CD34+ subpopulation in the BM of NSG mice, transplanted with CD34+ cells electroporated with GFP or CXCR4 mRNA.*

Next, we examined the potential advantage of CXCR4 overexpression in niche re-colonization following M-HSCT. NSGW41 mice, stably engrafted with $3x10^5$ CD34+ cells, were mobilized and then infused with the outgrowth of $2x10^5$ cells, counted on day

1 post-thawing, transduced with GFP-LV, and transiently overexpressing CXCR4 mRNA from the same donor as the original transplant. In parallel, control mice received cells overexpressing GFP mRNA (Figure 29A). The CXCR4 overexpressing cells effectively outcompeted mobilized HSPCs, establishing a stable chimerism in the human cell graft, whereas control cells overexpressing GFP engrafted to a lesser extent (Figures 29B-D). Furthermore, we confirmed that mobilization was essential to obtain chimerism with the newly infused cells, whether advantaged or not by CXCR4 overexpression, as evidenced by the lack of engrafted GFP+ cells in non-mobilized mice. By the end of the experiment, lineage composition in the peripheral blood was similar between mobilized and non-mobilized mice, and chimerism in each subset remained stable (Figures 29E-F).

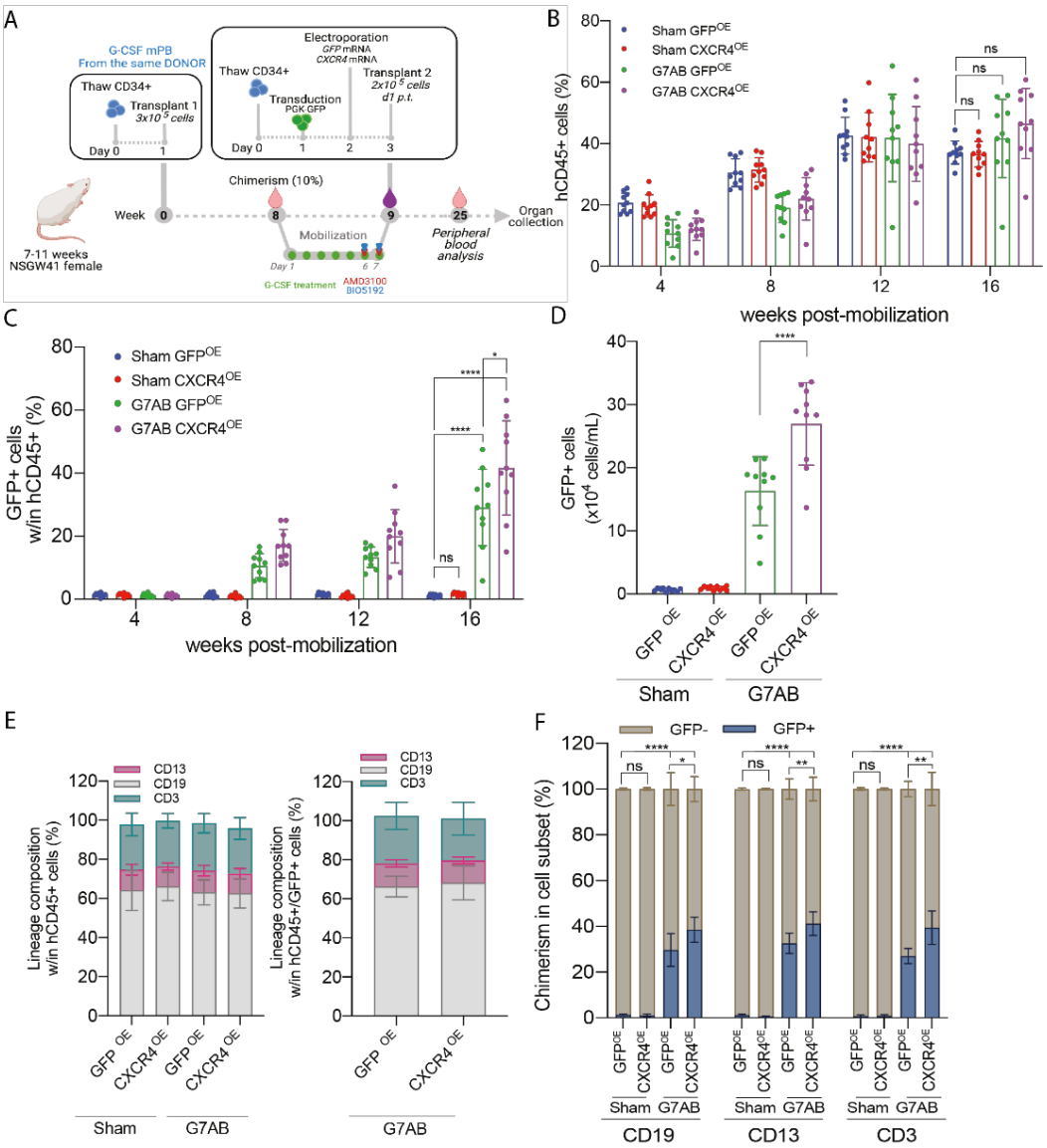


Figure 29. Transient CXCR4 overexpression confers an engraftment advantage in vivo. A) *Schematic illustration of competitive transplantation, after G7AB*

mobilization, between human resident cells and newly transplanted CD34+ G-CSF mPB GFP-transduced and electroporated cells in NSGW41 mice. ***B-C)*** *Long-term follow-up of human CD45+ (B) and CD45+/GFP+ (C) cells in the PB after M-HSCT with CD34+ cells transiently overexpressing GFP or CXCR4 mRNA, in NSGW41 mice.* ***D)*** *Counts of GFP+ cells per mL in the PB after M-HSCT with CD34+ cells transiently overexpressing GFP or CXCR4 mRNA, in NSGW41 mice.* ***E)*** *Myeloid and lymphoid lineage composition of human CD45+ (left panel) and CD45+/GFP+ cells (right panel) in the PB after M-HSCT, with CD34+ cells transiently overexpressing GFP or CXCR4, in NSGW41 mice.* ***F)*** *Chimerism of GFP+ cells was observed within CD19+, CD13+, and CD3+ cells in the PB after M-HSCT, with CD34+ cells transiently overexpressing GFP or CXCR4, in NSGW41 mice. The results are mean ± SEM, with n ≥ 10 biological replicates for data collected in vivo. In all the analyses, p less than 0.05 were considered significant (*p < 0.05, **p < 0.01, ***p < 0.001, ****p < 0.0001. ''ns'' means non-significance).*

These results were confirmed in the spleen, bone marrow, and thymus, where higher levels of GFP were detectable in mice transplanted with cells initially overexpressing CXCR4, without impacting the proportion of progenitors and differentiating cells within the hematopoietic organs (Figure 30A-F).

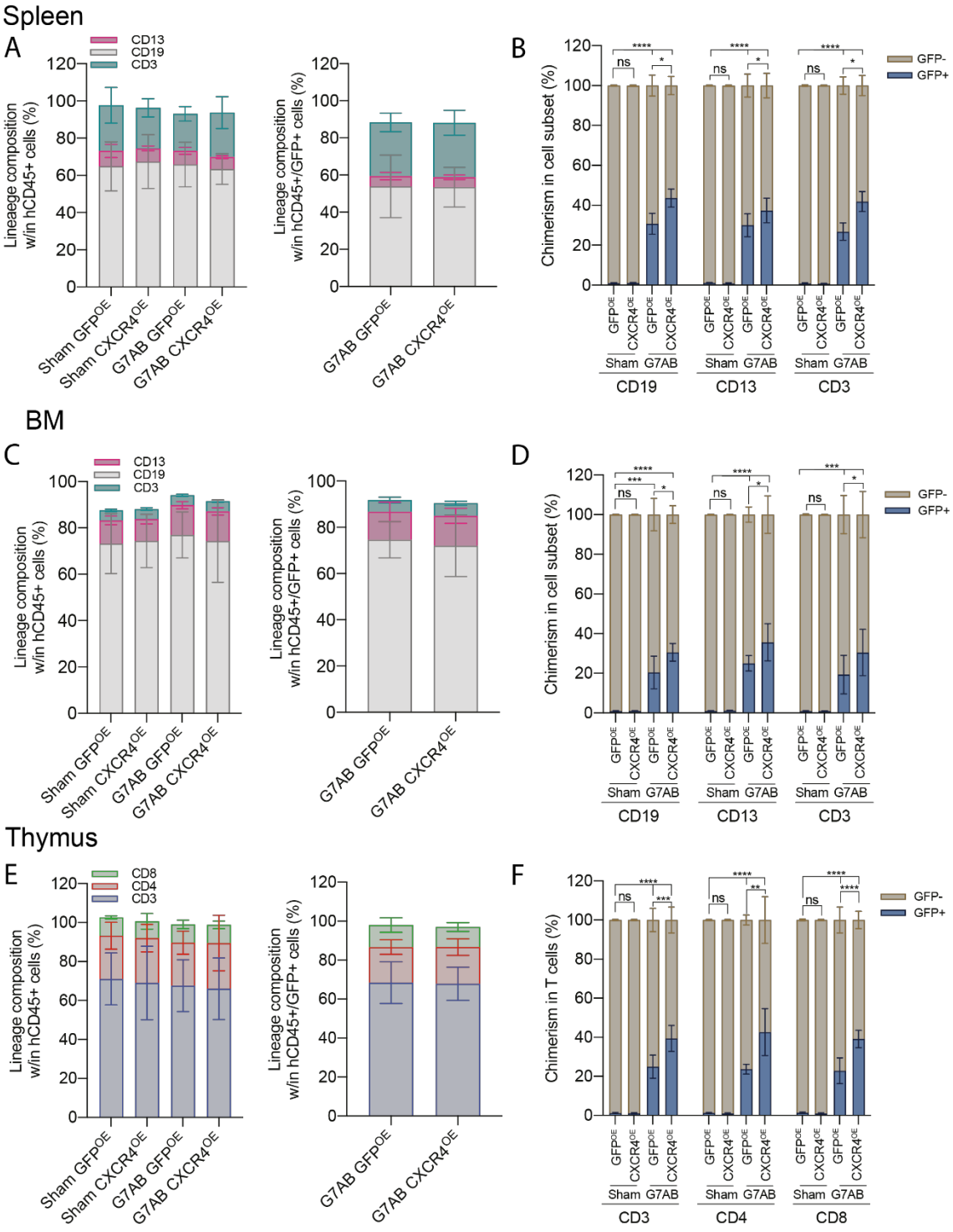


Figure 30. Lineage reconstitution and exchange efficiency across different organs.

A, C, E) *Myeloid and lymphoid lineage composition of human CD45+ (left panel) and CD45+/GFP+ cells (right panel) in the spleen (A), BM (C), and thymus (E) after M-HSCT with CD34+ cells transiently overexpressing GFP or CXCR4 in NSGW41 mice. The comparison of lineages between human CD45+ and CD45+/GFP+ cells was performed by a mixed-effect model (REML), followed by a post hoc analysis with Dunnett's.* ***B, D, F)*** *Chimerism of GFP+ cells was observed within CD19+, CD13+, and CD3+ cells in the spleen (B), BM (D), and within*

*CD3+, CD4+, and CD8+ T cells in the thymus (F) after M-HSCT with CD34+ cells transiently overexpressing GFP or CXCR4 in NSGW41 mice. A mixed-effect model (REML), followed by a post hoc analysis with Tukey's test (between groups) or by a post hoc analysis with Dunnett's test (within groups). The results are mean ± SEM, with n S 10. In all the analyses, p less than 0.05 were considered significant (*p < 0.05, **p < 0.01, ***p < 0.001, ****p < 0.0001. ''ns'' means non-significance).*

Secondary transplants of matched numbers of human CD34+ cells purified from the bone marrow of primary transplanted mice confirmed the presence of human GFP+ grafts in mice transplanted with cells harvested from mobilized groups only, demonstrating the successful engraftment of long-term HSCs following M-HSCT (Figure 31A-B). Moreover, the percentage of GFP+ cells in the secondary recipients was higher in the group transplanted with human cells from primary recipients overexpressing CXCR4 mRNA compared to those overexpressing control GFP mRNA, underscoring the advantage of employing an engraftment enhancer (Figure 31C).

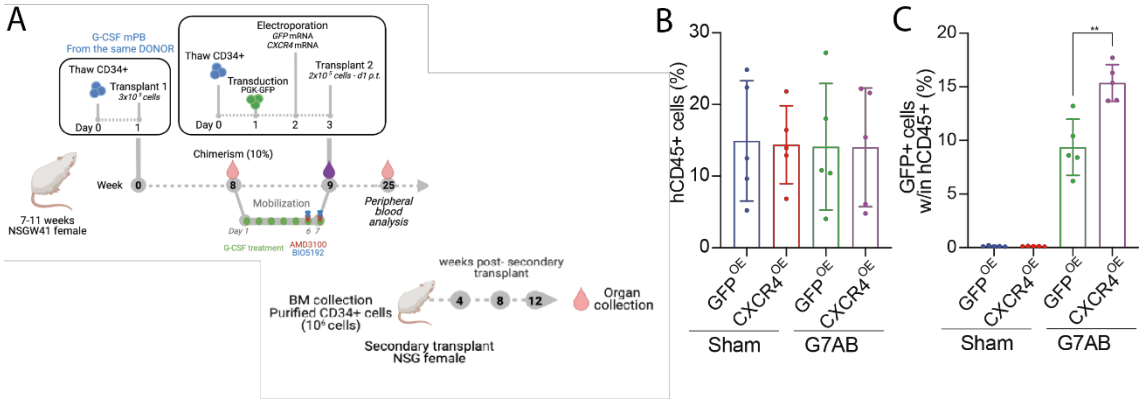


Figure 31. Secondary transplant

A) *Schematic illustration of competitive transplantation, after G7AB mobilization, between human resident cells and newly transplanted CD34+ G-CSF mPB GFP-transduced and electroporated cells in NSGW41 mice. After 12 weeks post-exchange, hCD34+ cells were isolated from donor BM and transplanted into secondary recipients.* ***B)*** *The percentage of human CD45+ cells in the PB of NSG mice at 16 weeks, following the secondary transplant of cells collected from groups described in Figure 25B.* ***C)*** *Percentage of human CD45+/GFP+ cells in PB of NSG mice at 16 weeks, following the secondary transplant of cells collected from groups described in Figure 25B.*

5.5 M-HSCT confers a clear advantage to gene-edited cells when paired with an engraftment enhancer

Ex vivo gene correction during autologous HSCT can reduce engraftment efficiency, particularly when using gene editing techniques (Schiroli *et al*, 2019). Initially, we monitored CXCR4 expression in cells edited for site-specific integration of a GFP-expressing cassette into the adeno-associated virus integration site 1 (AAVS1) safe harbor locus using an optimized protocol. CD34+ cells were electroporated with Cas9 ribonucleoprotein (RNP) assembled with sgRNA targeting AAVS1 and editing enhancers (GSE56/Ad5-E4orf6/7), immediately followed by transduction with a repair template carried by an AAV6-GFP vector (Figure 32A). CXCR4 expression decreased in gene-edited cells compared to electroporated-only cells (Figure 32B). To counteract this adverse effect on CXCR4, we co-electroporated cells with CXCR4 mRNA along with all the gene-editing components. Control cells received GFP mRNA with the same gene-editing machinery. Despite a decrease in migration potential observed in gene-edited cells with or without GFP overexpression, gene-edited HSPCs overexpressing CXCR4 showed higher migration potential in an in vitro migration assay, even when compared to electroporated-only control cells (Figure 32C).

We then investigated whether CXCR4 overexpression could confer an engraftment advantage to edited cells. While the chimerism level of edited cells (expressing GFP) only reached a median of 5% with the standard treatment, the addition of CXCR4 mRNA resulted in a 3-fold enhancement of engraftment, reaching a median of 15% (Figures 32D and 32E).

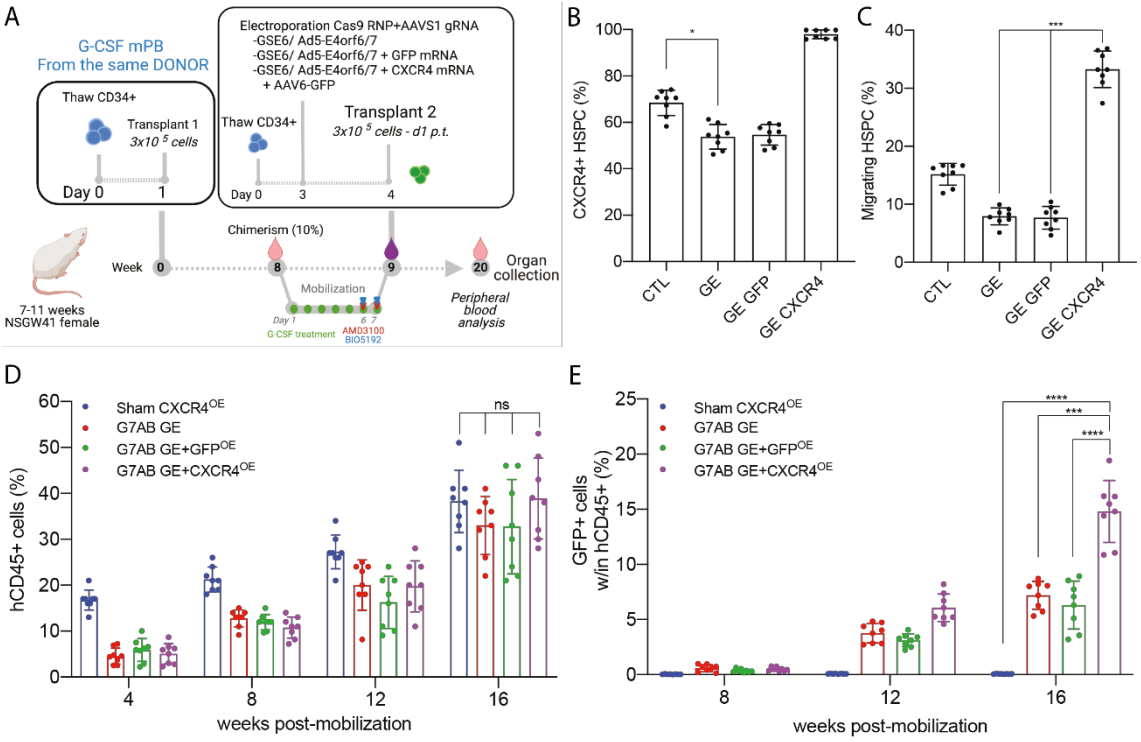


Figure 32. Coupling CXCR4 overexpression with HDR gene editing.
A) *Schematic illustration of competitive transplantation, after G7AB mobilization, between human resident cells (initially transplanted with 3 x10^5 CD34+ G-CSF mPB cells, counted on d1 p.t.) and newly transplanted CD34+ G-CSF mPB gene-edited cells (an outgrowth of 3 x10^5 CD34+ cells, counted on d1 p.t., and transplanted on d4 p.t.) in NSGW41 mice.* ***B-C)*** *The percentage of CXCR4+ cells in HSPCs (CD34+CD133+CD90+) (B) and of migrating HSPCs (C), following gene editing (GE; Cas9 RNA, AAVS1 sgRNA, and AAV6-GFP) combined or not with GFP (GE GFP) or CXCR4 (GE CXCR4) mRNA.* ***D-E)*** *Long-term follow-up of human CD45+ (D) and CD45+/GFP+ (E) cells in the PB after M-HSCT with CD34+ cells gene edited as in (A), in NSGW41 mice.*

Notably, because homology-directed repair (HDR) efficiency was approximately 40% as measured in the more primitive subset in vitro (Figure 33A), the total chimerism reached *in vivo* by cells edited together with CXCR4 mRNA would correspond to the levels reached by LV-transduced cells electroporated with CXCR4 mRNA in the previous experiment (40% GFP for cells transduced by LV to 90%). This result supports our earlier finding that editing with optimized enhancers can mitigate the impact of the procedure on HSPC repopulation properties (Ferrari et al., 2020). Lineage proportions within peripheral blood, bone marrow, and spleen remained similar for edited and non-edited cells, with or without the initial overexpression of CXCR4 (Figure 33B-G).

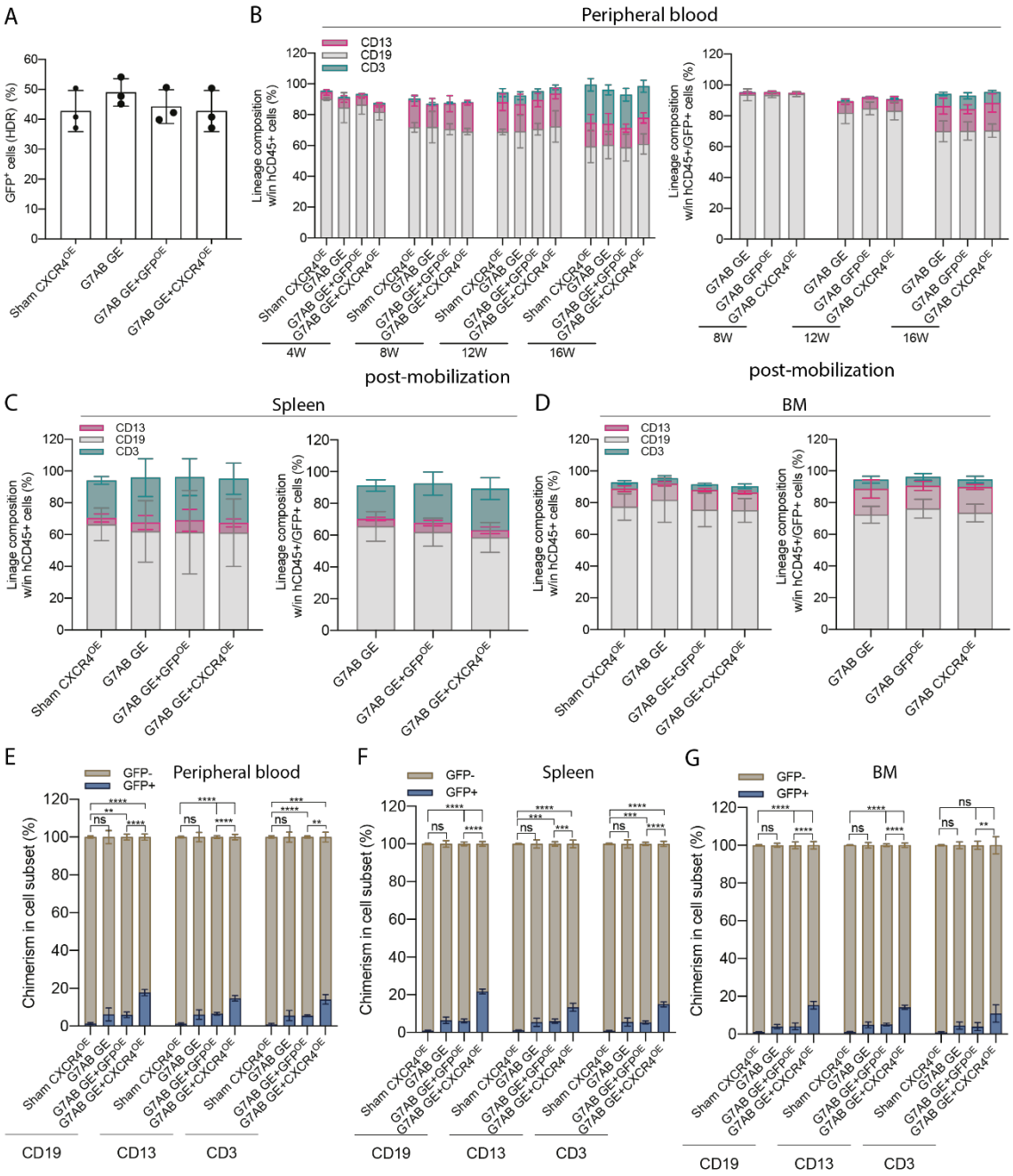


Figure 33. Transient CXCR4 overexpression confers HDR-edited cells an exchange advantage in different organs.

A) *HDR efficiency in edited cells (GFP+) on the bulk CD34+ population, assessed in vitro, 15 days post electroporation.* ***B)*** *The reconstitution of myeloid and lymphoid lineages over time of human CD45+ (left panel) and CD45+/GFP+ cells (right panel) in PB after M-HSCT with CD34+ cells gene edited as in main Figure 5A, in NSGW41 mice. The comparison of lineages between human CD45+ and CD45+/GFP+ cells was performed at the last time point by a mixed-effects model (REML), followed by a post hoc analysis with Dunnett's test (within groups).* ***C-D)*** *Myeloid and lymphoid lineage composition of human CD45+ (left panel) and CD45+/GFP+ cells (right panel) in the spleen (C) and BM (D) after M-HSCT with CD34+ cells gene edited as in main Figure 28B, in NSGW41 mice. The comparison of lineages between human CD45+ and CD45+/GFP+ cells was performed by a*

mixed-effect model (REML), followed by a post hoc analysis with Dunnett's test (within groups). ***E-G)*** *Chimerism of GFP+ cells was observed within CD19+ B cells, CD13+ myeloid cells, and CD3+ T cells at the end of the experiment in the PB (E), spleen (F), and BM (G) after M-HSCT with CD34+ cells gene edited as in main Figure 28B, in NSGW41 mice. A mixed-effect model (REML), followed by a post hoc analysis with Tukey's test (between groups) or by post hoc analysis with Dunnett's test (within groups). The results are mean ± SEM, with n ≥ 8 for data collected in vivo on NSGW41 mice, and n ≥ 5 for data collected in vitro (3 different donors). In all the analyses, p less than 0.05 were considered significant (*p < 0.05, **p < 0.01, ***p < 0.001, ****p < 0.0001. ''ns'' means non-significance).*

In conclusion, these findings demonstrate the adaptability of our strategy across various genetic engineering approaches and the feasibility of establishing a human hematopoietic graft comprising a fraction of edited cells sufficient to provide therapeutic benefits – as shown also for HIGM-1 – all without requiring preconditioning.

5.6 Investigating the engraftment advantage of AMD3100-resistant CXCR4 variants

While the results of M-HSCT described here are already promising, several strategies could further improve its efficacy. We tested different variants of CXCR4 (Rosenkilde *et al*, 2004, 2007; Ieranò *et al*, 2009; McDermott *et al*, 2011), all of which led to increased surface CXCR4 expression and conferred enhanced migration advantages to HSPCs (Figure 34A-C). Notably, two of these variants exhibited resistance to AMD3100 and even more so to AMD3465, while maintaining an efficient response to CXCL12, as demonstrated by the migration of overexpressing cells in the presence of CXCR4 antagonists (Figure 34D-E). These variants could be employed in the context of M-HSCT to further enhance the competitive advantage of infused cells over mobilized cells and potentially increase the extent of established chimerism.

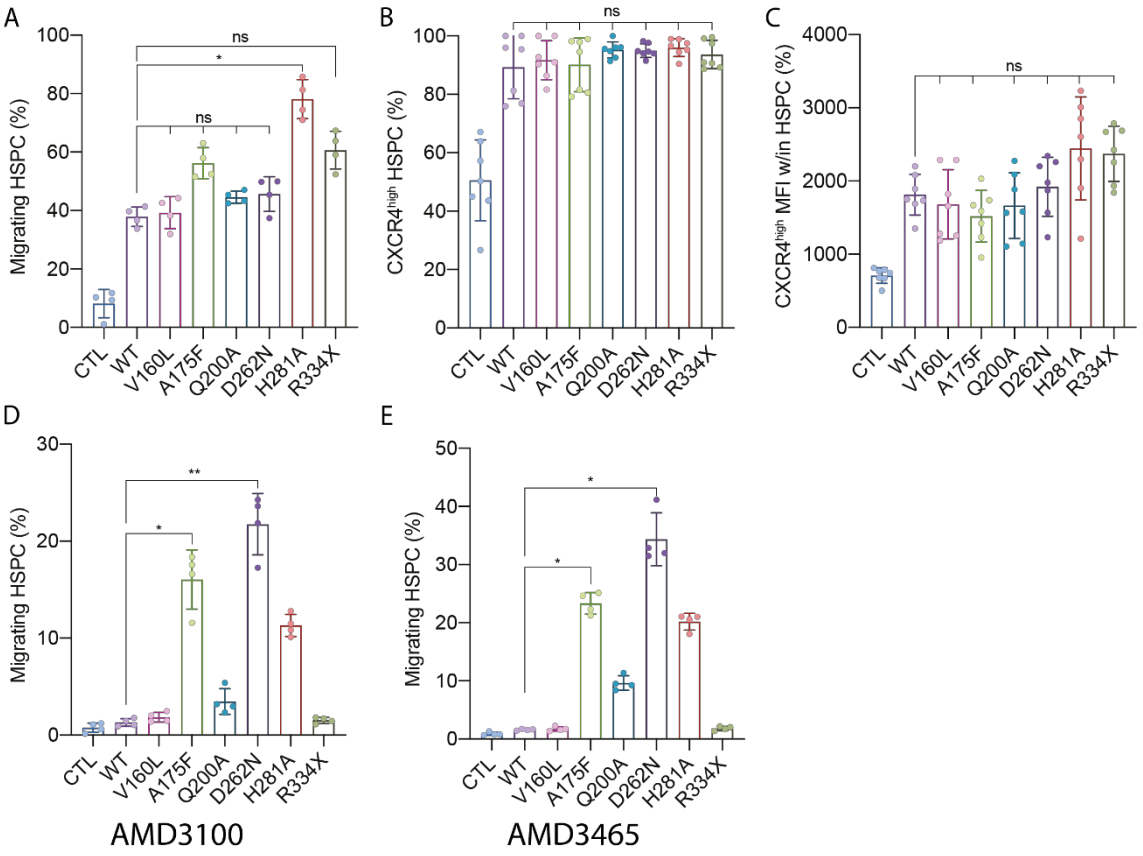


Figure 34. CXCR4 variants confer a migration advantage in presence of CXCR4 antagonists.
A-C) *The percentage of migrating HSPCs without treatment (A), in the presence of AMD3100 (B) or AMD3465 (C), electroporated with CXCR4 variants.* ***D)*** *The percentage of CXCR4^{high} cells in HSPCs (CD34+CD133+CD90+), electroporated with CXCR4 variants mRNA. A Kruskal-Wallis test, followed by a post hoc analysis with Dunn's test.* ***E)*** *CXCR4^{high} MFI in HSPCs (CD34+CD133+CD90+), electroporated with CXCR4 variants mRNA. A Kruskal-Wallis test, followed by a post hoc analysis with Dunn's test. The results are mean ± SEM, with n ≥ 5 for data collected in vitro (3 different donors). In all the analyses, p less than 0.05 were considered significant (*p < 0.05, **p < 0.01, ***p < 0.001, ****p < 0.0001. ''ns'' means non-significance).*

To investigate the potential of CXCR4 variants resistant to AMD3100 in or strategy, we employed the same mRNA-based transient overexpression approach described before to express these variants in human mobilized peripheral blood CD34+ cells. Our results showed that transplantation of HSPCs overexpressing the drug-resistant CXCR4 variant into hematochimeric mice resulted in enhanced exchange with the mobilized recipient cells, providing an advantage compared to cells overexpressing wild-type CXCR4, in particular when transplanting cells at the time of AMD3100 and BIO5192 injection

(Figure 35A-B). These findings suggest that the use of CXCR4 variants resistant to AMD3100 can further increase the advantage of donor cells.

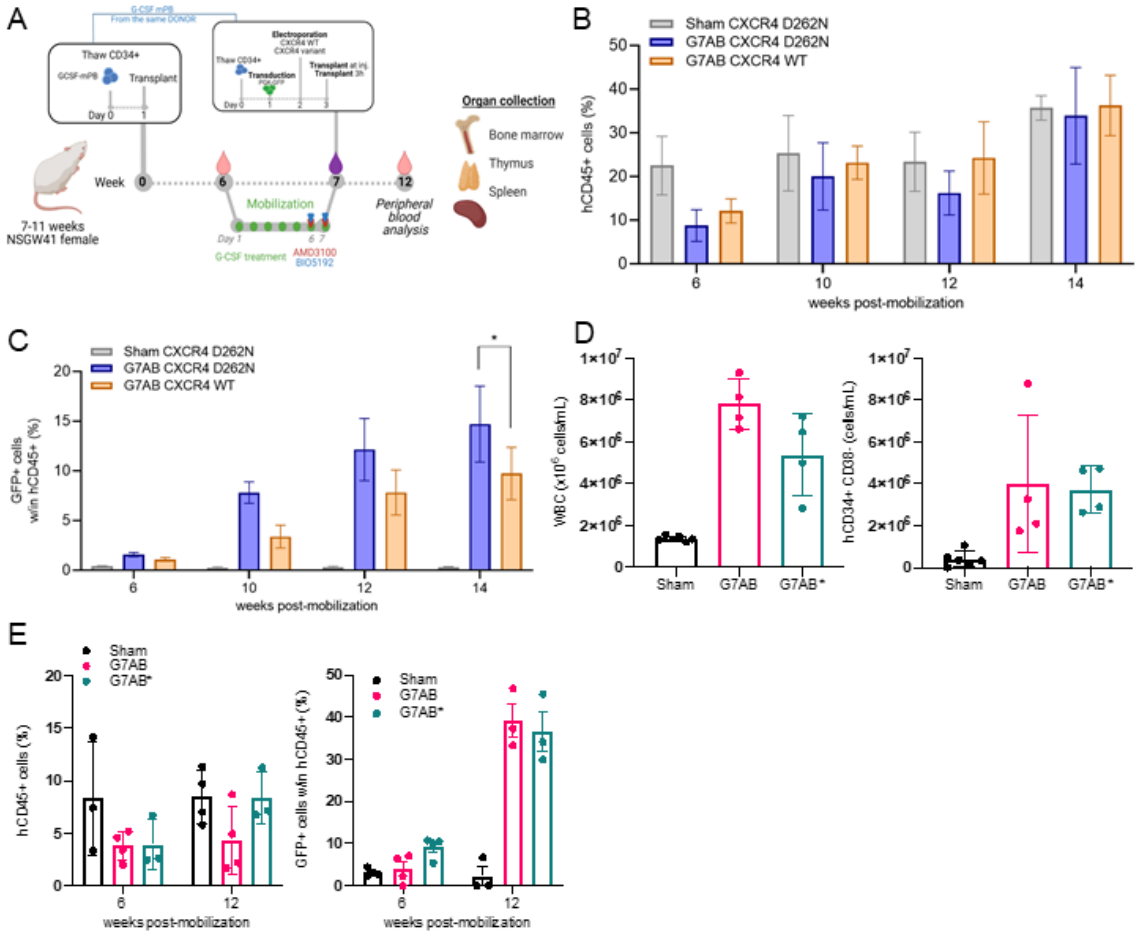


Figure 35. CXCR4 variant confers an engratment advantage in vivo.
A) *Schematic representation of the experimental design. NSGW41 or NBSGW mice were humanized with human mobilized peripheral blood CD34+ cells until 10% chimerism was achieved. Mice were then mobilized with G-CSF for 7 days through subcutaneous pump implantations and with two injections of AMD3100 and BIO5192 at day 6 and 7. For the second transplant, GFP lentiviral vector-transduced cells from the same donor used to humanize the mice were electroporated with either CXCR4 wild type or CXCR4^{D262N} variant. The donor cells were then transplanted either at 3h or immediately after the last injection of AMD3100.* ***B-C)*** *Human chimerism over time after mobilization, expressed as % of human CD45+ cells present in peripheral blood (B), and exchange efficiency (C) expressed as % of GFP+ cells within the hCD45+ population.* ***D)*** *Mobilization efficiency of the standard protocol (G7AB) or the modified protocol with AMD3465 (G7AB*) measured as white blood cell count (WBC, left panel), and human CD34+CD38- cells (right panel).* ***E)*** *Human chimerism over time after mobilization, expressed as % of hCD45+ cells in peripheral blood (right panel), and exchange efficiency (left panel) expressed as % of GFP+ cells within the hCD45+ population.*

In addition to their enhanced resistance to the AMD3100, we also evaluated the effect of CXCR4 variants on mobilization efficiency using the AMD3100 analogue AMD3465.

Mobilization efficiency was not affected by the use of AMD3465 compared to AMD3100 in the standard protocol with G-CSF, and BIO5192 (Figure 35C). Furthermore, we found that the exchange efficiency remained unchanged regardless of the use of AMD3100 or AMD3465 when transplanting donor cells at the peak of mobilization (Figure 35D).

Furthermore, besides CXCR4, other molecules could be explored to impart infused cells with a transient competitive advantage. As a proof of principle, we showed that the overexpression of KIT, ITGA4, or CD47 mRNA could provide *in vivo* engraftment advantages, similar to or even surpassing that observed for CXCR4. This supports the versatility and broad potential of our approach when coupled with mRNA-based genetic engineering of administered cells.

Altogether, these findings suggest that CXCR4 variants resistant to AMD3100 do not impair mobilization-based exchange. Moreover, preliminary results suggest that their use allows efficient exchange even when cells are administered at the time of AMD3100 injection, thus removing the constrain to infuse cells when the mobilizer is still high in circulation and potentially facilitating successful clinical translation.

5.7 Transient CXCR4 overexpression confers a migration advantage to non-human primate cells

In order to move forward our strategy towards clinical translation, we conducted a comprehensive investigation into key engraftment enhancers' expression in the BM of non-human primates (NHP), specifically Rhesus (*Macaca mulatta*) and Pigtail (*Macaca nemestrina*) models and found no significant disparities between the two sources. These NHP findings closely mirrored our earlier results obtained with human CD34+ cells, showing that CXCR4 expression, as well as KIT and ITGA4, are effectively restored during *ex vivo* culture of mPB HSPCs (Figure 36).

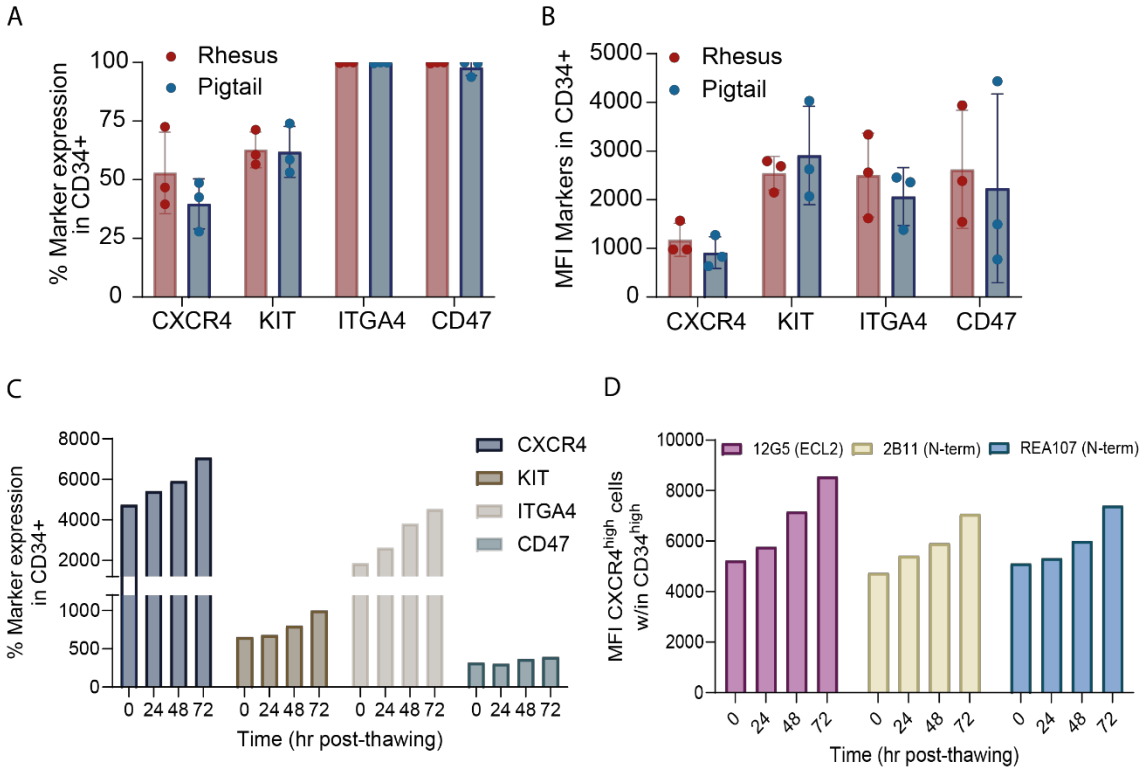


Figure 36. NHP cells characterization.
A-B) *Comparison of the percentage (A) and MFI (B) of BM CD34+ positive CXCR4, cKIT, ITGA4 and CD47 positive cells in Rhesus and Pigtail macaques.* ***C)*** *Kinetics of expression of CXCR4, cKIT, ITGA4 and CD47 in cultured pigtail mPB CD34+ cells.* ***D)*** *Expression kinetics of CXCR4 in pigtail mPB CD34+ cells with three different clones of Ab. Three biological replicates for each animal are shown.*

We subsequently studied the kinetics of CXCR4 overexpression in the NHP model using frozen mPB CD34+ cells electroporated with human CXCR4 mRNA. Concordantly with previous reports (Peterson *et al*, 2022), the addition of RNase inhibitor to the electroporation mix was necessary to obtain CXCR4 overexpression (Figure 37A and 37C). Interestingly, while the percentage of $CXCR4^{high}$ cells decreased gradually over time, the MFI returned to levels comparable with the mock electroporated control within 24h. We speculate that this shorter kinetics may be due to the higher RNase activity of this cell type or to an increased protein turnover compared to human cells. These results are concordant with *in vitro* migration assay data, showing a migration advantage for electroporated cells in both bulk CD34+ and the more primitive CD34+CD90+CD45RA- subpopulation at 6h post-electroporation (Figure 37B and 37D), and a lower advantage at 24h post-electroporation (Figure 37E).

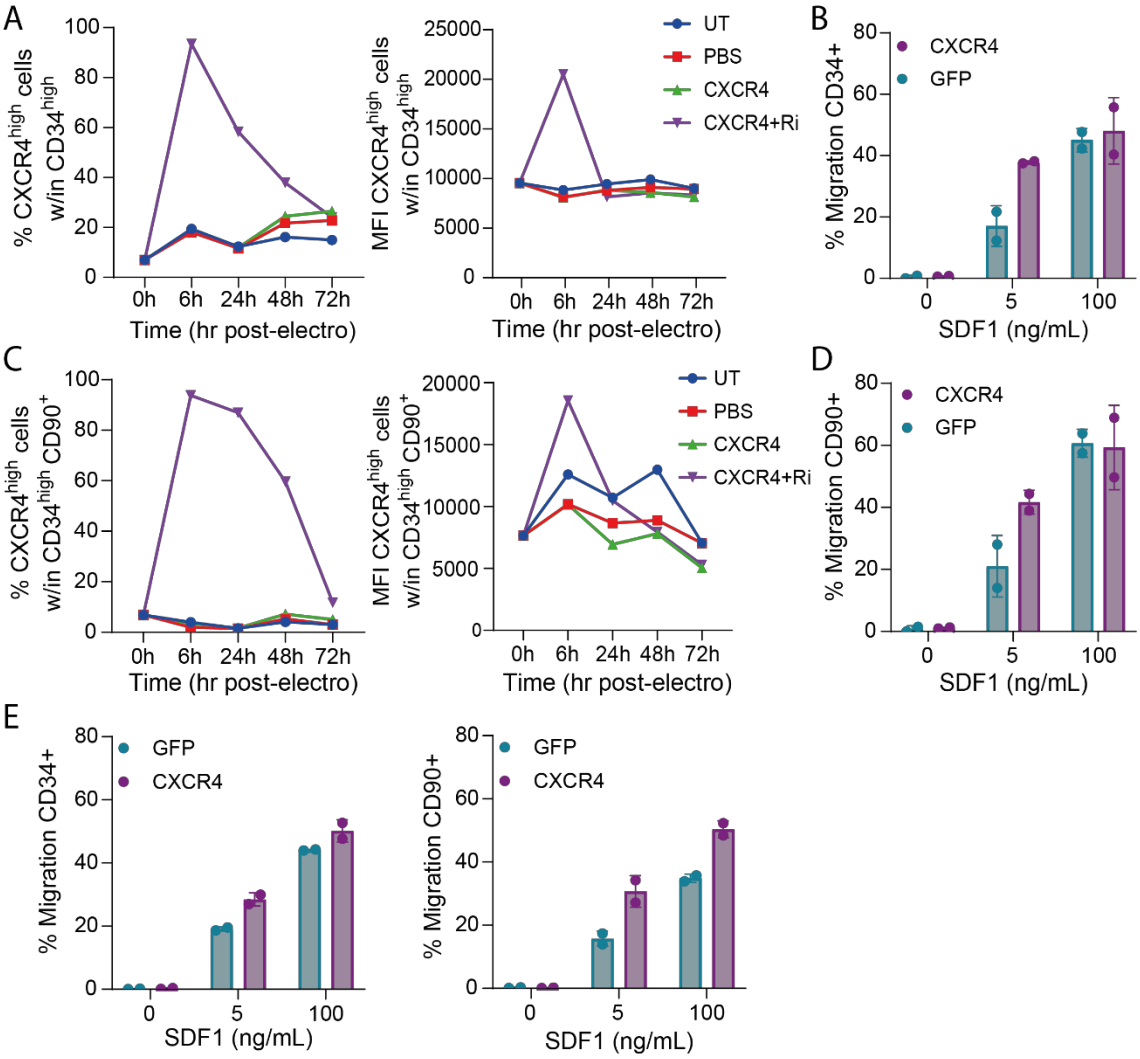


Figure 37. CXCR4 overexpression kinetics in NHP CD34+ cells.
A) Kinetics of CXCR4 overexpression in pigtail mPB CD34+ cells expressed as percentage (left panel) or MFI (right panel). B) Migration efficiency of CD34+ cells at 6h post-electroporation expressed as percentage of migrating cells over the total cells plated in the transwell. C) Kinetics of CXCR4 overexpression in pigtail mPB CD34+CD90+CD45RA- cells expressed as percentage (left panel) or MFI (right panel). D) Migration efficiency of CD34+CD90+CD45RA- cells at 6h post-electroporation expressed as percentage of migrating cells over the total cells plated in the transwell. E) Migration efficiency of CD34+ cells (left panel) and CD34+CD90+CD45RA- cells (right panel) at 24h post-electroporation expressed as percentage of migrating cells over the total cells plated in the transwell.

To eventually test and validate our strategy *in vivo*, resident cells need to be differentiated from the newly transfused ones. In NHP, the strategy applied in mouse models cannot be applied as LV-transduced cells stably expressing GFP can elicit strong immune responses leading to the clearance of edited cells (Berger *et al*, 2001). Therefore, we decided to

introduce a point mutation in the clinically relevant gene *CD33*, which is a myeloid differentiation antigen ubiquitously over-expressed on neoplastic cells in AML patients. This genetic modification aimed to render infused HSPCs CD33-negative while preserving their functionality and hematopoietic repopulation capacity, conferring resistance to targeted immunotherapies, including gemtuzumab ozogamicin (GO, Mylotarg^{TM}) and CD33-directed CAR-T cells (Borot *et al*, 2019; Humbert *et al*, 2019).

The predominant full-length CD33 isoform (CD33^{FL}) comprises seven exons, with treatments primarily focusing on epitopes within the domain encoded by exon 2 (Perez-Oliva *et al*, 2011). Therefore, Borot and colleagues explored the possibility of editing the *CD33* exon 2 splice acceptor site using the ABE8e adenine base editor (described by Richter *et al*, 2020), achieving over 95% editing at the targeted splicing acceptor adenine with minimal *indels* formation, as confirmed by Sanger sequencing (Borot *et al*, 2023). Prior studies revealed that both human and NHP CD33$^{\Delta 2}$ cells and CD33 KO cells can repopulate the BM niche and reconstitute functional myeloid cells upon transplantation in immunocompromised mice or NHPs (Kim *et al*, 2018; Borot *et al*, 2023). Moreover, it has been shown that approximately 30% of the human population is homozygous for a single nucleotide polymorphism (rs12459419) residing in the exon splicing enhancer site of exon 2, leading to increased expression of the CD33$^{\Delta 2}$ isoform (Karczewski *et al*, 2020), thus supporting the potential efficacy and safety of targeting this molecule in a future clinical application of epitope editing. Notably, Vor Biopharma is conducting a phase I/IIa clinical trial combining CD33 KO cells and Mylotarg^{TM} therapy in AML patients (NCT04849910).

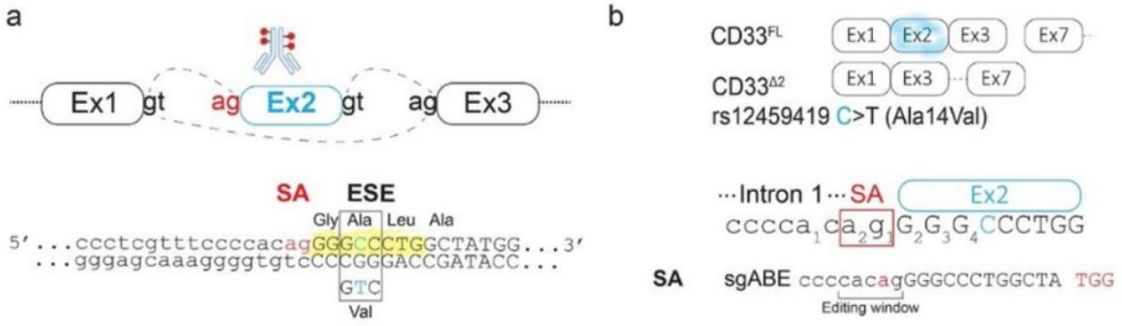


Figure 38. CD33 editing strategy.
A) *Top panel - Details of exon 1-3 region and possible splicing outcomes, ag: Splicing acceptor site (SA). gt: Splicing donor site. Dotted lines depict possible splicing event. GO Gentuzumab Ozogamicin (Ab icon) recognizes an epitope*

located in exon 2. Bottom panel - Details of the Intron1(lower case)/exon2(upper case) junction DNA sequence with highlight of exon 2 SA (red) and Exon Splicing Enhancer site (ESE in yellow). ***B)*** *Top panel - CD33 mRNA full length ($CD33^{FL}$) contains 7 exons, exon 2 encodes an Ig-like V-type domain. $CD33^{\Delta 2}$ lacks exon 2 due to a common polymorphism (rs12459419) which changes C>T. Bottom panel - Sequences of the protospacer design to edit the SA with ABE8e (sgABE). PAM is in red.*

We thus leveraged these findings to explore whether CXCR4 overexpression conferred an advantage to CD33-edited cells. Our observations indicated that these procedures could be successfully combined without compromising their individual efficiencies, thereby conferring a migration advantage in *in vitro* migration assays to edited cells (Figure 39A-D). However, when using an ABE8e ribonucleoprotein (ABE8e-RNP), we observed a substantial reduction in the CD90+ population, whereas electroporation with ABE8e mRNA showed similar levels of CD90+ cells to the mock electroporation condition (Figure 39E). This marked discrepancy in the effects is likely due to the relatively low purity of the ABE8e RNP, possibly arising from technical challenges in the purification process, thereby leading to increased cellular toxicity. We thus selected an all mRNA protocol for further studies.

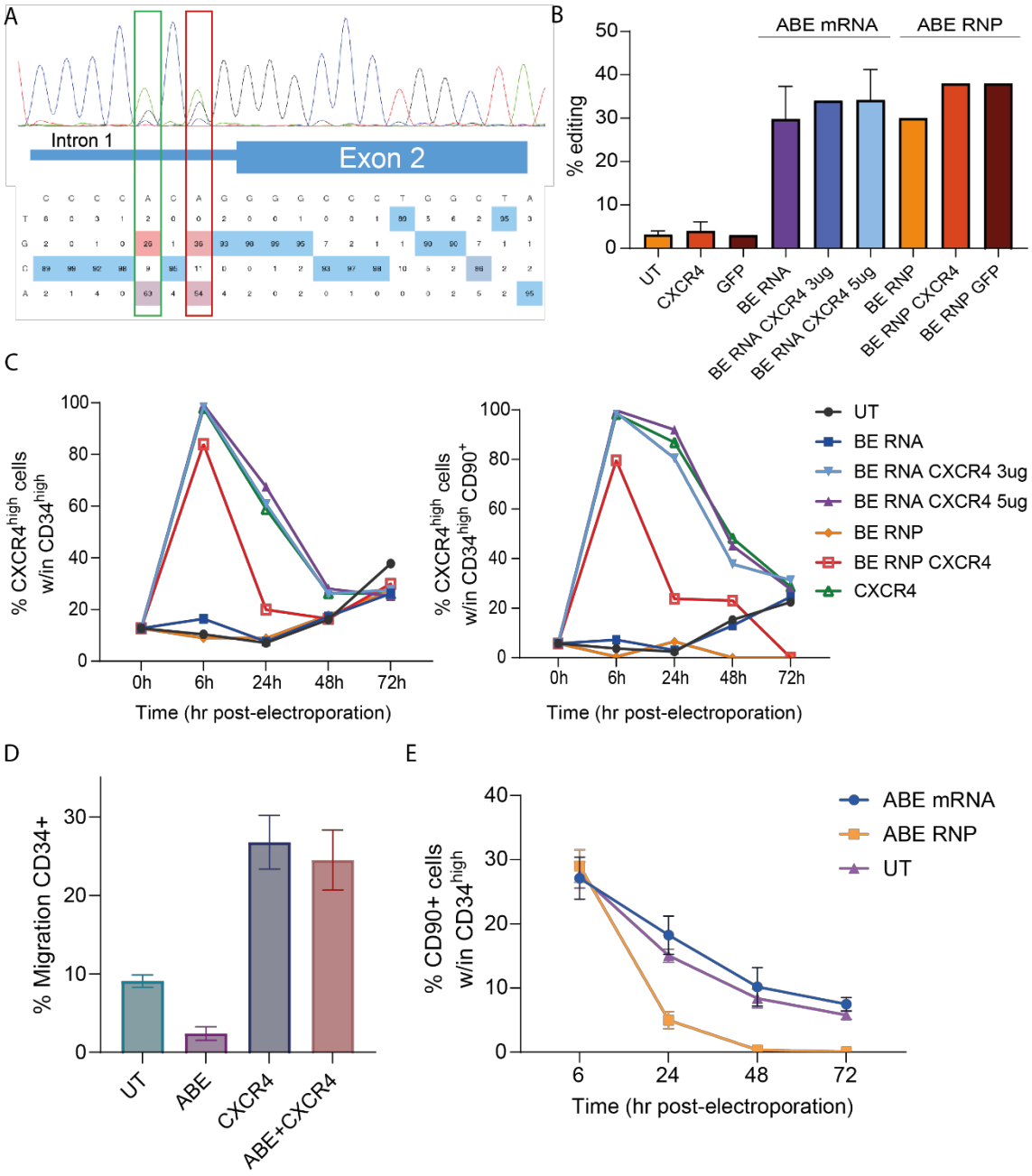


Figure 39. Coupling CXCR4 overexpression and CD33 base editing.
A) *Schematic representation of editing efficiency at the CD33 locus. Red square shows the on-target adenine editing efficiency, while the green square shows the bystander editing efficiency.* ***B)*** *Editing efficiency by Sanger sequencing expressed as percentage of edited on-target events.* ***C)*** *Kinetics of CXCR4 overexpression in pigtail mPB CD34+ cells (left panel) and CD34+CD90+CD45RA- cells (right panel)over time.* ***D)*** *Migration efficiency of mPB CD34+ cells at 6h post-electroporation expressed as percentage of migrating cells over the total cells plated in the transwell.* ***E)*** *Percentage of CD34+CD90+CD45RA- cells in different editing conditions. RNP=ABE8e ribonucleoprotein; BE=base editor (ABE8e+sgRNA).*

Using this protocol, we obtained similar results to those obtained with human CD34+ cells when an AMD3100-resistant CXCR4 variant was employed, showing a 2-fold migration advantage in presence of the drug (Figure 40).

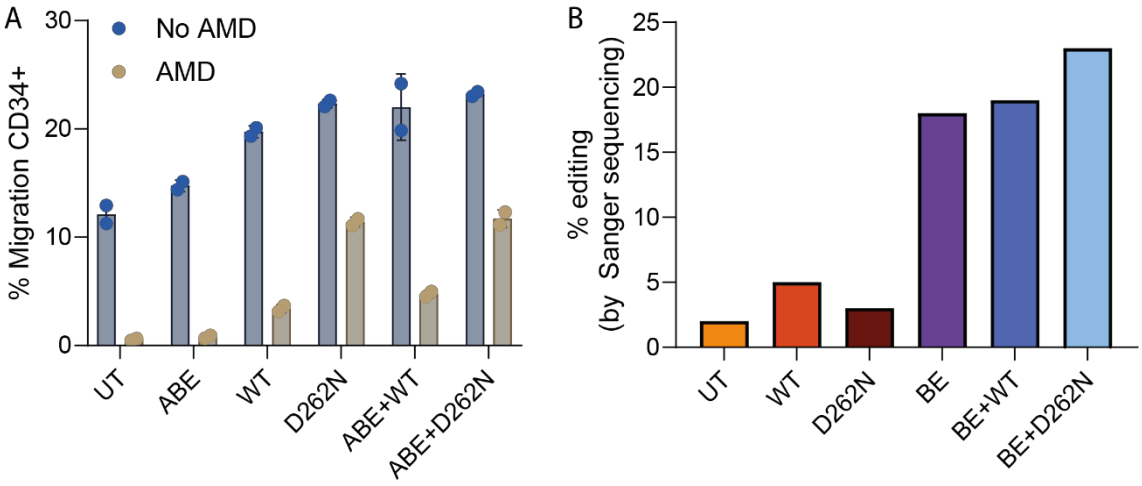


Figure 40. Coupling CD33 editing and overexpression of CXCR4 variant.
A) *Migration efficiency of mPB CD34+ cells at 6h post-electroporation expressed as percentage of migrating cells over the total cells plated in the transwell.* ***B)*** *Editing efficiency by Sanger sequencing expressed as percentage of edited on-target events.*

Overall, our in vitro findings with NHP HSPCs overlap with those observed with human CD34+ cells, although with a shorter kinetic of CXCR4 overexpression. Moreover, recent data from the literature show that CXCR4 overexpression increases HSC engraftment in NHPs (Wang *et al*, 2022). Therefore, successful translation of our approach in the NHP model will enable us to move toward clinical trials with greater confidence. To achieve this goal, we plan to test two different approaches. In the first strategy, we will mobilize one NHP with G-CSF for 6 days, performing two AMD3100 injections on days 5 and 6. After the first dose of AMD3100, we will isolate CD34+ cells from leukapheresis and, after overnight culture, cells will be electroporated with CXCR4 mRNA, ABE8e mRNA, and the CD33 sgRNA. At six hours after electroporation (i.e. at CXCR4 peak of expression), cells will be infused in the donor animal. This approach will mimic our strategy already validated in the mouse model. The second approach will be based on the actual clinical practice for HSPC-GT. In this second strategy, the animal will be mobilized for 5 days with G-CSF and will receive only one dose of AMD3100 on the last day. Upon cell isolation from the apheresis product and overnight culture, cells will be electroporated with CXCR4 mRNA, ABE8e mRNA, and the CD33 sgRNA and

subsequently frozen down. We will then wait 6-8 weeks to allow the animal to recover from the procedure and perform a second cycle of mobilization and apheresis before transplant. This apheresis procedure will be performed to eliminate competing cells from the circulation and, in a clinical setting, would be useful to store cells for an eventual second transplant. Moreover, the delay between cell editing and transplant would allow to perform quality tests and evaluate the genome integrity. A control animal will be mobilized as the second animal although after the 6-8 weeks resting period, edited cells will be infused without a second mobilization cycle. This would allow us to assess the engraftment efficiency without prior mobilization-based conditioning.

6 DISCUSSION

In this study, we present evidence supporting the potential of harnessing HSPC mobilization as a promising strategy in HSCT and HSPC-GT. This approach leverages a crucial time window, at the peak of mobilization, when donor cells possess a competitive advantage over circulating ones, allowing them to efficiently repopulate the depleted BM niches. Donor cell superiority arises from the rescue of HSPC functionality during *ex vivo* culture, mitigating the detrimental impact of mobilization agents. The transient overexpression of key engraftment effectors further enhances this advantage. We offered a proof of concept for this approach using a mouse model of Hyper-IgM Syndrome-1 (HIGM-1), employing healthy bone marrow cells as surrogates for autologous genetically corrected cells. Subsequently, we demonstrated the method's applicability to human HSPCs and its adaptability to diverse genetic engineering strategies. Although it remains challenging to properly define and investigate the most primitive HSC population, we confirmed the efficient engraftment of LT-HSCs by serial transplantation into xenogenic recipients.

6.1 Limitations of the mouse model

Our study of human HSCT has been necessarily performed in the hematochimeric mouse model, which represents the most frequently adopted model for testing new experimental manipulations of human HSPC. Although powerful, this model still imposes some limitations on the prediction of the results in a future clinical setting, as the murine BM niche may not fully represent the human architecture and local factors may have lower specific activity toward human cells and/or different biodistribution. Indeed, NSGW41 hosts were required to demonstrate an efficient exchange of infused human HSPCs as they provide for less competition from mouse resident cells and compensate for the lower specific activity of murine factors on human HSPC. Nevertheless, we do expect that our findings might still be predictive of a fully human setting as the mobilization yields resemble those obtained in the clinic (50–100 CD34+/mL mobilized) and we obtained overlapping results with both mouse and human HSPCs. Additionally, clonal composition of the graft and biodistribution studies are required to confirm the heterogeneity of the exchanged population.

Other factors requiring consideration encompass the kinetics and variability of HSPC mobilization in human patients, crucial for the timely infusion of the drug product. Precise timing is paramount, as infusing edited cells too early or too late may result in occupied niches, hindering successful engraftment. However, the potential benefits of combining mobilization with the removal of circulating HSPCs through apheresis have not been modelled in our hematochimeric mice. In theory, this combination might further diminish the competition between resident and infused cells. These inquiries are anticipated to be most effectively addressed in NHPs, which is considered to be the most rigorous model for human HSPC physiology. Additionally, as NHPs are presumed to more accurately mirror human tissue distribution of CXCL12 compared to mice, they are better suited for validating the engraftment advantage of transiently overexpressed CXCR4 in infused cells (Wang *et al*, 2022). Encouragingly, our preliminary results in this model overlap with what was observed in human cells and in our humanized mouse model.

6.2 Leveraging mRNA-based transient overexpression to confer an engraftment advantage

Although we were able to successfully engraft HSPCs after mobilization, we also observed that this was due to the advantage acquired by *ex vivo* cultured cells, which recovered the expression of CXCR4 and other factors involved in homing and retention. Subsequently, the transient overexpression of CXCR4 offered a significant advantage to infused cells. The approach we present is streamlined into the *ex vivo* HSPC engineering process, facilitating the recovery of essential surface molecules for homing and engraftment that are compromised by the mobilization protocol itself. Furthermore, we observed that the electroporation step used to introduce the genetic engineering machinery in the cell, negatively affects HSPC engraftment or repopulation potential by downregulating CXCR4 expression. Therefore, transient overexpression of CXCR4 or other molecules involved in HSPC homing and retention can enhance HSPC fitness and rescue engraftment efficiency. This strategy aligns with recent advancements in mRNA engineering, utilizing modified nucleotides and optimized designs to achieve sustained gene expression without provoking innate immune responses. Importantly, the mRNA-only platform mitigates the risk of accidental genomic integration of effector transgenes. These effector molecules encompass critical homing receptors, adhesion molecules, and

phagocytosis inhibitors, potentially expanding to other genes involved in self-renewal. Overall, our mRNA-based strategy has proven to be compatible with gene transfer, gene replacement, and base editing, showing compatibility with a great diversity of gene therapy strategies and, therefore, it may easily be streamlined in the editing protocol for a plethora of diseases.

Engineering these engraftment enhancers may endow transplanted cells with an even greater advantage as demonstrated by our proof-of-principle studies with AMD3100-resistant CXCR4 variants or by editing the targets of different immunotherapy strategies (Casirati *et al*, 2023; Borot *et al*, 2023). To achieve this goal, it would be possible to employ traditional protein engineering methods like rational design and directed evolution, or emerging AI-assisted approaches (Ferruz & Höcker, 2022). While rational design relies on known protein structures for precise modifications, AI models show promise for designing novel proteins and studying conformational changes caused by different mutations (Yang *et al*, 2019; Ferruz *et al*, 2022; Madani *et al*, 2023; Cheng *et al*, 2023). On the other hand, directed evolution creates diverse variants through random mutations, improving functions through iterative selection without requiring prior knowledge of protein structure (Arnold, 1998). Although its application in mammalian cells poses challenges in translation due to differences in protein folding and cellular signaling (Packer & Liu, 2015), efforts to shift directed evolution to mammalian systems have proven successful (Hendel & Shoulders, 2021; Hess *et al*, 2016; Chen *et al*, 2020). Therefore, we can envision the possibility to engineer engraftment enhancers to further improve the advantage of transplanted cells, eventually allowing a broader time window for the transplant, and thus removing the constrain of timely infusion of edited cells at the peak of mobilization.

6.3 Enhancing mobilization to deplete the BM niche

Overall, we showed that mobilization can be enhanced to efficiently vacate the BM niche, thus allowing the exchange between donor and recipient cells. Notably, the extent by which the niche is emptied depends on the mobilization protocol. Importantly, we could achieve an exchange using the clinically approved combination of G-CSF and Plerixafor, though the exchange efficiency significantly improved when we included BIO5192, which is currently not approved for clinical use. Nevertheless, we could

envision to repurpose the mAb Natalizumab, which is currently approved for the treatment of multiple sclerosis, to target the same pathway as BIO5192 (ITGA4/VICAM1), as already tested by other groups (Zohren *et al*, 2008; Jing *et al*, 2010, NCT05618301). Moreover, considering the detrimental impact on the BM niche induced by G-CSF treatment, ongoing developments in mobilization agents – as the Motixafortide (CXCR4/SDF1 inhibitor, Crees *et al*, 2023) and Natalizumab combination (NCT05618301) – or HSPC-targeting immunotoxins, may offer promising alternatives, potentially reducing or eliminating the need for G-CSF treatment. This shift could preserve BM niches, enabling more rapid hematopoietic reconstitution by gene-corrected cells. In circumstances where the removal of G-CSF might compromise the competitiveness of mobilized cells, the use of engraftment enhancers could become essential. Despite the focus of this study did not encompass the toxicity profile, we anticipate it to be in line with that associated with clinically used mobilizers, which have demonstrated an excellent safety record with minimal adverse effects. Additionally, the serial administration of corrected cells from a stored cell product following additional mobilization cycles could further enhance engraftment of gene-corrected cells.

6.4 Future perspectives and clinical translation

A significant advantage of mobilization-based conditioning lies in its ability to spare the host's immune system, thereby eliminating the occurrence of cytopenias. This departure from conventional conditioning methods helps avoid the profound immunosuppression typically associated with such approaches, along with their short- and long-term consequences, including infections, mucositis, veno-occlusive disease, and endocrine dysfunction (Inamoto & Lee, 2017; Carreras *et al*, 2019; Grupp *et al*, 2023). This, in turn, would result in a substantial reduction in the morbidity and hospital stay associated with the procedure. Once mobilization-based HSCT has undergone comprehensive validation for its first clinical testing, its initial application may be best suited for autologous HSCT settings that do not necessitate a high threshold of correction or lymphodepletion/immune suppression. Autologous HSC-GT for severe combined immunodeficiencies (SCIDs) and DNA repair diseases could be particularly suitable (Dufour, 2017), as these conditions are prone to chemotherapy toxicity and are often treated with low-dose conditioning regimens that could potentially be replaced by HSPC

mobilization. The historical use of congenital disorders of hematopoiesis as model diseases for the development of innovative therapies further supports this potential application (Schmidt *et al*, 2017; Naldini, 2019; Rüesch *et al*, 2022). In this regard, we demonstrate the proof of concept for phenotypic rescue of Hyper-IgM Syndrome-1 (HIGM-1) through M-HSCT in a mouse model, albeit utilizing wild-type cells as a surrogate for edited cells. Allogeneic HSCT remains the sole curative treatment for HIGM-1 as the limited availability of matched donors and the associated risks of graft rejection, GvHD, infections, and other complications result in restricted survival improvements for HIGM-1 patients (Ferrua *et al*, 2019). Thus, the pursuit of alternative therapeutic approaches that are safer and more effective, particularly for patients with a higher risk profile for HSCT, becomes crucial. M-HSCT involving autologous cells corrected via gene editing may offer a promising solution, with engraftment enhancers compensating for the HDR efficiency limitations in primitive HSPCs (Vavassori *et al*, 2021). Additionally, there is promise for mobilization-based conditioning in emerging HSPC-based anticancer gene therapies, which rely on gain of function in specific lineages emerging from a fraction of HSPCs (Mucci *et al*, 2021; Birocchi *et al*, 2022).

As described before, in a typical autologous HSPC-GT procedure cells are collected post-mobilization, they subsequently undergo genetic modification, and are then cryopreserved for quality control assessments. Upon successfully passing these evaluations, the patient undergoes chemotherapy before receiving the drug product. In the context of mobilization-based HSPC-GT protocols, integration into this established clinical framework is essential. A prospective approach involves mobilizing HSPCs once for harvest and drug product manufacturing, conducting quality controls, and subsequently administering mobilizers just before drug product infusion. However, the potential development of all-in-one mobilization and engraftment protocols hinges on achieving a feasible *ex vivo* manufacturing process within a 24–48-hour timeframe (as seen in some ongoing clinical studies) that is both reproducible and yields satisfactory outcomes. The option of repeat administration of a stored drug product might be considered if engraftment proves unsatisfactory across successive mobilization cycles, given the established safety profile of the mobilization protocol. Nevertheless, a more comprehensive understanding of the kinetics of HSPC egression and recirculation during subsequent mobilization rounds necessitates further modelling efforts.

Expansion to more common conditions, such as allogenic HSCT, or HSCT for malignant diseases will be far more challenging, as HSPC exchange on its own does not suppress the immune system, nor does it kill tumour cells. Different approaches could be envisioned here: (i) combination with low-dose chemotherapy (Konopleva *et al*, 2015) or (ii) combination with immune-depleting agents, both antibody based (alemtuzumab, anti-thymocyte globulin) or not (cyclophosphamide, fludarabine).

Eventually, the combination of mobilization and enhanced engraftment efficiency explored in our research could revolutionize the HSPC-GT landscape, potentially eliminating the need for chemo/radiotherapy. This innovative approach could deliver long-term therapeutic benefits to patients with significantly reduced risks and long-term toxicity. Furthermore, new conditioning regimens, such as those involving selective immunodepletion, may align with our strategy by implementing engraftment enhancers tailored to the specific requirements of each approach.

7 MATERIALS AND METHODS

7.1 Experimental models

7.1.1 Cell lines

HEK293T cells were cultured in Iscove's modified Dulbecco's medium (Corning) supplemented with 10% heat-inactivated fetal bovine serum (Euroclone), 100 IU.ml^{-1} penicillin, 100 µg.ml^{-1}, streptomycin and 2% glutamine.

7.1.2 Primary human CD34+ cells

G-CSF mPB CD34^{+} HSPCs and G-CSF/Mozobil mPB CD34^{+} HSPCs were purchased from Mobilized Leukopak (AllCells) according to TIGET-HPCT protocol approved by the San Raffaele Institute Bioethical Committee and purified with the CliniMACS CD34 Reagent System (Miltenyi Biotec) according to the manufacturer's instructions. HSPCs were seeded at the concentration of 1×10^{6} cells per ml in serum-free StemSpan medium (StemCell Technologies) supplemented with 100 IU.ml^{-1} penicillin, 100µg.ml^{-1} streptomycin, 2% glutamine, 300ng.ml^{-1} hSCF, 300ng.ml^{-1} hFlt3-L, 100ng.ml^{-1} hTPO, 1µM SR1, 35nM UM171 and 10µM PGE2 (except when a subsequent transduction is planned). All cells were cultured in a 5% CO2 humidified atmosphere at 37 °C. *In vivo*, the human HSPC population was defined as CD34^{+}CD38^{-}CD90^{+}, and *in vitro* as CD34^{+}CD133^{+}CD90^{+}.

7.1.3 Xenogeneic mouse transplantation models

NSG, NSGW41, and NBSGW mice were purchased from The Jackson Laboratory and maintained in specific-pathogen-free (SPF) conditions. The procedures involving animals were designed and performed with the approval of the Animal Care and Use Committee of the San Raffaele Hospital (IACUC #876 for NSGW41 and NSG, #1358 for NBSGW) and communicated to the Italian Ministry of Health and local authorities according to Italian law.

7.1.4 Syngeneic mouse transplantation model

C57Bl/6 Ly45.1, C57Bl/6 Ly45.2 mice were purchased from Charles River Laboratory. *Cd40lg*$^{-/-}$ (B6.129S2-Cd40lgtm1Imx/J) mice were purchased from The

Jackson Laboratory and maintained in specific-pathogen-free conditions. The procedures involving animals were performed with the approval of the Animal Care and Use Committee of the San Raffaele Hospital (IACUC #818) and communicated to the Italian Ministry of Health and local authorities according to Italian law.

Donor mice between 6 and 10 weeks of age were euthanized by CO_2, and BM cells were retrieved from femurs, tibias, and humeri. HSPCs were purified by Lin- selection using the mouse Lineage Cell Depletion Kit (Miltenyi Biotec) according to the manufacturer's instructions. Cells were either directly transplanted in recipient mice, or cultured (for 2 hours or overnight) in serum-free StemSpan medium (StemCell Technologies) containing penicillin, streptomycin, glutamine, and a combination of mouse cytokines (20 ng/ml IL-3, 100 ng/ml SCF, 100 ng/ml Flt-3L, 50 ng/ml TPO all from PeproTech), at a concentration of 2-5x10^6 cells.ml^{-1}. Purified Lin^- cells were transplanted at a total dose of 2x10^6 cells/mouse into 8 to 12-week-old mobilized mice, three hours after the last injection of AMD3100 and/or Bio5192. Serial collections of blood from the retro-orbital vein were performed to monitor the hematological parameters and donor cell engraftment. At the end of the experiment, BM, thymus and spleen, and lymph nodes were harvested and analyzed.

7.1.5 Non-human primates animal housing and care/Ethics Statement

Healthy juvenile rhesus macaques were housed at the University of Washington National Primate Research Center (WaNPRC) under conditions approved by the American Association for the Accreditation of Laboratory Animal Care. All experimental procedures performed were reviewed and approved by the Institutional Animal Care and Use Committee of the Fred Hutchinson Cancer Research Center and University of Washington (Protocol no. 3235-01, -04, and -06). This study was performed in strict accordance with the recommendations in the Guide for the Care and Use of Laboratory Animals of the National Institutes of Health (they were HLA typed and assigned based on their genotype as described in the results section. No random assignment). This study included at least twice daily observation by animal technicians for basic husbandry parameters (eg, food intake, activity, stool consistency, and overall appearance) as well as daily observation by a veterinary technician and/or veterinarian. Animals were housed in cages approved by The Guide and in accordance with Animal Welfare Act regulations.

Animals were fed twice daily and were fasted for up to 14 h before sedation. If a clinical abnormality was noted by the WaNPRC personnel, standard WaNPRC procedures were followed to notify the veterinary staff for evaluation and determination for admission as a clinical case. Animals were sedated by administration of ketamine HCl and telazol and supportive agents before all procedures. Following sedation, animals were monitored according to WaNPRC standard protocols. Analgesics were provided as prescribed by the Clinical Veterinary staff for at least 48 h after the procedures and could be extended at the discretion of the veterinarians, based on clinical observations. Decisions to euthanize animals were made in close consultation with veterinary staff and were performed in accordance with guidelines as established by the American Veterinary Medical Association Panel on Euthanasia (2013). Prior to euthanasia, animals were sedated by administration of ketamine HCl.

7.1.6 Non-human Primates CD34+ cells enrichment and in vitro *culture*

NHP CD34+ cells were isolated from BM aspirates, and/or mobilized leukapheresis. G-CSF (Amgen) was injected subcutaneously (s.c.) at 50 µg/kg for 5 days. AMD3100/Plerixafor was given s.c. at 5 mg/kg on the last day of mobilization, 6h before leukapheresis. From both BM aspirates and leukapheresis samples, CD34+ cells were isolated by immunomagnetic cell separation with the aid of an anti-CD34 antibody (clone12.8) and anti-IgM microbeads (magnetic-assisted cell sorting technology [MACS]; Miltenyi Biotech).

Enriched CD34+ cells were cultured overnight prior to electroporation in serum-free expansion medium StemSpan SFEM II (STEMCELL Technologies, Vancouver, Canada) supplemented with 1% penicillin-streptomycin (Gibco), and 100 ng/mL each of recombinant human stem cell factor (SCF-1) (PeproTech, Rocky Hill, NJ), thrombopoietin (TPO-1) (PeproTech), and FMS-like tyrosine kinase 3 ligand (FLT-3) (PeproTech).

7.2 LV vector production and titration

VSV.G-pseudotyped third-generation self-inactivating lentiviral vectors (SINLV) were produced by calcium phosphate transient transfection into 293Tcells. 293T cells were transfected with a solution containing a mix of the LV genome transfer plasmid,

bearing the expression cassette for GFP, the packaging plasmids pMDLg/pRRE, pMD2.VSV.G, pKRev(pILVV01) and pAdVantage (Promega). Medium was changed 14-16 hours after transfection and supernatant was collected 30 hours after medium change. LV-containing supernatants were passed through a 0.22 μm filter (Millipore) and transferred into sterile polyallomer tubes (Beckman) and centrifuged at 20,000 g for 120 min at 20° C (Beckman Optima XL-100KUltracentrifuge). LV pellet was dissolved in the appropriate volume of phosphate buffered saline (PBS) to allow 500X concentration. Concentrated vector stock was aliquoted and stored at -80°C. LV titer was determined by flow cytometry 4-5 days after LV transduction analysis or ddPCR, 10-14 days after LV transduction.

7.2.1 Transduction

10^6 $CD34^+$ cells/ml were stimulated with 10μM PGE2 20 hours post-thawing. After 2 hours of pre-stimulation, cells were infected for 14 hours with LV-GFP at multiplicity of infection (MOI) 100. When necessary, cells were electroporated 14 hours post-transduction.

7.3 mRNA IVT

GFP, ITGA4, CXCR4, CD47 and *KIT* cDNA coding RNA were synthetized (GeneArt, Thermo Fisher) using Homo Sapiens codon-optimized algorithm. A complementary *CXCR4* sequence was produced with reduced uridine content (dU). Coding sequences were subcloned in 'pVax' plasmids under the control of the following 5' aptamer sequence: CapAG – eIF4G aptamer (GACTCACTATTTGTTTTCGCGCCCAGTTGCAAAAAGTGTCG) - Kozak sequence (CCACC) – start codon (ATG). Downstream the codon-optimized sequence follows a woodchuck hepatitis virus posttranscriptional regulatory element and a 120-bp polyA sequence.

For mRNA IVT, pVAX plasmids were linearized with SpeI (New England Biolabs) restriction enzyme and purified by phenol-chloroform extraction. mRNA was *in vitro* transcribed using the commercial 5X MEGAscript T7 kit (Thermo Fisher) and capped with 5mM of CleanCapAG (Trilink). Different modified nucleotides were used: 5-Methoxyuridine-5'-Triphosphate (moU), Pseudouridine-5'-Triphosphate (pU), 5-

Methylcytidine-5'-Triphosphate (mC; Trilink) at a concentration of 7.5mM. mRNA was purified using RNeasy Plus Mini Kit (Qiagen) followed by high-performance liquid chromatography purification (ADS BIOTEC WAVE System) and Amicon Ultra- 15 (30 K) tube (Millipore) concentration. mRNA productions were aliquoted and stored at −80 °C. All RNA samples were analyzed by denaturing agarose gel electrophoresis to assess the quality and integrity.

7.4 Electroporation

Cells were electroporated with 5µg of encoding mRNA, two days post-thawing. Transfections were performed using the 4D-NucleofectorTM System (Lonza) and following manufacturer's instructions primary cells (P3 Primary Cell 4D-Nucleofector X Kit, program EO-100; Lonza). From 6h to day 10 after electroporation, target protein expression within HSPC subpopulations was evaluated by flow cytometry.

7.5 Gene editing of human HSPCs and analyses

For AAV6-based gene editing, 1×10^6 $CD34^+$ cells (mobilized with G-CSF) after 3 days of culture in the medium described above were washed with ten volumes of DPBS and electroporated using P3 Primary Cell 4D-Nucleofector X Kit and program EO-100 (Lonza). Cells were electroporated with RNPs at a final concentration of 2.5 µM together with 0.1 nmol of Alt-R Cas9 Electroporation Enhancer (Integrated DNA Technologies), according to the manufacturer's instructions. AAV6 transduction was performed at a dose of 1×10^4 vg per cell 15 min after electroporation. Additional mRNAs were added in the gene editing mixture as follows: (i) 3.5µg *GSE56/Ad5-E4orf6/7* (Fusion protein with P2A self-cleaving peptide) mRNA, (ii) 3.5µg *GSE56/Ad5-E4orf6/7* mRNA and 3.5µg *GFP* mRNA or *CXCR4* mRNA. Three and fifteen days after the editing procedure, cells were harvested to measure the percentage of cells expressing the GFP marker by flow cytometry and to extract genomic DNA for molecular analyses, as described (Ferrari *et al*, 2020).

7.6 Adenine base editing

ABE8e-NG mRNA was ordered as custom product from Trilink Biotechnologies. mRNAs were transcribed *in vitro* from PCR product using full substitution of N1-methylpseudouridine for uridine and was capped co-transcriptionally using the CleanCap AG analogue (Trilink Biotechnologies), resulting in a 5' Cap 1 structure. Mammalian - optimized UTR sequences (Trilink) and a 120-base poly-A tail were included in the transcribed PCR. Chemically modified sgRNA (CCCCACAGGGGCCCTGGCTA) was purchased from IDT.

Electroporation was performed with the BTX Harvard Apparatus Electroporator ECM830. Briefly, cells were washed twice with PBS and resuspended in High Performance Electroporation Solution BTX (Cat# 45-0805) at a concentration of 20 $x10^6$ cells/mL. For 1 million cells, were added 2ug ABE8e-NG mRNA, 100 pmol CD33 sgRNA, and 2uL RNAse Inhibitor (Promega Cat# N2515). When not specified differently, 5ug of home-made CXCR4 mRNA were used. The cells/mRNA mix was then transferred in a 1mm cuvette and electroporate with a 5 msec. pulse at 125V. After electroporation, cells were rapidly transferred in pre-warmed medium and plated in non-TC treated plates at 37 °C.

To investigate ABE8e-mediated editing, genomic DNA was extracted from cells following the QIAamp DNA Blood Mini Kit (QIAGEN # 51104). CD33 locus was amplified from genomic DNA using forward (5'-CATGAGGTTCAATCTGTGTG-3') and reverse (5'-GGAATTCCTGGTGTGGTAGGG-3') primers following the Thermofisher Phusion High-Fidelity DNA polymerase kit (2U/uL) (Cat # F530L). PCR samples were then purified with the QIAQuick PCR Purification Kit (QIAGEN # 28104) and sequenced by Sanger method with the Reverse primer. Editing efficiency in resulting fastq files, was analyzed with CRISPResso2 to align each read to the reference amplicon and quantify indels or base changes.

7.7 Molecular analysis

For HDR digital droplet PCR (ddPCR) analysis, 5–50 ng of gDNA were analyzed using the QX200 Droplet Digital PCR System (Bio-Rad) according to the manufacturer's instructions. HDR ddPCR primers and probes were designed on the junction between the vector sequence and the targeted locus. Human TTC5 (Bio-Rad) was used for

normalization. DNA was extracted using Qiamp DNA micro kit (Qiagen) or Qiamp DNA mini kit according to starting number of cells (as suggested by manufacturers). DNA was subsequently quantified and checked for purity. Vector copies per diploid genome (vector copy number, VCN) were quantified by ddPCR starting from 5-50 ng of template gDNA using the following primers (HIV sense: 5′-TACTGACGCTCTCGCACC-3′; HIV antisense: 5′-TCTCGACGCAGGACTCG-3′) and probe (FAM-ATCTCTCTCCTTCTAGCCTC-MGBNFQ) against the primer binding site region of LVs. Endogenous DNA amount was quantified by a primer/probe set against the human telomerase gene (Telo sense: 5′- GGCACACGTGGCTTTTCG-3′; Telo antisense: 5′-GGTGAACCTCGTAAGTTTATGCAA-3′; Telo probe: VIC 5′-TCAGGACGTCGAGTGGACACGGTG-3′ TAMRA). Copies per genome were calculated by the formula = [ng LV/ng endogenous DNA] × [no of LV integrations in the standard curve]. All reactions were carried out in duplicate. Each ddPCR run carries an internal control in the form of a CEMA301 cell line stably carrying a single vector integrant previously validated by Southern blot analysis.

For gene expression analyses, total RNA was extracted using RNeasy Plus Micro Kit (QIAGEN), according to the manufacturer's instructions and DNAse treatment was performed using RNase-free DNAse Set (QIAGEN). Complementary DNA was synthesized with SuperScript VILO IV cDNA Synthesis Kit (Thermo Fisher) with EzDNAse treatment. cDNA was then used for quantitative PCR (qPCR) in a Viia7 Real-time PCR thermal cycler using TaqMan Gene Expression Assays (Applied Biosystems) mapping to human IRF7, OAS1, ISG15 and RIG-I genes. Data were analyzed with QuantStudio Real-Time PCR software v.1.1 (Applied Biosystem). Relative expression of each target gene was first normalized to HPRT and then represented as fold changes ($2^{-\Delta\Delta Ct}$) relative to the untreated cells.

7.8 *In vitro* migration assay

Migration was performed using transwells permeable supports (Costar, 5µm polycarbonate membrane). Briefly, $2x10^5$ mPB $CD34^+$ previously electroporated with target mRNA, were seeded in the upper chamber, in StemSpan medium with cytokines. The lower chamber was filled with 600 µl of StemSpan medium with cytokines, supplemented with recombinant CXCL12 (PeproTech, 125ng/ml). After 3 hours,

migrating cells were recovered from the lower chamber and quantitatively evaluated on the BD Accuri™ C6 flow cytometer. For the migration inhibition experiment, Mozobil/AMD3100 and AMD3465 were added at 200 μM.

7.9 Flow cytometry

Immunophenotypic analyses were performed on fluorescence activated cell sorting FACS Canto II (BD Pharmingen) according to manufacturers' instructions, equipped with DIVA Software and analyzed with the FSC express software (v. 6, 7, De Novo Software). 5×10^4 - 2×10^5 cells (from culture or mouse samples) were harvested, washed with PBS or MACS buffer (PBS pH 7.2, 0.5% BSA, 2mM EDTA), treated with fragment crystallizable (Fc) Receptor-Block (Miltenyi Biotec), when antibody stained, and then re-suspended in the buffer used for washing. Staining was performed in MACS buffer, incubating cells for 15 minutes at 4° C in dark with a mix of antibodies listed below, in a final volume of 100 μL. Sphero Rainbow Calibration Particles (Spherotech) beads were used to calibrate the instrument detectors, for consistent MFI measurement, for analysis performed at different times. Single stained and Fluorescence Minus One (FMO)-stained cells were used as controls.

LIVE/DEAD Fixable Dead Cell Stain Kit (Thermo Fisher) or 7-aminoactinomycin (Sigma-Aldrich) was included in the sample preparation for flow cytometry according to the manufacturer's instructions to exclude dead cells from the analysis. Apoptosis analysis was performed on $CD34^+$ cells one day after electroporation using Annexin V (Biolegend) and Apoptosis Detection kit with 7-Aminoactinomycin D (7AAD, BD Pharmingen) according to the manufacturers' instructions. Percentages of live ($7AAD^-$, $AnnexinV^-$), early apoptotic ($7AAD^-$, $AnnexinV^+$) and late apoptotic ($7AAD^+$, $AnnexinV^+$) cells are reported.

For intracellular staining, surface antigens were stained prior to fixation and permeabilization steps, performed using the BD Cytofix/Cytoperm fixation/permeabilization Kit, according to the manufacturer's instructions.

Blood samples were also analysed with the hemocytometer Sysmex KX-21N (Block scientific, Sysmex corporation) to quantify absolute numbers.

7.10 Human CD34$^+$ HSPC xenotransplantation experiments

For transplantation into sublethally irradiated (150–180 cGy) NSG mice, 3x10^5 cord blood CD34$^+$ cells, diluted in 200 µL of PBS, were injected intravenously 24 hours after electroporation (performed 48hours post-thawing).

For transplantation into NOD-B6-SCID Il2rγ-/- Kit(W41/W41) mice, 3x10^5 G-CSF mPB CD34$^+$ cells, diluted in 200 µL of PBS, were injected intravenously 48-72hours post-thawing. Once the human chimerism reached 10%, humanized NSGW41 mice were mobilized and transplanted with 1-3x10^5 G-CSF mPB CD34$^+$ cells, transduced (for stable overexpression of a fluorescent marker) the first day post-thawing and/or electroporated on the third day post-thawing, and transplanted on the fourth day. Mice were randomly distributed to each experimental group. Human CD45$^+$ cell engraftment, cell lineages and/or GFP$^+$ cells were monitored by serial collection of blood from the retro-orbital vein and, at the end of the experiment (>12 weeks after transplantation), BM, thymus and spleen were harvested and analysed by flow cytometry for end-point analyses.

BM was flushed with PBS 2% BSA and 50 µL were stained for surface markers. The remaining cells were mouse cell-depleted and used for additional surface- or intracellular human antigen staining. For mouse cell depletion, BM cells flushed from the femurs and tibia of mice were processed with the Mouse Cell depletion Kit (Miltenyi Biotec) according to the manufacturer's instructions. Thymus was smashed and resuspended in PBS 2% BSA, and spleen was smashed, lysate with ACK Lysing Buffer (ThermoFisher) and resuspended in PBS 2% BSA. After processing, all samples were stained for surface marker and analyzed by flow cytometry. In some experiments, secondary transplantations were performed upon intravenous injection of 10^6 human CD34+ harvested and purified (CD34 MicroBead Kit – following manufacturer instruction) from the BM of primary engrafted NSGW41 mice to NSG mice (16 weeks).

7.11 Mobilization *in vivo*

NSGW41 mice were injected i.v. with CD34$^+$ cells as previously described above. After stable engraftment (10 weeks after injection), mice were treated for mobilization. G-CSF (Lenograstim, 250µg/kg/day) was delivered for 7 days through osmotic pumps positioned subcutaneously (s.c.) (Micro-osmotic pump 1007D, Alzet). At days 6 and 7 after pumps implantation, mice received i.p. injections of AMD3100 (Mozobil,

5mg/kg/day) and BIO5192 (R&D System, 1mg/kg/day). 6 hours after last i.p. injections, mice were transplanted i.v. with mobilized-derived $CD34^+$ cells, from the same donor, transduced with LV-GFP vector for stable overexpression and electroporated with mRNA for transient overexpression of the indicated gene products.

Different protocols were tested in *Cd40lg*$^{-/-}$ mice: (i) s.c. pump delivering 250µg/kg/day of G-CSF for 7 days (G7); (ii) s.c. pump delivering 250µg/kg/day of G-CSF for 7 days, with i.p. injections of AMD3100 (5mg/kg/day) on day 6 and 7 (G7A); (iii) s.c. pump delivering 250µg/kg/day of G-CSF for 7 days, with i.p. injections of AMD3100 (5mg/kg/day) and BIO5192 (1mg/kg/day) on day 6 and 7 (G7AB); (iv) s.c. pump delivering 125µg/kg/day of G-CSF for 7 days, with i.p. injections of AMD3100 (5mg/kg/day) and BIO5192 (1mg/kg/day) on day 6 and 7 (G7AB-H); (v) G-CSF delivered by i.p. injections (125 µg/kg) every 12 hours for four days, with AMD3100 s.c. injections (5 mg/kg) 14 hours after the last dose of G-CSF (G5A); (vi) G-CSF delivered by i.p. injections (125 µg/kg) every 12 hours for four days, with AMD3100 (5 mg/kg) and BIO5192 (1mg/kg) s.c. injections 14 hours after the last dose of G-CSF (G5AB); (vii) s.c. pump delivering 250µg/kg/day of G-CSF for 3 days, with i.p. injections of AMD3100 (5mg/kg/day) and BIO5192 (1mg/kg/day) on day 6 and 7 (G3AB); (viii) s.c. pump delivering 125µg/kg/day of G-CSF for 3 days, with i.p. injections of AMD3100 (5mg/kg/day) and BIO5192 (1mg/kg/day) on day 6 and 7 (G3AB-H); and (ix) AMD3100 (5mg/kg/day) and BIO5192 (1mg/kg/day) i.p. injected for three days.

Bone marrow vacancy and estimated chimerism were calculated based on the following formulas in *Cd40lg*$^{-/-}$ mice (Table 1):

To determine the total number of SLAM HSC per mouse at steady state (Figure 2G, left panel), lower limbs (which account for 20% of the total BM, Nombela-Arrieta and Manz, 2017) were collected in a define volume and counted, paralleled with their characterization through FACS. We found 2500 SLAM HSC/lower limbs, therefore reaching a total of 12 500 SLAM HSC/mouse (2500*100/20). This number is in accordance with other published paper (Chen et al., 2008; Karpova et al., 2017; Singh et al., 2020). To determine the total number of SLAM HSC that egressed from the BM post-G7AB mobilization, we examined the BM of mobilized mice. 1100 SLAM HSC were recovered in the lower limbs, reaching a total of 5500 SLAM HSC in the BM of mobilized mice. Therefore, to determine the number of SLAM HSC egressed, the number of SLAM

HSC present post-mobilization was subtracted from the total number of SLAM HSC present in the steady state mouse, leading to an assessment of 7,000 SLAM HSC egressing from the BM (12,500 – 5,500).

The mobilized SLAM HSC/mL was calculated based on the bleeding performed at the peak of mobilization in mobilized mice (Figure 2G, right panel). The blood was analyzed through hematocytometer (WBC/mL) and FACS staining (% subpopulation). Based on the WBC and the percentage of each subpopulation, the mobilized SLAM HSC/mL was estimated. To calculate the total number of mobilized SLAM HSC, the concentration of mobilized SLAM HSC/mL was multiplied by the total blood volume estimated to 1.5mL. Thereby, counts of SLAM HSC in the circulation of mobilized mice (Figure 2G, right panel) were valued to 3500 SLAM HSC/mL, leading to an estimation of 5250 total SLAM HSC total in the circulation (2500*1.5), corresponding to 75% of the 7000 SLAM HSC egressed from the BM.

Fig. 2G		**Steady state mice (Sham)**	**Mobilized mice (G7AB)**
Left panel	# SLAM HSC in lower limbs	2500	1100
	# SLAM HSC total BM Lower limbs = 20% total BM	12500	5500
	#SLAM HSC egressed (# SLAM HSC total BM Sham - # SLAM HSC total BM mobilized)	12500 – 5500 = 7000	
Right panel	# SLAM HSC circulation (Total blood volume = 1.5mL)	28*1.5 = 43	3500*1.5 = 5250
% SLAM HSC in circulation to SLAM HSC egressed from the BM		5250*100/7000 = 75%	

Concerning the transplanted Lin- BM cells:

$2x10^6$ Lin^- BM cells were used / transplantation. Upon purification of Lin^- cells from the BM, we characterized the Lin^- population using FACS and determined the percentage of LSK (average 9% Lin-; $9x10^4$ LSK/million of Lin^-) and SLAM HSC (average 2%; 2000 SLAM HSC/million of Lin^-) subpopulation. We next calculated the transplanted number of LSK and SLAM HSC from $2x10^6$ Lin^- cells, corresponding to 4000 SLAM HSC total.

The ratio recipient to donor was determined by dividing the mobilized recipient SLAM HSC by the transplanted SLAM HSC. As $2x10^6$ Lin^- were transplanted each time, except

for the dose response experiment (Supplementary Figure 2M), the SLAM HSC transplanted always correspond to 4000 (Table 1).

$$BM\ vacancy\ (\%) = \frac{Total\ mobilized\ SLAM\ HSC * 100}{Total\ SLAM\ HSC\ in\ the\ BM}$$

$$Estimated\ chimerism\ (\%) = \frac{BM\ vacancy}{\frac{total\ SLAM\ HSC\ mobilized}{total\ SLAM\ HSC\ infused} + 1}$$

Humanized bone marrow vacancy and estimated chimerism were calculated based on the following formulas:

$$BM\ vacancy\ (\%) = \frac{Total\ mobilized\ CD34 * 100}{Total\ CD34\ in\ the\ BM}$$

$$Estimated\ chimerism\ (\%) = \frac{BM\ vacancy}{\frac{total\ CD34\ mobilized}{total\ CD34\ infused} + 1}$$

7.12 *In vivo* immunization and IgG quantification

Mice were immunized by intraperitoneal injection (i.p.) with 100 µg of TNP-KLH (Lgc Biosearch Technologies) in Imject Alum Adjuvant (1:2) (ThermoFisher Scientific), as described before (Vavassori et al., 2021). Serum was collected at day 0, 7, and 14 after immunization. Mice were boosted as described above on day 21, and serum was collected on day 7 after re-challenge. For IgG quantification, the concentration of antigen-specific IgGs in mouse sera was determined by an enzyme-linked immunosorbent assay (ELISA). Plates were coated with 100 µL/well of 5 µg/ml TNP-KLH in carbonate buffer. Following incubation, plates were washed three times in PBS containing 0.05% Tween20 (Sigma-Aldrich) (Wash Buffer). The plates were then blocked for 1 h using 100 µL/well of PBS containing 1% Bovine Serum Albumine (BSA), followed by a washing step, as described above. Serum samples were serially diluted in wash buffer and 100 µL/well of each diluted sample was added into the plate and incubated for 2 h at room temperature. For determination of the plate background optical density (OD) values, some wells were incubated with wash buffer alone. Following incubation, plates were washed and 100 µL/well of HRP-conjugated goat anti-mouse (Southern Biotech 1:10,000) was added and incubated for 1 h at room temperature. After washing, the plates were incubated for 5 min with 3,3',5,5'0-tetramethyl benzidine (TMB, Sigma-Aldrich) substrate at room

temperature. The reaction was stopped by the addition of 50 µL of 1 M H_2SO_4. The OD values at 450 nm were determined for each well using a Multiskan GO microplate reader (Thermo Fisher Scientific) and normalized to IgG1 standard curves. Results were expressed as mean of duplicate determinations.

7.13 ELISA

For ELISA performed on BM matrix, femurs and tibias were repeatedly flushed with 1mL of cold PBS. Cells were pelleted by centrifugation at 300 *g* for 10 minutes at 4°C, supernatant was then collected and stored at –80°C. ELISA has been performed following manufacturer instruction after a 1:100 dilution with 1x Assay Diluent for MMP9 (Thermo Scientific) or on undiluted BM matrix for CXCL12 (Sigma-Aldrich).

7.14 Statistical analysis

Here, the n indicates the number of biologically independent samples, animals or experiments. For some experiments, different HSPC donors were pooled. Data were summarized as mean ± SEM. Inferential techniques were carried out whenever they were necessary for the interpretation of the data, otherwise descriptive statistics are reported. The Mann–Whitney test was performed to compare two independent groups, while in presence of more than two independent groups the Kruskal–Wallis test followed by post hoc analysis using Dunn's test was used. In presence of dependent observations and longitudinal comparisons the mixed-effects model (REML) were performed, followed by post hoc analysis with Sidak's test (when groups =2) or Tukey's test (when groups >2) and/or by post hoc analysis with Dunnett's test (within group). In all the analyses, P-values less than 0.05 were considered significant (*P < 0.05, **P < 0.01, ***P < 0.001, ****P < 0.0001. "ns" means non-significance). All statistical analyses were performed using R 3.5.0 (http://www.R-project.org/) or GraphPad Prism v8.

REFERENCES

Abee CR ed. (2012) Nonhuman primates in biomedical research Second edition. Amsterdam: Academic Press, an imprint of Elsevier

Abraham DM, Lozano RJ, Guitart X, Liang JA, Mortlock RD, Espinoza DA, Fan X, Krouse A, Bonifacino A, Hong SG, *et al* (2023) Comparison of busulfan and total body irradiation conditioning on hematopoietic clonal dynamics following lentiviral gene transfer in rhesus macaques. *Molecular Therapy - Methods & Clinical Development* 28: 62–75

Acar M, Kocherlakota KS, Murphy MM, Peyer JG, Oguro H, Inra CN, Jaiyeola C, Zhao Z, Luby-Phelps K & Morrison SJ (2015) Deep imaging of bone marrow shows non-dividing stem cells are mainly perisinusoidal. *Nature* 526: 126–130

Ailles LE & Naldini L (2002) HIV-1-Derived Lentiviral Vectors. In *Lentiviral Vectors*, Trono D (ed) pp 31–52. Berlin, Heidelberg: Springer Berlin Heidelberg

Altuntaş F & Korkmaz S (2017) Hematopoietic progenitor cell mobilization. *Transfusion and Apheresis Science* 56: 787

Anderson BR, Muramatsu H, Nallagatla SR, Bevilacqua PC, Sansing LH, Weissman D & Karikó K (2010) Incorporation of pseudouridine into mRNA enhances translation by diminishing PKR activation. *Nucleic Acids Research* 38: 5884–5892

Andreani M, Testi M, Gaziev J, Condello R, Bontadini A, Tazzari PL, Ricci F, De Felice L, Agostini F, Fraboni D, *et al* (2011) Quantitatively different red cell/nucleated cell chimerism in patients with long-term, persistent hematopoietic mixed chimerism after bone marrow transplantation for thalassemia major or sickle cell disease. *Haematologica* 96: 128–133

Anzalone AV, Koblan LW & Liu DR (2020) Genome editing with CRISPR–Cas nucleases, base editors, transposases and prime editors. *Nat Biotechnol* 38: 824–844

Anzalone AV, Randolph PB, Davis JR, Sousa AA, Koblan LW, Levy JM, Chen PJ, Wilson C, Newby GA, Raguram A, *et al* (2019) Search-and-replace genome editing without double-strand breaks or donor DNA. *Nature* 576: 149–157

Ara T, Itoi M, Kawabata K, Egawa T, Tokoyoda K, Sugiyama T, Fujii N, Amagai T & Nagasawa T (2003) A Role of CXC Chemokine Ligand 12/Stromal Cell-Derived Factor-1/Pre-B Cell Growth Stimulating Factor and Its Receptor CXCR4 in Fetal and Adult T Cell Development in Vivo. *The Journal of Immunology* 170: 4649–4655

Arnold FH (1998) Design by Directed Evolution. *Acc Chem Res* 31: 125–131

Asada N, Kunisaki Y, Pierce H, Wang Z, Fernandez NF, Birbrair A, Ma'ayan A & Frenette PS (2017) Differential cytokine contributions of perivascular haematopoietic stem cell niches. *Nat Cell Biol* 19: 214–223

Babic A & Trigoso E (2018) Cell Source and Apheresis. In *The European Blood and Marrow Transplantation Textbook for Nurses*, Kenyon M & Babic A (eds) pp 71–87. Cham: Springer International Publishing

Baccin C, Al-Sabah J, Velten L, Helbling PM, Grünschläger F, Hernández-Malmierca P, Nombela-Arrieta C, Steinmetz LM, Trumpp A & Haas S (2020) Combined single-cell and spatial transcriptomics reveal the molecular, cellular and spatial bone marrow niche organization. *Nat Cell Biol* 22: 38–48

Bacigalupo A, Ballen K, Rizzo D, Giralt S, Lazarus H, Ho V, Apperley J, Slavin S, Pasquini M, Sandmaier BM, *et al* (2009) Defining the Intensity of Conditioning Regimens: Working Definitions. *Biology of Blood and Marrow Transplantation* 15: 1628–1633

Baryawno N, Przybylski D, Kowalczyk MS, Kfoury Y, Severe N, Gustafsson K, Kokkaliaris KD, Mercier F, Tabaka M, Hofree M, *et al* (2019) A Cellular Taxonomy of the Bone Marrow Stroma in Homeostasis and Leukemia. *Cell* 177: 1915-1932.e16

Baum CM, Weissman IL, Tsukamoto AS, Buckle AM & Peault B (1992) Isolation of a candidate human hematopoietic stem-cell population. *Proc Natl Acad Sci USA* 89: 2804–2808

Bazinet A & Popradi G (2019) A General Practitioner's Guide to Hematopoietic Stem-cell Transplantation. *Current Oncology* 26: 187–191

Beagles KE, Peterson L, Zhang X, Morris J & Kiem H-P (2005) Cyclosporine Inhibits the Development of Green Fluorescent Protein (GFP)-Specific Immune Responses After Transplantation of GFP-Expressing Hematopoietic Repopulating Cells in Dogs. *Human Gene Therapy* 16: 725–733

Becker AJ, McCULLOCH EA & Till JE (1963) Cytological Demonstration of the Clonal Nature of Spleen Colonies Derived from Transplanted Mouse Marrow Cells. *Nature* 197: 452–454

Belkacemi Y, Labopin M, Giebel S, Loganadane G, Miszczyk L, Michallet M, Socié G, Schaap NPM, Cornelissen JJ, Yakoub-Agha I, *et al* (2018) Single-Dose Daily Fractionation Is Not Inferior to Twice-a-Day Fractionated Total-Body Irradiation Before Allogeneic Stem Cell Transplantation for Acute Leukemia: A Useful Practice Simplification Resulting From the SARASIN Study. *International Journal of Radiation Oncology*Biology*Physics* 102: 515–526

Benveniste P, Frelin C, Janmohamed S, Barbara M, Herrington R, Hyam D & Iscove NN (2010) Intermediate-Term Hematopoietic Stem Cells with Extended but Time-Limited Reconstitution Potential. *Cell Stem Cell* 6: 48–58

Benz C, Copley MR, Kent DG, Wohrer S, Cortes A, Aghaeepour N, Ma E, Mader H, Rowe K, Day C, *et al* (2012) Hematopoietic Stem Cell Subtypes Expand Differentially during Development and Display Distinct Lymphopoietic Programs. *Cell Stem Cell* 10: 273–283

Berenson RJ, Andrews RG, Bensinger WI, Kalamasz D, Knitter G, Buckner CD & Bernstein ID (1988) Antigen CD34+ marrow cells engraft lethally irradiated baboons. *J Clin Invest* 81: 951–955

Berger C, Huang M-L, Gough M, Greenberg PD, Riddell SR & Kiem H-P (2001) Nonmyeloablative Immunosuppressive Regimen Prolongs In Vivo Persistence of Gene-Modified Autologous T Cells in a Nonhuman Primate Model. *J Virol* 75: 799–808

Bhatia M, Wang JCY, Kapp U, Bonnet D & Dick JE (1997) Purification of primitive human hematopoietic cells capable of repopulating immune-deficient mice. *Proc Natl Acad Sci USA* 94: 5320–5325

Biasco L, Pellin D, Scala S, Dionisio F, Basso-Ricci L, Leonardelli L, Scaramuzza S, Baricordi C, Ferrua F, Cicalese MP, *et al* (2016) In Vivo Tracking of Human Hematopoiesis Reveals Patterns of Clonal Dynamics during Early and Steady-State Reconstitution Phases. *Cell Stem Cell* 19: 107–119

Birocchi F, Cusimano M, Rossari F, Beretta S, Rancoita PM, Ranghetti A, Colombo S, Costa B, Angel P, Sanvito F, *et al* (2022) Targeted inducible delivery of immunoactivating cytokines reprograms glioblastoma microenvironment and inhibits growth in mouse models. *SCIENCE TRANSLATIONAL MEDICINE*

Bloomgren G, Richman S, Hotermans C, Subramanyam M, Goelz S, Natarajan A, Lee S, Plavina T, Scanlon JV, Sandrock A, *et al* (2012) Risk of Natalizumab-Associated Progressive Multifocal Leukoencephalopathy. *N Engl J Med* 366: 1870–1880

Bonig H, Wundes A, Chang K-H, Lucas S & Papayannopoulou T (2008) Increased numbers of circulating hematopoietic stem/progenitor cells are chronically maintained in patients treated with the CD49d blocking antibody natalizumab. *Blood* 111: 3439–3441

Borot F, Humbert O, Newby GA, Fields E, Kohli S, Radtke S, Laszlo GS, Mayuranathan T, Ali AM, Weiss MJ, *et al* (2023) Multiplex Base Editing to Protect from CD33-Directed Therapy: Implications for Immune and Gene Therapy Cell Biology

Borot F, Wang H, Ma Y, Jafarov T, Raza A, Ali AM & Mukherjee S (2019) Gene-edited stem cells enable CD33-directed immune therapy for myeloid malignancies. *Proc Natl Acad Sci USA* 116: 11978–11987

Boulais PE & Frenette PS (2015) Making sense of hematopoietic stem cell niches. *Blood* 125: 2621–2629

Broxmeyer HE (2012) Preclinical Experience with AMD3100 for Mobilization of Hematopoietic Stem and Progenitor Cells. In *Novel Developments in Stem Cell*

Mobilization, Fruehauf S Zeller WJ & Calandra G (eds) pp 3–22. Boston, MA: Springer US

Burns LJ, Logan BR, Chitphakdithai P, Miller JP, Drexler R, Spellman S, Switzer GE, Wingard JR, Anasetti C & Confer DL (2016) Recovery of Unrelated Donors of Peripheral Blood Stem Cells versus Recovery of Unrelated Donors of Bone Marrow: A Prespecified Analysis from the Phase III Blood and Marrow Transplant Clinical Trials Network Protocol 0201. *Biology of Blood and Marrow Transplantation* 22: 1108–1116

Calvanese V & Mikkola HKA (2023) The genesis of human hematopoietic stem cells. *Blood* 142: 519–532

Canarutto D, Omer Javed A, Pedrazzani G, Ferrari S & Naldini L (2023) Mobilization-based engraftment of haematopoietic stem cells: a new perspective for chemotherapy-free gene therapy and transplantation. *British Medical Bulletin*: ldad017

Carreras E, Dufour C, Mohty M & Kröger N eds. (2019) The EBMT Handbook: Hematopoietic Stem Cell Transplantation and Cellular Therapies Cham: Springer International Publishing

Case SS, Price MA, Jordan CT, Yu XJ, Wang L, Bauer G, Haas DL, Xu D, Stripecke R, Naldini L, *et al* (1999) Stable transduction of quiescent CD34 $^{+}$ CD38 $^{-}$ human hematopoietic cells by HIV-1-based lentiviral vectors. *Proc Natl Acad Sci USA* 96: 2988–2993

Cashman J, Clark-Lewis I, Eaves A & Eaves C (2002) Stromal-derived factor 1 inhibits the cycling of very primitive human hematopoietic cells in vitro and in NOD/SCID mice. *Blood* 99: 792–799

Casirati G, Cosentino A, Mucci A, Salah Mahmoud M, Ugarte Zabala I, Zeng J, Ficarro SB, Klatt D, Brendel C, Rambaldi A, *et al* (2023) Epitope editing enables targeted immunotherapy of acute myeloid leukaemia. *Nature*

Castagnoli R, Delmonte OM, Calzoni E & Notarangelo LD (2019) Hematopoietic Stem Cell Transplantation in Primary Immunodeficiency Diseases: Current Status and Future Perspectives. *Front Pediatr* 7: 295

Chabanon A, Desterke C, Rodenburger E, Clay D, Guerton B, Boutin L, Bennaceur-Griscelli A, Pierre-Louis O, Uzan G, Abecassis L, *et al* (2008) A Cross-Talk Between Stromal Cell-Derived Factor-1 and Transforming Growth Factor- β Controls the Quiescence/Cycling Switch of CD34+ Progenitors Through FoxO3 and Mammalian Target of Rapamycin. *Stem Cells* 26: 3150–3161

Charlesworth CT, Hsu I, Wilkinson AC & Nakauchi H (2022) Immunological barriers to haematopoietic stem cell gene therapy. *Nat Rev Immunol*

Chen H, Liu S, Padula S, Lesman D, Griswold K, Lin A, Zhao T, Marshall JL & Chen F (2020) Efficient, continuous mutagenesis in human cells using a pseudo-random DNA editor. *Nat Biotechnol* 38: 165–168

Chen Y-F, Li J, Xu L-L, Găman M-A & Zou Z-Y (2023) Allogeneic stem cell transplantation in the treatment of acute myeloid leukemia: An overview of obstacles and opportunities. *World J Clin Cases* 11: 268–291

Cheng H, Zheng Z & Cheng T (2020) New paradigms on hematopoietic stem cell differentiation. *Protein Cell* 11: 34–44

Cheng J, Novati G, Pan J, Bycroft C, Žemgulytė A, Applebaum T, Pritzel A, Wong LH, Zielinski M, Sargeant T, *et al* (2023) Accurate proteome-wide missense variant effect prediction with AlphaMissense. *Science* 381: eadg7492

Cheshier SH, Morrison SJ, Liao X & Weissman IL (1999) *In vivo* proliferation and cell cycle kinetics of long-term self-renewing hematopoietic stem cells. *Proc Natl Acad Sci USA* 96: 3120–3125

Chevallier P, Labopin M, Buchholz S, Ganser A, Ciceri F, Lioure B, Faul C, Guillerm G, Finke J, Huynh A, *et al* (2012) Clofarabine-containing conditioning regimen for allo-SCT in AML/ALL patients: a survey from the Acute Leukemia Working Party of EBMT. *Eur J Haematol* 89: 214–219

Christian M, Cermak T, Doyle EL, Schmidt C, Zhang F, Hummel A, Bogdanove AJ & Voytas DF (2010) Targeting DNA Double-Strand Breaks with TAL Effector Nucleases. *Genetics* 186: 757–761

Christodoulou C, Spencer JA, Yeh S-CA, Turcotte R, Kokkaliaris KD, Panero R, Ramos A, Guo G, Seyedhassantehrani N, Esipova TV, *et al* (2020) Live-animal imaging of native haematopoietic stem and progenitor cells. *Nature* 578: 278–283

Civin CI, Strauss LC, Brovall C, Fackler MJ, Schwartz JF & Shaper JH (1984) Antigenic analysis of hematopoiesis. III. A hematopoietic progenitor cell surface antigen defined by a monoclonal antibody raised against KG-1a cells. *J Immunol* 133: 157–165

Clift RA, Buckner CD, Appelbaum FR, Bearman SI, Petersen FB, Fisher LD, Anasetti C, Beatty P, Bensinger WI & Doney K (1990) Allogeneic marrow transplantation in patients with acute myeloid leukemia in first remission: a randomized trial of two irradiation regimens. *Blood* 76: 1867–1871

Colella P, Ronzitti G & Mingozzi F (2018) Emerging Issues in AAV-Mediated In Vivo Gene Therapy. *Molecular Therapy - Methods & Clinical Development* 8: 87–104

Cosgun KN, Rahmig S, Mende N, Reinke S, Hauber I, Schäfer C, Petzold A, Weisbach H, Heidkamp G, Purbojo A, *et al* (2014) Kit Regulates HSC Engraftment across the Human-Mouse Species Barrier. *Cell Stem Cell* 15: 227–238

Craddock CF, Nakamoto B, Andrews RG, Priestley GV & Papayannopoulou T (1997) Antibodies to VLA4 integrin mobilize long-term repopulating cells and augment cytokine-induced mobilization in primates and mice. *Blood* 90: 4779–4788

Crees ZD, Rettig MP, Jayasinghe RG, Stockerl-Goldstein K, Larson SM, Arpad I, Milone GA, Martino M, Stiff P, Sborov D, *et al* (2023) Motixafortide and G-CSF to mobilize hematopoietic stem cells for autologous transplantation in multiple myeloma: a randomized phase 3 trial. *Nat Med* 29: 869–879

Czechowicz A, Kraft D, Weissman IL & Bhattacharya D (2007) Efficient Transplantation via Antibody-Based Clearance of Hematopoietic Stem Cell Niches. *Science* 318: 1296–1299

Czechowicz A, Palchaudhuri R, Scheck A, Hu Y, Hoggatt J, Saez B, Pang WW, Mansour MK, Tate TA, Chan YY, *et al* (2019) Selective hematopoietic stem cell ablation using CD117-antibody-drug-conjugates enables safe and effective transplantation with immunity preservation. *Nat Commun* 10: 617

Dausset J (1981) The Major Histocompatibility Complex in Man. *Science* 213: 1469–1474

Dausset J & Brecy H (1957) Identical Nature of the Leucocyte Antigens detectable in Monozygotic Twins by means of Immune Iso-Leuco-agglutinins. *Nature* 180: 1430–1430

De Saint-Georges L & Miller SC (1992) The micocirculation of bone and marrow in the diaphysis of the rat hemopoietic long bones. *Anat Rec* 233: 169–177

Demirci S, Zeng J, Wu Y, Uchida N, Shen AH, Pellin D, Gamer J, Yapundich M, Drysdale C, Bonanno J, *et al* (2020) BCL11A enhancer–edited hematopoietic stem cells persist in rhesus monkeys without toxicity. *Journal of Clinical Investigation* 130: 6677–6687

Deotare U, Al-Dawsari G, Couban S & Lipton JH (2015) G-CSF-primed bone marrow as a source of stem cells for allografting: revisiting the concept. *Bone Marrow Transplant* 50: 1150–1156

Di Bartolomeo P, Santarone S, De Angelis G, Picardi A, Cudillo L, Cerretti R, Adorno G, Angelini S, Andreani M, De Felice L, *et al* (2013) Haploidentical, unmanipulated, G-CSF–primed bone marrow transplantation for patients with high-risk hematologic malignancies. *Blood* 121: 849–857

DiPersio JF, Stadtmauer EA, Nademanee A, Micallef INM, Stiff PJ, Kaufman JL, Maziarz RT, Hosing C, Früehauf S, Horwitz M, *et al* (2009) Plerixafor and G-CSF versus placebo and G-CSF to mobilize hematopoietic stem cells for autologous stem cell transplantation in patients with multiple myeloma. *Blood* 113: 5720–5726

Doulatov S, Notta F, Laurenti E & Dick JE (2012) Hematopoiesis: A Human Perspective. *Cell Stem Cell* 10: 120–136

Drysdale CM, Tisdale JF & Uchida N (2020) Immunoresponse to Gene-Modified Hematopoietic Stem Cells. *Molecular Therapy - Methods & Clinical Development* 16: 42–49

Dufour C (2017) How I manage patients with Fanconi anaemia. *Br J Haematol* 178: 32–47

Dunbar CE, Seidel NE, Doren S, Sellers S, Cline AP, Metzger ME, Agricola BA, Donahue RE & Bodine DM (1996) Improved retroviral gene transfer into murine and Rhesus peripheral blood or bone marrow repopulating cells primed in vivo with stem cell factor and granulocyte colony-stimulating factor. *Proc Natl Acad Sci USA* 93: 11871–11876

Eder S, Beohou E, Labopin M, Sanz J, Finke J, Arcese W, Or R, Bonifazi F, Aljurf M, Socié G, *et al* (2017) Thiotepa-based conditioning for allogeneic stem cell transplantation in acute lymphoblastic leukemia-A survey from the Acute Leukemia Working Party of the European Society for Blood and Marrow Transplantation: Thiotepa for allo-HSCT in ALL. *Am J Hematol* 92: 18–22

El Kharrag R, Berckmueller K, Cui M, Madhu R, Perez AM, Humbert O, Kiem H-P & Radtke S (2021) Efficient Nanoparticle-Mediated Delivery of Gene Editing Reagents into Human Hematopoietic Stem and Progenitor Cells. *Blood* 138: 2933–2933

Epstein RB, Graham TC, Buckner CD, Bryant J & Thomas ED (1966) Allogeneic Marrow Engraftment by Cross Circulation in Lethally Irradiated Dogs. *Blood* 28: 692–707

Fares I, Chagraoui J, Lehnertz B, MacRae T, Mayotte N, Tomellini E, Aubert L, Roux PP & Sauvageau G (2017) EPCR expression marks UM171-expanded CD34+ cord blood stem cells. *Blood* 129: 3344–3351

Ferrari S, Jacob A, Beretta S, Unali G, Albano L, Vavassori V, Cittaro D, Lazarevic D, Brombin C, Cugnata F, *et al* (2020) Efficient gene editing of human long-term hematopoietic stem cells validated by clonal tracking. *Nat Biotechnol* 38: 1298–1308

Ferrari S, Jacob A, Cesana D, Laugel M, Beretta S, Varesi A, Unali G, Conti A, Canarutto D, Albano L, *et al* (2022) Choice of template delivery mitigates the genotoxic risk and adverse impact of editing in human hematopoietic stem cells. *Cell Stem Cell* 29: 1428-1444.e9

Ferrari S, Valeri E, Conti A, Scala S, Aprile A, Di Micco R, Kajaste-Rudnitski A, Montini E, Ferrari G, Aiuti A, *et al* (2023) Genetic engineering meets hematopoietic stem cell biology for next-generation gene therapy. *Cell Stem Cell* 30: 549–570

Ferrua F, Galimberti S, Courteille V, Slatter MA, Booth C, Moshous D, Neven B, Blanche S, Cavazzana M, Laberko A, *et al* (2019) Hematopoietic stem cell transplantation

for CD40 ligand deficiency: Results from an EBMT/ESID-IEWP-SCETIDE-PIDTC study. *Journal of Allergy and Clinical Immunology* 143: 2238–2253

Ferruz N & Höcker B (2022) Controllable protein design with language models. *Nat Mach Intell* 4: 521–532

Ferruz N, Schmidt S & Höcker B (2022) ProtGPT2 is a deep unsupervised language model for protein design. *Nat Commun* 13: 4348

Follenzi A & Naldini L (2001) HIV-Based Vectors: Preparation and Use. In *Gene Therapy Protocols* pp 259–274. New Jersey: Humana Press

Frangoul H, Altshuler D, Cappellini MD, Chen Y-S, Domm J, Eustace BK, Foell J, De La Fuente J, Grupp S, Handgretinger R, *et al* (2021) CRISPR-Cas9 Gene Editing for Sickle Cell Disease and β-Thalassemia. *N Engl J Med* 384: 252–260

Friedenstein A (1989) Stromal-Hematopoietic Interrelationships: Maximov's Ideas and Modern Models. In *Modern Trends in Human Leukemia VIII*, Neth R Gallo RC Greaves MF Gaedicke G Gohla S Mannweiler K & Ritter J (eds) pp 159–167. Berlin, Heidelberg: Springer Berlin Heidelberg

Fukuda S, Bian H, King AG & Pelus LM (2007) The chemokine GRO^{M_L} mobilizes early hematopoietic stem cells characterized by enhanced homing and engraftment. 110: 10

Gaudelli NM, Lam DK, Rees HA, Solá-Esteves NM, Barrera LA, Born DA, Edwards A, Gehrke JM, Lee S-J, Liquori AJ, *et al* (2020) Directed evolution of adenine base editors with increased activity and therapeutic application. *Nat Biotechnol* 38: 892–900

Genovese P, Schiroli G, Escobar G, Di Tomaso T, Firrito C, Calabria A, Moi D, Mazzieri R, Bonini C, Holmes MC, *et al* (2014) Targeted genome editing in human repopulating haematopoietic stem cells. *Nature* 510: 235–240

George BM, Kao KS, Kwon H-S, Velasco BJ, Poyser J, Chen A, Le AC, Chhabra A, Burnett CE, Cajuste D, *et al* (2019) Antibody Conditioning Enables MHC-Mismatched Hematopoietic Stem Cell Transplants and Organ Graft Tolerance. *Cell Stem Cell* 25: 185-192.e3

Gonzalez MA & Bernad A (2012) Characteristics of Adult Stem Cells. In *Stem Cell Transplantation*, López-Larrea C López-Vázquez A & Suárez-Álvarez B (eds) pp 103–120. New York, NY: Springer US

Goodman JW & Hodgson GS (1962) Evidence for Stem Cells in the Peripheral Blood of Mice. *Blood* 19: 702–714

Goyama S, Wunderlich M & Mulloy JC (2015) Xenograft models for normal and malignant stem cells. *Blood* 125: 2630–2640

Greenbaum A, Hsu Y-MS, Day RB, Schuettpelz LG, Christopher MJ, Borgerding JN, Nagasawa T & Link DC (2013) CXCL12 in early mesenchymal progenitors is required for haematopoietic stem-cell maintenance. *Nature* 495: 227–230

Greenbaum AM & Link DC (2011) Mechanisms of G-CSF-mediated hematopoietic stem and progenitor mobilization. *Leukemia* 25: 211–217

Grupp SA, Corbacioglu S, Kang HJ, Teshima T, Khaw SL, Locatelli F, Maertens J, Stelljes M, Stepensky P, Lopez P, *et al* (2023) Defibrotide plus best standard of care compared with best standard of care alone for the prevention of sinusoidal obstruction syndrome (HARMONY): a randomised, multicentre, phase 3 trial. *The Lancet Haematology* 10: e333–e345

Gyurkocza B & Sandmaier BM (2014) Conditioning regimens for hematopoietic cell transplantation: one size does not fit all. *Blood* 124: 344–353

Hansen JA, Clift RA, Thomas ED, Buckner CD, Storb R & Giblett ER (1980) Transplantation of Marrow from an Unrelated Donor to a Patient with Acute Leukemia. *N Engl J Med* 303: 565–567

Hendel SJ & Shoulders MD (2021) Directed evolution in mammalian cells. *Nature Methods* 18: 12

Henderson JM, Ujita A, Hill E, Yousif-Rosales S, Smith C, Ko N, McReynolds T, Cabral CR, Escamilla-Powers JR & Houston ME (2021) Cap 1 Messenger RNA Synthesis with Co-transcriptional CleanCap ® Analog by In Vitro Transcription. *Current Protocols* 1: e39

Hess GT, Frésard L, Han K, Lee CH, Li A, Cimprich KA, Montgomery SB & Bassik MC (2016) Directed evolution using dCas9-targeted somatic hypermutation in mammalian cells. *Nat Methods* 13: 1036–1042

Hoggatt J, Singh P, Tate TA, Chou B-K, Datari SR, Fukuda S, Liu L, Kharchenko PV, Schajnovitz A, Baryawno N, *et al* (2018) Rapid Mobilization Reveals a Highly Engraftable Hematopoietic Stem Cell. *Cell* 172: 191-204.e10

Hsu W-L, Preston DL, Soda M, Sugiyama H, Funamoto S, Kodama K, Kimura A, Kamada N, Dohy H, Tomonaga M, *et al* (2013) The Incidence of Leukemia, Lymphoma and Multiple Myeloma among Atomic Bomb Survivors: 1950–2001. *Radiation Research* 179: 361

Huang X, Kong N, Zhang X, Cao Y, Langer R & Tao W (2022) The landscape of mRNA nanomedicine. *Nat Med* 28: 2273–2287

Humbert O, Laszlo GS, Sichel S, Ironside C, Haworth KG, Bates OM, Beddoe ME, Carrillo RR, Kiem H-P & Walter RB (2019) Engineering resistance to CD33-targeted immunotherapy in normal hematopoiesis by CRISPR/Cas9-deletion of CD33 exon 2. *Leukemia* 33: 762–808

Ieranò C, Giuliano P, D'Alterio C, Cioffi M, Mettivier V, Portella L, Napolitano M, Barbieri A, Arra C, Liguori G, *et al* (2009) A point mutation (G574A) in the chemokine receptor CXCR4 detected in human cancer cells enhances migration. *Cell Cycle* 8: 1228–1237

Inamoto Y & Lee SJ (2017) Late effects of blood and marrow transplantation. *Haematologica* 102: 614–625

Itkin T, Gur-Cohen S, Spencer JA, Schajnovitz A, Ramasamy SK, Kusumbe AP, Ledergor G, Jung Y, Milo I, Poulos MG, *et al* (2016) Distinct bone marrow blood vessels differentially regulate haematopoiesis. *Nature* 532: 323–328

Iversen PO (1997) Blood flow to the haemopoietic bone marrow. *Acta Physiologica Scandinavica* 159: 269–276

Jacobsohn DA & Vogelsang GB (2007) Acute graft versus host disease. *Orphanet J Rare Dis* 2: 35

Jang H-K, Song B, Hwang G-H & Bae S (2020) Current trends in gene recovery mediated by the CRISPR-Cas system. *Exp Mol Med* 52: 1016–1027

Jinek M, Chylinski K, Fonfara I, Hauer M, Doudna JA & Charpentier E (2012) A Programmable Dual-RNA–Guided DNA Endonuclease in Adaptive Bacterial Immunity. *Science* 337: 816–821

Jing D, Oelschlaegel U, Ordemann R, Hölig K, Ehninger G, Reichmann H, Ziemssen T & Bornhäuser M (2010) CD49d blockade by natalizumab in patients with multiple sclerosis affects steady-state hematopoiesis and mobilizes progenitors with a distinct phenotype and function. *Bone Marrow Transplant* 45: 1489–1496

Judson G, Jones A, Kellogg R, Buckner D, Eisel R, Perry S & Greenough W (1968) Closed Continuous-flow Centrifuge. *Nature* 217: 816–818

Kamel-Reid S & Dick JE (1988) Engraftment of Immune-Deficient Mice with Human Hematopoietic Stem Cells. *Science* 242: 1706–1709

Kandarakov O, Belyavsky A & Semenova E (2022) Bone Marrow Niches of Hematopoietic Stem and Progenitor Cells. *IJMS* 23: 4462

Kang Y & Chao NJ (2012) Strategies to Enhance Hematopoietic Stem Cell Engraftment Following Transplantation. In *Novel Developments in Stem Cell Mobilization*, Fruehauf S Zeller WJ & Calandra G (eds) pp 439–456. Boston, MA: Springer US

Karczewski KJ, Francioli LC, Tiao G, Cummings BB, Alföldi J, Wang Q, Collins RL, Laricchia KM, Ganna A, Birnbaum DP, *et al* (2020) The mutational constraint spectrum quantified from variation in 141,456 humans. *Nature* 581: 434–443

Karikó K, Buckstein M, Ni H & Weissman D (2005) Suppression of RNA Recognition by Toll-like Receptors: The Impact of Nucleoside Modification and the Evolutionary Origin of RNA. *Immunity* 23: 165–175

Kiel MJ, Yilmaz ÖH, Iwashita T, Yilmaz OH, Terhorst C & Morrison SJ (2005) SLAM Family Receptors Distinguish Hematopoietic Stem and Progenitor Cells and Reveal Endothelial Niches for Stem Cells. *Cell* 121: 1109–1121

Kim HK, Yu G, Park J, Min S, Lee S, Yoon S & Kim HH (2021) Predicting the efficiency of prime editing guide RNAs in human cells. *Nat Biotechnol* 39: 198–206

Kim MY, Yu K-R, Kenderian SS, Ruella M, Chen S, Shin T-H, Aljanahi AA, Schreeder D, Klichinsky M, Shestova O, *et al* (2018) Genetic Inactivation of CD33 in Hematopoietic Stem Cells to Enable CAR T Cell Immunotherapy for Acute Myeloid Leukemia. *Cell* 173: 1439-1453.e19

Kobayashi M, Wei H, Yamanashi T, Azevedo Portilho N, Cornelius S, Valiente N, Nishida C, Cheng H, Latorre A, Zheng WJ, *et al* (2023) HSC-independent definitive hematopoiesis persists into adult life. *Cell Reports* 42: 112239

Koç ON, Gerson SL, Cooper BW, Dyhouse SM, Haynesworth SE, Caplan AI & Lazarus HM (2000) Rapid Hematopoietic Recovery After Coinfusion of Autologous-Blood Stem Cells and Culture-Expanded Marrow Mesenchymal Stem Cells in Advanced Breast Cancer Patients Receiving High-Dose Chemotherapy. *JCO* 18: 307–307

Kohn DB, Kantoff PW, Eglitis MA, McLachlin JR, Moen RC, Karson E, Zwiebel JA, Nienhuis A, Karlsson S & O'Reilly R (1987) Retroviral-mediated gene transfer into mammalian cells. *Blood Cells* 13: 285–298

Komor AC, Kim YB, Packer MS, Zuris JA & Liu DR (2016) Programmable editing of a target base in genomic DNA without double-stranded DNA cleavage. *Nature* 533: 420–424

Konopleva M, Benton CB, Thall PF, Zeng Z, Shpall E, Ciurea S, Kebriaei P, Alousi A, Popat U, Anderlini P, *et al* (2015) Leukemia cell mobilization with G-CSF plus plerixafor during busulfan–fludarabine conditioning for allogeneic stem cell transplantation. *Bone Marrow Transplant* 50: 939–946

Kotin RM, Siniscalco M, Samulski RJ, Zhu XD, Hunter L, Laughlin CA, McLaughlin S, Muzyczka N, Rocchi M & Berns KI (1990) Site-specific integration by adeno-associated virus. *Proc Natl Acad Sci USA* 87: 2211–2215

Kunisaki Y, Bruns I, Scheiermann C, Ahmed J, Pinho S, Zhang D, Mizoguchi T, Wei Q, Lucas D, Ito K, *et al* (2013) Arteriolar niches maintain haematopoietic stem cell quiescence. *Nature* 502: 637–643

Kwon H-S, Logan AC, Chhabra A, Pang WW, Czechowicz A, Tate K, Le A, Poyser J, Hollis R, Kelly BV, *et al* (2019) Anti-human CD117 antibody-mediated bone marrow niche clearance in nonhuman primates and humanized NSG mice. *Blood* 133: 2104–2108

Lapidot T, Dar A & Kollet O (2005) How do stem cells find their way home? *Blood* 106: 1901–1910

Lapidot T, Pflumio F, Doedens M, Murdoch B, Williams DE & Dick JE (1992) Cytokine Stimulation of Multilineage Hematopoiesis from Immature Human Cells Engrafted in SCID Mice. *Science* 255: 1137–1141

Lattanzi A, Camarena J, Lahiri P, Segal H, Srifa W, Vakulskas CA, Frock RL, Kenrick J, Lee C, Talbott N, *et al* (2021) Development of β-globin gene correction in human hematopoietic stem cells as a potential durable treatment for sickle cell disease. *Sci Transl Med* 13: eabf2444

Laurenti E & Göttgens B (2018) From haematopoietic stem cells to complex differentiation landscapes. *Nature* 553: 418–426

Le Blanc K, Samuelsson H, Gustafsson B, Remberger M, Sundberg B, Arvidson J, Ljungman P, Lönnies H, Nava S & Ringdén O (2007) Transplantation of mesenchymal stem cells to enhance engraftment of hematopoietic stem cells. *Leukemia* 21: 1733–1738

Lee Y, Gotoh A, Kwon H-J, You M, Kohli L, Mantel C, Cooper S, Hangoc G, Miyazawa K, Ohyashiki K, *et al* (2002) Enhancement of intracellular signaling associated with hematopoietic progenitor cell survival in response to SDF-1/CXCL12 in synergy with other cytokines. *Blood* 99: 4307–4317

Lévesque J-P, Hendy J, Takamatsu Y, Simmons PJ & Bendall LJ (2003a) Disruption of the CXCR4/CXCL12 chemotactic interaction during hematopoietic stem cell mobilization induced by GCSF or cyclophosphamide. *J Clin Invest* 111: 187–196

Lévesque J-P, Hendy J, Winkler IG, Takamatsu Y & Simmons PJ (2003b) Granulocyte colony-stimulating factor induces the release in the bone marrow of proteases that cleave c-KIT receptor (CD117) from the surface of hematopoietic progenitor cells. *Experimental Hematology* 31: 109–117

Li C & Samulski RJ (2020) Engineering adeno-associated virus vectors for gene therapy. *Nat Rev Genet* 21: 255–272

Lidonnici MR, Aprile A, Frittoli MC, Mandelli G, Paleari Y, Spinelli A, Gentner B, Zambelli M, Parisi C, Bellio L, *et al* (2017) Plerixafor and G-CSF combination mobilizes hematopoietic stem and progenitors cells with a distinct transcriptional profile and a reduced *in vivo* homing capacity compared to plerixafor alone. *Haematologica* 102: e120–e124

Liesveld JL, Sharma N & Aljitawi OS (2020) Stem cell homing: From physiology to therapeutics. *Stem Cells* 38: 1241–1253

Liu G, Lin Q, Jin S & Gao C (2022) The CRISPR-Cas toolbox and gene editing technologies. *Molecular Cell* 82: 333–347

Lo Celso C, Fleming HE, Wu JW, Zhao CX, Miake-Lye S, Fujisaki J, Côté D, Rowe DW, Lin CP & Scadden DT (2009) Live-animal tracking of individual haematopoietic stem/progenitor cells in their niche. *Nature* 457: 92–96

Lomova A, Clark DN, Campo-Fernandez B, Flores-Bjurström C, Kaufman ML, Fitz-Gibbon S, Wang X, Miyahira EY, Brown D, DeWitt MA, *et al* (2019) Improving Gene Editing Outcomes in Human Hematopoietic Stem and Progenitor Cells by Temporal Control of DNA Repair. *Stem Cells* 37: 284–294

Lozier JN, Metzger ME, Donahue RE & Morgan RA (1999) The Rhesus Macaque as an Animal Model for Hemophilia B Gene Therapy. *Blood* 93: 1875–1881

MacMillan ML, Blazar BR, DeFor TE & Wagner JE (2009) Transplantation of ex-vivo culture-expanded parental haploidentical mesenchymal stem cells to promote engraftment in pediatric recipients of unrelated donor umbilical cord blood: results of a phase I–II clinical trial. *Bone Marrow Transplant* 43: 447–454

Madani A, Krause B, Greene ER, Subramanian S, Mohr BP, Holton JM, Olmos JL, Xiong C, Sun ZZ, Socher R, *et al* (2023) Large language models generate functional protein sequences across diverse families. *Nat Biotechnol*

Magnani A, Pondarré C, Bouazza N, Magalon J, Miccio A, Six E, Roudaut C, Arnaud C, Kamdem A, Touzot F, *et al* (2020) Extensive multilineage analysis in patients with mixed chimerism after allogeneic transplantation for sickle cell disease: insight into hematopoiesis and engraftment thresholds for gene therapy. *Haematologica* 105: 1240–1247

Matthys P, Hatse S, Vermeire K, Wuyts A, Bridger G, Henson GW, De Clercq E, Billiau A & Schols D (2001) AMD3100, a Potent and Specific Antagonist of the Stromal Cell-Derived Factor-1 Chemokine Receptor CXCR4, Inhibits Autoimmune Joint Inflammation in IFN-γ Receptor-Deficient Mice. *The Journal of Immunology* 167: 4686–4692

McCredie KB, Hersh EM & Freireich EJ (1971) Cells Capable of Colony Formation in the Peripheral Blood of Man. *Science* 171: 293–294

McDermott DH, Lopez J, Deng F, Liu Q, Ojode T, Chen H, Ulrick J, Kwatemaa N, Kelly C, Anaya-O'Brien S, *et al* (2011) AMD3100 is a potent antagonist at CXCR4R334X, a hyperfunctional mutant chemokine receptor and cause of WHIM syndrome. *Journal of Cellular and Molecular Medicine* 15: 2071–2081

McIntosh BE, Brown ME, Duffin BM, Maufort JP, Vereide DT, Slukvin II & Thomson JA (2015) Nonirradiated NOD,B6.SCID Il2rγ−/− KitW41/W41 (NBSGW) Mice Support Multilineage Engraftment of Human Hematopoietic Cells. *Stem Cell Reports* 4: 171–180

Méndez-Ferrer S, Lucas D, Battista M & Frenette PS (2008) Haematopoietic stem cell release is regulated by circadian oscillations. *Nature* 452: 442–447

Méndez-Ferrer S, Michurina TV, Ferraro F, Mazloom AR, MacArthur BD, Lira SA, Scadden DT, Ma'ayan A, Enikolopov GN & Frenette PS (2010) Mesenchymal and haematopoietic stem cells form a unique bone marrow niche. *Nature* 466: 829–834

Miyoshi H, Blömer U, Takahashi M, Gage FH & Verma IM (1998) Development of a Self-Inactivating Lentivirus Vector. *J Virol* 72: 8150–8157

Mohty M, Labopin M, Volin L, Gratwohl A, Socié G, Esteve J, Tabrizi R, Nagler A, Rocha V, & on behalf of the Acute Leukemia Working Party of EBMT (2010) Reduced-intensity versus conventional myeloablative conditioning allogeneic stem cell transplantation for patients with acute lymphoblastic leukemia: a retrospective study from the European Group for Blood and Marrow Transplantation. *Blood* 116: 4439–4443

Morrison SJ & Scadden DT (2014) The bone marrow niche for haematopoietic stem cells. *Nature* 505: 327–334

Mucci A, Antonarelli G, Caserta C, Vittoria FM, Desantis G, Pagani R, Greco B, Casucci M, Escobar G, Passerini L, *et al* (2021) Myeloid cell-based delivery of IFN-γ reprograms the leukemia microenvironment and induces anti-tumoral immune responses. *EMBO Mol Med* 13: e13598

Nagler A, Rocha V, Labopin M, Unal A, Ben Othman T, Campos A, Volin L, Poire X, Aljurf M, Masszi T, *et al* (2013) Allogeneic Hematopoietic Stem-Cell Transplantation for Acute Myeloid Leukemia in Remission: Comparison of Intravenous Busulfan Plus Cyclophosphamide (Cy) Versus Total-Body Irradiation Plus Cy As Conditioning Regimen—A Report From the Acute Leukemia Working Party of the European Group for Blood and Marrow Transplantation. *JCO* 31: 3549–3556

Naldini L (2019) Genetic engineering of hematopoiesis: current stage of clinical translation and future perspectives. *EMBO Mol Med* 11: e9958

Naldini L, Blömer U, Gallay P, Ory D, Mulligan R, Gage FH, Verma IM & Trono D (1996) In Vivo Gene Delivery and Stable Transduction of Nondividing Cells by a Lentiviral Vector. *Science* 272: 263–267

Nelson JW, Randolph PB, Shen SP, Everette KA, Chen PJ, Anzalone AV, An M, Newby GA, Chen JC, Hsu A, *et al* (2022) Engineered pegRNAs improve prime editing efficiency. *Nat Biotechnol* 40: 402–410

Nilsson SK, Johnston HM & Coverdale JA (2001) Spatial localization of transplanted hemopoietic stem cells: inferences for the localization of stem cell niches. *Blood* 97: 2293–2299

Nombela-Arrieta C & Manz MG (2017) Quantification and three-dimensional microanatomical organization of the bone marrow. *Blood Advances* 1: 407–416

Notta F, Doulatov S, Laurenti E, Poeppl A, Jurisica I & Dick JE (2011) Isolation of Single Human Hematopoietic Stem Cells Capable of Long-Term Multilineage Engraftment. *Science* 333: 218–221

Omer-Javed A, Pedrazzani G, Albano L, Ghaus S, Latroche C, Manzi M, Ferrari S, Fiumara M, Jacob A, Vavassori V, *et al* (2022) Mobilization-based

chemotherapy-free engraftment of gene-edited human hematopoietic stem cells. *Cell*: S0092867422005372

Packer MS & Liu DR (2015) Methods for the directed evolution of proteins. *Nat Rev Genet* 16: 379–394

Palchaudhuri R, Saez B, Hoggatt J, Schajnovitz A, Sykes DB, Tate TA, Czechowicz A, Kfoury Y, Ruchika F, Rossi DJ, *et al* (2016) Non-genotoxic conditioning for hematopoietic stem cell transplantation using a hematopoietic-cell-specific internalizing immunotoxin. *Nat Biotechnol* 34: 738–745

Panch SR, Szymanski J, Savani BN & Stroncek DF (2017) Sources of Hematopoietic Stem and Progenitor Cells and Methods to Optimize Yields for Clinical Cell Therapy. *Biology of Blood and Marrow Transplantation* 23: 1241–1249

Passegué E, Wagers AJ, Giuriato S, Anderson WC & Weissman IL (2005) Global analysis of proliferation and cell cycle gene expression in the regulation of hematopoietic stem and progenitor cell fates. *The Journal of Experimental Medicine* 202: 1599–1611

Passmore LA & Coller J (2022) Roles of mRNA poly(A) tails in regulation of eukaryotic gene expression. *Nat Rev Mol Cell Biol* 23: 93–106

Peled A, Petit I, Kollet O, Magid M, Ponomaryov T, Byk T, Nagler A, Ben-Hur H, Many A, Shultz L, *et al* (1999) Dependence of Human Stem Cell Engraftment and Repopulation of NOD/SCID Mice on CXCR4. *Science* 283: 845–848

Perez-Oliva AB, Martinez-Esparza M, Vicente-Fernandez JJ, Corral-San Miguel R, Garcia-Penarrubia P & Hernandez-Caselles T (2011) Epitope mapping, expression and post-translational modifications of two isoforms of CD33 (CD33M and CD33m) on lymphoid and myeloid human cells. *Glycobiology* 21: 757–770

Perlin JR, Sporrij A & Zon LI (2017) Blood on the tracks: hematopoietic stem cell-endothelial cell interactions in homing and engraftment. *J Mol Med* 95: 809–819

Peterson CW, Venkataraman R, Reddy SS, Pande D, Enstrom MR, Radtke S, Humbert O & Kiem H-P (2022) Intracellular RNase activity dampens zinc finger nuclease-mediated gene editing in hematopoietic stem and progenitor cells. *Molecular Therapy - Methods & Clinical Development* 24: 30–39

Petit I, Szyper-Kravitz M, Nagler A, Lahav M, Peled A, Habler L, Ponomaryov T, Taichman RS, Arenzana-Seisdedos F, Fujii N, *et al* (2002) G-CSF induces stem cell mobilization by decreasing bone marrow SDF-1 and up-regulating CXCR4. *Nat Immunol* 3: 687–694

Pietras EM, Warr MR & Passegué E (2011) Cell cycle regulation in hematopoietic stem cells. *Journal of Cell Biology* 195: 709–720

Pinho S & Frenette PS (2019) Haematopoietic stem cell activity and interactions with the niche. *Nat Rev Mol Cell Biol* 20: 303–320

Pinho S, Marchand T, Yang E, Wei Q, Nerlov C & Frenette PS (2018) Lineage-Biased Hematopoietic Stem Cells Are Regulated by Distinct Niches. *Developmental Cell* 44: 634-641.e4

Pittenger MF, Discher DE, Péault BM, Phinney DG, Hare JM & Caplan AI (2019) Mesenchymal stem cell perspective: cell biology to clinical progress. *npj Regen Med* 4: 22

Pittenger MF, Mackay AM, Beck SC, Jaiswal RK, Douglas R, Mosca JD, Moorman MA, Simonetti DW, Craig S & Marshak DR (1999) Multilineage Potential of Adult Human Mesenchymal Stem Cells. *Science* 284: 143–147

Porto EM, Komor AC, Slaymaker IM & Yeo GW (2020) Base editing: advances and therapeutic opportunities. *Nat Rev Drug Discov* 19: 839–859

Pulsipher MA, Chitphakdithai P, Logan BR, Navarro WH, Levine JE, Miller JP, Shaw BE, O'Donnell PV, Majhail NS & Confer DL (2014) Lower risk for serious adverse events and no increased risk for cancer after PBSC vs BM donation. *Blood* 123: 3655–3663

Pulsipher MA, Chitphakdithai P, Logan BR, Shaw BE, Wingard JR, Lazarus HM, Waller EK, Seftel M, Stroncek DF, Lopez AM, *et al* (2013) Acute toxicities of unrelated bone marrow versus peripheral blood stem cell donation: results of a prospective trial from the National Marrow Donor Program. *Blood* 121: 197–206

Pulsipher MA, Logan BR, Chitphakdithai P, Kiefer DM, Riches ML, Rizzo JD, Anderlini P, Leitman SF, Varni JW, Kobusingye H, *et al* (2019) Effect of Aging and Predonation Comorbidities on the Related Peripheral Blood Stem Cell Donor Experience: Report from the Related Donor Safety Study. *Biology of Blood and Marrow Transplantation* 25: 699–711

Radtke S, Chan Y-Y, Giese MA, Norgaard ZK, Schefter LE, Adair JE & Kiem H-P (2016) Conserved Lineage Development in Human and Nonhuman Primate Hematopoiesis. *Blood* 128: 2646–2646

Ramamoorth M (2015) Non Viral Vectors in Gene Therapy- An Overview. *JCDR*

Ramanathan A, Robb GB & Chan S-H (2016) mRNA capping: biological functions and applications. *Nucleic Acids Res* 44: 7511–7526

Rambaldi A, Grassi A, Masciulli A, Boschini C, Micò MC, Busca A, Bruno B, Cavattoni I, Santarone S, Raimondi R, *et al* (2015) Busulfan plus cyclophosphamide versus busulfan plus fludarabine as a preparative regimen for allogeneic haemopoietic stem-cell transplantation in patients with acute myeloid leukaemia: an open-label, multicentre, randomised, phase 3 trial. *The Lancet Oncology* 16: 1525–1536

Ramirez P, Rettig MP, Uy GL, Deych E, Holt MS, Ritchey JK & DiPersio JF (2009) BIO5192, a small molecule inhibitor of VLA-4, mobilizes hematopoietic stem and progenitor cells. *Blood* 114: 1340–1343

Ratajczak W, Niedźwiedzka-Rystwej P, Tokarz-Deptuła B & Deptuła W (2018) Immunological memory cells. *cejoi* 43: 194–203

Renshaw BR, Fanslow WC, Armitage RJ, Campbell KA, Liggitt D, Wright B, Davison BL & Maliszewski CR (1994) Humoral immune responses in CD40 ligand-deficient mice. *The Journal of experimental medicine* 180: 1889–1900

Richter MF, Zhao KT, Eton E, Lapinaite A, Newby GA, Thuronyi BW, Wilson C, Koblan LW, Zeng J, Bauer DE, *et al* (2020) Phage-assisted evolution of an adenine base editor with improved Cas domain compatibility and activity. *Nat Biotechnol* 38: 883–891

Rohner E, Yang R, Foo KS, Goedel A & Chien KR (2022) Unlocking the promise of mRNA therapeutics. *Nat Biotechnol* 40: 1586–1600

Rongvaux A, Takizawa H, Strowig T, Willinger T, Eynon EE, Flavell RA & Manz MG (2013) Human Hemato-Lymphoid System Mice: Current Use and Future Potential for Medicine. *Annu Rev Immunol* 31: 635–674

Rongvaux A, Willinger T, Martinek J, Strowig T, Gearty SV, Teichmann LL, Saito Y, Marches F, Halene S, Palucka AK, *et al* (2014) Development and function of human innate immune cells in a humanized mouse model. *Nat Biotechnol* 32: 364–372

Rosenkilde MM, Gerlach L-O, Hatse S, Skerlj RT, Schols D, Bridger GJ & Schwartz TW (2007) Molecular Mechanism of Action of Monocyclam Versus Bicyclam Non-peptide Antagonists in the CXCR4 Chemokine Receptor. *Journal of Biological Chemistry* 282: 27354–27365

Rosenkilde MM, Gerlach L-O, Jakobsen JS, Skerlj RT, Bridger GJ & Schwartz TW (2004) Molecular Mechanism of AMD3100 Antagonism in the CXCR4 Receptor. *Journal of Biological Chemistry* 279: 3033–3041

Rüesch M, Amar El Dusouqui S, Buhrfeind E, Buser A, Chalandon Y, Frey BM, Güngör T, Holbro A, Huguet S, Infanti L, *et al* (2022) Basic characteristics and safety of donation in related and unrelated haematopoietic progenitor cell donors – first 10 years of prospective donor follow-up of Swiss donors. *Bone Marrow Transplant* 57: 918–924

Samulski RJ, Zhu X, Xiao X, Brook JD, Housman DE, Epstein N & Hunter LA (1991) Targeted integration of adeno-associated virus (AAV) into human chromosome 19. *The EMBO Journal* 10: 3941–3950

Sánchez-Guijo FM, Orfao A & Del Cañizo MC (2012) Bone Marrow Transplantation Extends Its Scope. In *Stem Cell Transplantation*, López-Larrea C López-Vázquez A & Suárez-Álvarez B (eds) pp 121–134. New York, NY: Springer US

Santos GW, Tutschka PJ, Brookmeyer R, Saral R, Beschorner WE, Bias WB, Braine HG, Burns WH, Elfenbein GJ, Kaizer H, *et al* (1983) Marrow Transplantation for Acute Nonlymphocytic Leukemia after Treatment with Busulfan and Cyclophosphamide. *N Engl J Med* 309: 1347–1353

Saraceni F, Labopin M, Hamladji R-M, Mufti G, Socié G, Shimoni A, Delage J, Deconinck E, Chevallier P, Blaise D, *et al* (2018) Thiotepa-busulfan-fludarabine compared to busulfan-fludarabine for sibling and unrelated donor transplant in acute myeloid leukemia in first remission. *Oncotarget* 9: 3379–3393

Schiroli G, Conti A, Ferrari S, della Volpe L, Jacob A, Albano L, Beretta S, Calabria A, Vavassori V, Gasparini P, *et al* (2019) Precise Gene Editing Preserves Hematopoietic Stem Cell Function following Transient p53-Mediated DNA Damage Response. *Cell Stem Cell* 24: 551-565.e8

Schiroli G, Ferrari S, Conway A, Jacob A, Capo V, Albano L, Plati T, Castiello MC, Sanvito F, Gennery AR, *et al* (2017) Preclinical modeling highlights the therapeutic potential of hematopoietic stem cell gene editing for correction of SCID-X1. *Sci Transl Med* 9: eaan0820

Schmidt AH, Mengling T, Hernández-Frederick CJ, Rall G, Pingel J, Schetelig J & Ehninger G (2017) Retrospective Analysis of 37,287 Observation Years after Peripheral Blood Stem Cell Donation. *Biology of Blood and Marrow Transplantation* 23: 1011–1020

Schmitt N, Streuer A, Danner J, Altrock E, Riabov V, Xu Q, Rapp F, Weimer N, Palme I, Nowak V, *et al* (2022) Direct Comparison of NSG and NBSGW Mice for MDS Patient-Derived Xenograft Models. *Blood* 140: 4009–4010

Schönberger S, Niehues T, Meisel R, Bernbeck B, Laws HJ, Kögler G, Enzmann J, Wernet P, Göbel U & Dilloo D (2004) Transplantation of Haematopoietic Stem Cells Derived from Cord Blood, Bone Marrow or Peripheral Blood: A Single Centre Matched-Pair Analysis in a Heterogeneous Risk Population. *Klin Padiatr* 216: 356–363

Scully R, Panday A, Elango R & Willis NA (2019) DNA double-strand break repair-pathway choice in somatic mammalian cells. *Nat Rev Mol Cell Biol* 20: 698–714

Seita J & Weissman IL (2010) Hematopoietic stem cell: self-renewal versus differentiation. *WIREs Mechanisms of Disease* 2: 640–653

Shepherd BE, Kiem H-P, Lansdorp PM, Dunbar CE, Aubert G, LaRochelle A, Seggewiss R, Guttorp P & Abkowitz JL (2007) Hematopoietic stem-cell behavior in nonhuman primates. *Blood* 110: 1806–1813

Shimoni A, Labopin M, Savani B, Hamladji R-M, Beelen D, Mufti G, Socié G, Delage J, Blaise D, Chevallier P, *et al* (2018) Intravenous Busulfan Compared with Treosulfan-Based Conditioning for Allogeneic Stem Cell Transplantation in Acute Myeloid Leukemia: A Study on Behalf of the Acute Leukemia Working

Party of European Society for Blood and Marrow Transplantation. *Biology of Blood and Marrow Transplantation* 24: 751–757

Shin JJ, Schröder MS, Caiado F, Wyman SK, Bray NL, Bordi M, Dewitt MA, Vu JT, Kim W-T, Hockemeyer D, *et al* (2020) Controlled Cycling and Quiescence Enables Efficient HDR in Engraftment-Enriched Adult Hematopoietic Stem and Progenitor Cells. *Cell Reports* 32: 108093

Shultz LD, Schweitzer PA, Christianson SW, Gott B, Schweitzer IB, Tennent B, McKenna S, Mobraaten L, Rajan TV & Greiner DL (1995) Multiple defects in innate and adaptive immunologic function in NOD/LtSz-scid mice. *J Immunol* 154: 180–191

Shy BR, Vykunta VS, Ha A, Talbot A, Roth TL, Nguyen DN, Pfeifer WG, Chen YY, Blaeschke F, Shifrut E, *et al* (2023) High-yield genome engineering in primary cells using a hybrid ssDNA repair template and small-molecule cocktails. *Nat Biotechnol* 41: 521–531

Socie G, Lawler M, Gluckman E, McCann SR & Brison O (1995) Studies on hemopoietic chimerism following allogeneic bone marrow transplantation in the molecular biology era. *Leukemia Research* 19: 497–504

Spencer JA, Ferraro F, Roussakis E, Klein A, Wu J, Runnels JM, Zaher W, Mortensen LJ, Alt C, Turcotte R, *et al* (2014) Direct measurement of local oxygen concentration in the bone marrow of live animals. *Nature* 508: 269–273

Suárez-Álvarez B, López-Vázquez A & López-Larrea C (2012) Mobilization and Homing of Hematopoietic Stem Cells. In *Stem Cell Transplantation*, López-Larrea C López-Vázquez A & Suárez-Álvarez B (eds) pp 152–170. New York, NY: Springer US

Sullivan KM (2000) Bone Marrow Transplantation for Non-Malignant Disease. *Hematology* 2000: 319–338

Thomas ED, Clift RA, Hersman J, Sanders JE, Stewart P, Buckner CD, Fefer A, McGuffin R, Smith JW & Storb R (1982) Marrow transplantation for acute nonlymphoblastic leukemia in first remission using fractionated or single-dose irradiation. *International Journal of Radiation Oncology*Biology*Physics* 8: 817–821

Till JE & McCulloch EA (1961) A direct measurement of the radiation sensitivity of normal mouse bone marrow cells. *Radiat Res* 14: 213–222

Trobridge GD, Beard BC, Gooch C, Wohlfahrt M, Olsen P, Fletcher J, Malik P & Kiem H-P (2008) Efficient transduction of pigtailed macaque hematopoietic repopulating cells with HIV-based lentiviral vectors. *Blood* 111: 5537–5543

Tusup M, French LE, De Matos M, Gatfield D, Kundig T & Pascolo S (2019) Design of in vitro Transcribed mRNA Vectors for Research and Therapy. *Chimia* 73: 391

Tutschka P, Copelan E & Klein J (1987) Bone marrow transplantation for leukemia following a new busulfan and cyclophosphamide regimen. *Blood* 70: 1382–1388

Tzeng Y-S, Li H, Kang Y-L, Chen W-C, Cheng W-C & Lai D-M (2011) Loss of Cxcl12/Sdf-1 in adult mice decreases the quiescent state of hematopoietic stem/progenitor cells and alters the pattern of hematopoietic regeneration after myelosuppression. *Blood* 117: 429–439

Uchida N, Nassehi T, Drysdale CM, Gamer J, Yapundich M, Bonifacino AC, Krouse AE, Linde N, Hsieh MM, Donahue RE, *et al* (2019) Busulfan Combined with Immunosuppression Allows Efficient Engraftment of Gene-Modified Cells in a Rhesus Macaque Model. *Molecular Therapy* 27: 1586–1596

Urnov FD, Miller JC, Lee Y-L, Beausejour CM, Rock JM, Augustus S, Jamieson AC, Porteus MH, Gregory PD & Holmes MC (2005) Highly efficient endogenous human gene correction using designed zinc-finger nucleases. *Nature* 435: 646–651

Vavassori V, Ferrari S, Beretta S, Asperti C, Albano L, Annoni A, Gaddoni C, Varesi A, Soldi M, Cuomo A, *et al* (2023) Lipid Nanoparticles Allow Efficient and Harmless *Ex Vivo* Gene Editing of Human Hematopoietic Cells. *Blood Journal*: blood.2022019333

Vavassori V, Mercuri E, Marcovecchio GE, Castiello MC, Schiroli G, Albano L, Margulies C, Buquicchio F, Fontana E, Beretta S, *et al* (2021) Modeling, optimization, and comparable efficacy of T cell and hematopoietic stem cell gene editing for treating hyper-IgM syndrome. *EMBO Mol Med* 13

Verma IM & Weitzman MD (2005) GENE THERAPY: Twenty-First Century Medicine. *Annu Rev Biochem* 74: 711–738

Vigna E & Naldini L (2000) Lentiviral vectors: excellent tools for experimental gene transfer and promising candidates for gene therapy. *The Journal of Gene Medicine* 2: 308–316

Walters MC, Patience M, Leisenring W, Rogers ZR, Aquino VM, Buchanan GR, Roberts IAG, Yeager AM, Hsu L, Adamkiewicz T, *et al* (2001) Stable mixed hematopoietic chimerism after bone marrow transplantation for sickle cell anemia. *Biology of Blood and Marrow Transplantation* 7: 665–673

Wang H, Germond A, Li C, Gil S, Kim J, Kiem H-P & Lieber A (2022) In vivo HSC transduction in rhesus macaques with an HDAd5/3 + vector targeting desmoglein 2 and transiently overexpressing cxcr4. *Blood Advances* 6: 4360–4372

Waskow C, Madan V, Bartels S, Costa C, Blasig R & Rodewald H-R (2009) Hematopoietic stem cell transplantation without irradiation. *Nat Methods* 6: 267–269

Weissman IL & Shizuru JA (2008) The origins of the identification and isolation of hematopoietic stem cells, and their capability to induce donor-specific transplantation tolerance and treat autoimmune diseases. *Blood* 112: 3543–3553

Wolock SL, Krishnan I, Tenen DE, Matkins V, Camacho V, Patel S, Agarwal P, Bhatia R, Tenen DG, Klein AM, *et al* (2019) Mapping Distinct Bone Marrow Niche Populations and Their Differentiation Paths. *Cell Reports* 28: 302-311.e5

Wong C (2023) UK first to approve CRISPR treatment for diseases: what you need to know. *Nature* 623: 676–677

Wu Y, Zeng J, Roscoe BP, Liu P, Yao Q, Lazzarotto CR, Clement K, Cole MA, Luk K, Baricordi C, *et al* (2019) Highly efficient therapeutic gene editing of human hematopoietic stem cells. *Nat Med* 25: 776–783

Wunderlich M, Chou F-S, Sexton C, Presicce P, Chougnet CA, Aliberti J & Mulloy JC (2018) Improved multilineage human hematopoietic reconstitution and function in NSGS mice. *PLoS ONE* 13: e0209034

Yang KK, Wu Z & Arnold FH (2019) Machine-learning-guided directed evolution for protein engineering. *Nat Methods* 16: 687–694

Yin AH, Miraglia S, Zanjani ED, Almeida-Porada G, Ogawa M, Leary AG, Olweus J, Kearney J & Buck DW (1997) AC133, a novel marker for human hematopoietic stem and progenitor cells. *Blood* 90: 5002–5012

Yu VWC & Scadden DT (2016) Hematopoietic Stem Cell and Its Bone Marrow Niche. In *Current Topics in Developmental Biology* pp 21–44. Elsevier

Zhang J, Niu C, Ye L, Huang H, He X, Tong W-G, Ross J, Haug J, Johnson T, Feng JQ, *et al* (2003) Identification of the haematopoietic stem cell niche and control of the niche size. *Nature* 425: 836–841

Zhao Z, Shang P, Mohanraju P & Geijsen N (2023) Prime editing: advances and therapeutic applications. *Trends in Biotechnology* 41: 1000–1012

Zhou BO, Yue R, Murphy MM, Peyer JG & Morrison SJ (2014) Leptin-Receptor-Expressing Mesenchymal Stromal Cells Represent the Main Source of Bone Formed by Adult Bone Marrow. *Cell Stem Cell* 15: 154–168

Zohren F, Toutzaris D, Klärner V, Hartung H-P, Kieseier B & Haas R (2008) The monoclonal anti–VLA-4 antibody natalizumab mobilizes CD34+ hematopoietic progenitor cells in humans. *Blood* 111: 3893–3895

